

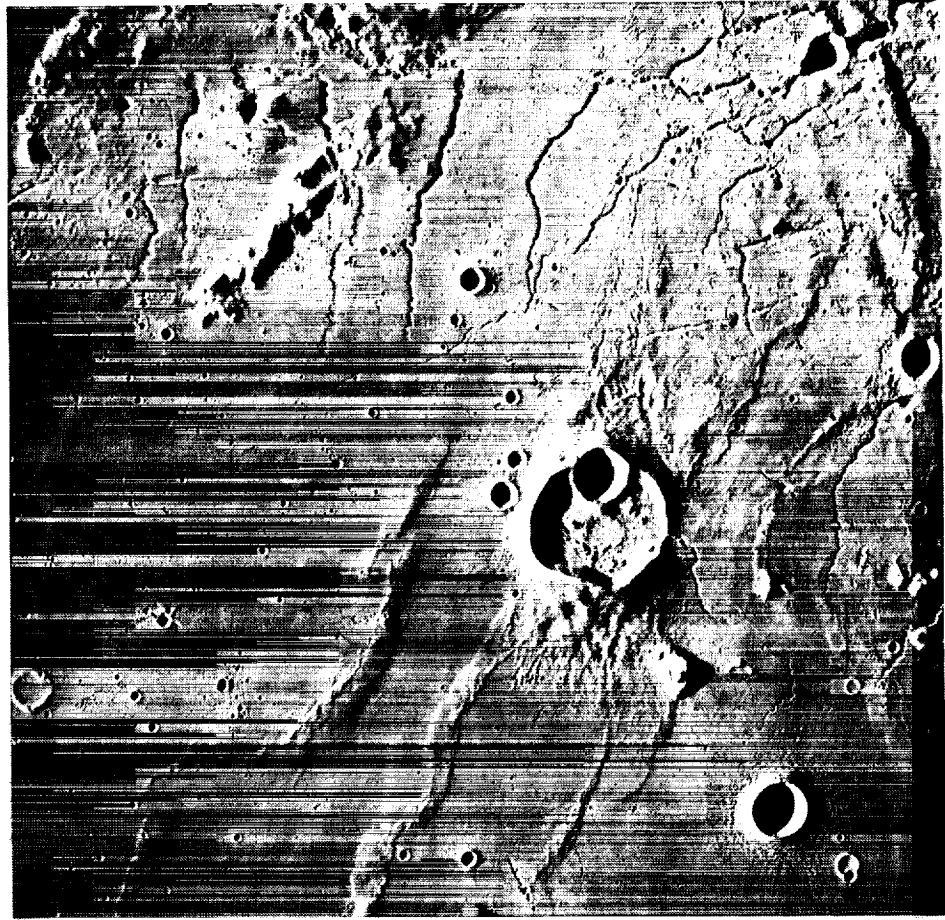
11-91-CR

P. 75

# WORKSHOP ON MARE VOLCANISM AND BASALT PETROGENESIS: "ASTOUNDING FUNDAMENTAL CONCEPTS (AFC)" DEVELOPED OVER THE LAST FIFTEEN YEARS

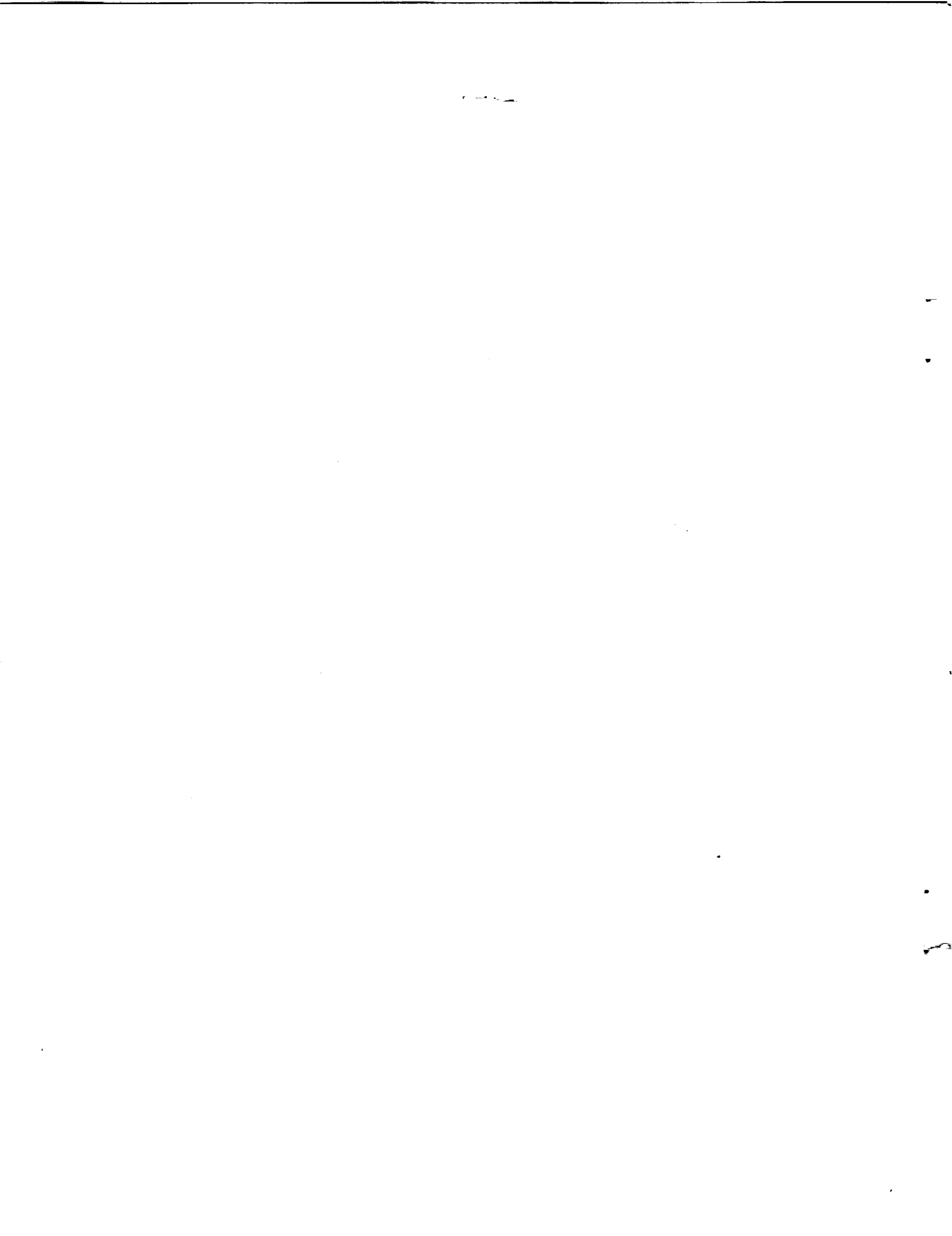
N92-10961  
--THRU--  
N92-10965  
Unclass  
0046150

(NASA-CR-188810) WORKSHOP ON MARE VOLCANISM  
AND BASALT PETROGENESIS: ASTOUNDING  
FUNDAMENTAL CONCEPTS (AFC) DEVELOPED OVER  
THE LAST FIFTEEN YEARS (Lunar and Planetary  
Inst.) 75 p  
CSCL 03B G3/91



## LPI Technical Report Number 91-03

LUNAR AND PLANETARY INSTITUTE 3303 NASA ROAD 1 HOUSTON TX 77058-4399  
LPI/TR--91-03



WORKSHOP ON MARE VOLCANISM AND BASALT PETROGENESIS:  
"ASTOUNDING FUNDAMENTAL CONCEPTS (AFC)" DEVELOPED  
OVER THE LAST FIFTEEN YEARS

Conveners:

Lawrence A. Taylor

John Longhi

Held at

Park Plaza Hotel

Dallas, Texas

October 27-28, 1990

Sponsored by

Lunar and Planetary Institute

Lunar and Planetary Sample Team (LAPST)

Lunar and Planetary Institute

3303 NASA Road 1

Houston TX 77058-4399

LPI Technical Report Number 91-03

LPI/TR--91-03

Compiled in 1991 by  
LUNAR AND PLANETARY INSTITUTE

The Institute is operated by Universities Space Research Association under Contract NASW-4574 with the National Aeronautics and Space Administration.

Material in this document may be copied without restraint for library, abstract service, educational, or personal research purposes; however, republication of any portion requires the written permission of the authors as well as appropriate acknowledgment of this publication.

This report may be cited as:

Taylor L. A. and Longhi J., eds. (1991) *Mare Volcanism and Basalt Petrogenesis Workshop: "Astounding Fundamental Concepts (AFC)" Developed Over the Last Fifteen Years*. LPI Tech. Rpt. 91-03, Lunar and Planetary Institute, Houston. 69 pp.

Papers in this report may be cited as:

Author A. A. (1991) Title of paper (abstract). In *Mare Volcanism and Basalt Petrogenesis Workshop: "Astounding Fundamental Concepts (AFC)" Developed Over the Last Fifteen Years* (L. A. Taylor and J. Longhi, eds.), pp. xx-yy. LPI Tech. Rpt. 91-03, Lunar and Planetary Institute, Houston.

This report is distributed by:

ORDER DEPARTMENT  
Lunar and Planetary Institute  
3303 NASA Road 1  
Houston TX 77058-4399

*Mail order requestors will be invoiced for the cost of shipping and handling.*

---

Cover: Central Krieger Crater north-northeast of Aristarchus Crater in Oceanus Procellarum. (Notice the several wrinkle ridges to the north and abundant sinuous rilles to the south.)

## Preface

---

A workshop that was devoted solely to mare basalts and volcanism had not been convened since 1975. Several topical workshops had touched on this subject (e.g., the Workshop on the Geology and Petrology of the Apollo 15 Landing Site that was held in 1985), but considerable new results have come forth in the intervening 15 or so years. Some major developments include the recognition that mare volcanism is as old as 4.3 Ga; the recognition that there are numerous groups of glass beads, produced by fire fountaining, that require unique source regions; the discovery of new basalt types (e.g., VHK from Apollo 14 and Group D of Apollo 17 basalts); an increased understanding of the basic physical principles of basaltic magma ascent and eruption; knowledge of the implications of volcanic landform and deposit morphology for eruption conditions (e.g., pyroclastic dark-mantled deposits); and the application of new petrogenetic modeling techniques. The advances of desktop PCs in the last 10 years have led to the increased use of computers in all aspects of lunar scientific endeavors; indeed, older petrogenetic models have been readily examined and modified, and applications of recently developed models and principles (e.g., assimilation and fractional crystallization, AFC) have provided new insight to the genesis of basaltic magmas.

Many of these significant new developments have never been brought together in their own forum until this workshop. The discussion of recent ideas and concepts within the context of this workshop has permitted many of us to catch up on the myriad developments during the last 15 years. And very importantly, although this workshop emphasized the knowns, it revealed many avenues for potential investigations on mare basalts and, hopefully, has stimulated participants to undertake additional mare basalt research well into the next century.

*Lawrence A. Taylor, University of Tennessee  
John Longhi, Lamont-Doherty Geological Observatory*



# Program

---

Saturday, October 27, 1990

8:00-8:45 a.m. REGISTRATION/CONTINENTAL BREAKFAST

8:45-8:55 INTRODUCTION

## GEOLOGICAL SETTING

- 8:55-9:40 J. W. Head\*  
*Geological Setting and Morphology of Mare Volcanic Deposits: Implications for Chronology, Petrogenesis, and Eruption Conditions*
- 9:40-10:00 R. Jaumann\*, G. Neukum, and H. Hoffmann  
*Mare Serenitatis/Mare Tranquillitatis Shelf Region: Identification of Basalt Types from Multispectral Reflectance Measurements*
- 10:00-10:20 J. M. Sunshine\* and C. M. Pieters  
*Titanium-rich Basalts Within the Flamsteed-P Region of Oceanus Procellarum: New Results from High Spatial Resolution CCD Data*
- 10:20-10:40 COFFEE BREAK
- 10:40-11:00 P. H. Warren\* and G. W. Kallemeyn  
*Lunar Mare Meteorites*
- 11:00-11:20 B. R. Hawke\*, P. G. Lucey, J. F. Bell, and P. D. Spudis  
*Ancient Mare Volcanism*
- 11:20-11:40 C. R. Coombs\*, D. S. McKay, and B. R. Hawke  
*The Violent Side of Mare Volcanism*
- 11:40-12:00 P. H. Schultz\*  
*The Moon: Dead or Alive*
- 12:00-1:20 p.m. LUNCH

## MAGMA EVOLUTION AND SOURCE REGIONS

- 1:20-1:50 C. R. Neal\* and L. A. Taylor - INVITED  
*Models for Mare Basalt Petrogenesis Developed over the Last 20 Years*
- 1:50-2:20 J. W. Shervais\* and S. K. Vetter - INVITED  
*Lunar Mare Volcanism: Recent Advances in Petrogenesis*

---

\*Denotes speaker

- 2:20-2:40 G. McKay\*, J. Wagstaff, and L. Le  
*REE Distribution Coefficients for Pigeonite: Constraints on the Origin of the Mare Basalt Europium Anomaly, III*
- 2:40-3:10 G. A. Snyder\*, L. A. Taylor, and C. R. Neal - COMBINED TALK  
*The Sources of Mare Basalts: A Model Involving Lunar Magma Ocean Crystallization, Plagioclase Flotation, and Trapped Instantaneous Residual Liquid*  
and  
*Geochemical Constraints (and Pitfalls) on Remelting of Lunar Magma Ocean Cumulates for the Generation of High-Ti Mare Basalts*
- 3:10-3:30 S. K. Vetter\* and J. W. Shervais  
*Apollo 15 Olivine-Normative and Quartz-Normative Mare Basalts: A Common Origin by Dynamic Melting*
- 3:30-3:50 COFFEE BREAK
- 3:50-4:10 T. L. Dickinson\* and D. O. Nelson  
*Formation of Apollo 14 Aluminous Mare Basalts by Replenishment Fractional Crystallization and Assimilation of Precursor Crust*
- 4:10-4:30 P. H. Warren\*, E. A. Jerde, and G. W. Kallemeyn  
*A Spinifex-Textured Mare Basalt: Comparison with Komatiites*
- 4:30-4:50 J. H. Jones\* and J. W. Delano  
*Exploration of Relationships Between Low-Ti and High-Ti Pristine Lunar Glasses Using an Armalcolite Assimilation Model*
- 4:50-5:10 C. K. Shearer\*, J. J. Papike, and N. Shimizu  
*The Relevance of Picritic Glasses to Mare Basalt Volcanism*
- 5:10-6:30 RECEPTION

Sunday, October 28, 1990

### MAGMA SOURCE AND ASCENT PROCESSES

- 8:00-8:30 a.m. CONTINENTAL BREAKFAST
- 8:30-9:15 F. J. Spera\* - INVITED  
*Lunar Magma Transport Phenomena*
- 9:15-9:45 P. C. Hess\* - INVITED  
*Pristine Mare Glasses: Primary Magmas?*
- 9:45-10:05 J. Longhi\*  
*Dynamical Melting Models of Mare Basalts*
- 10:05-10:25 M. Manga\* and J. Arkani-Hamed  
*Remelting Mechanisms for Shallow Source Regions of Mare Basalts*

## HISTORY OF VOLCANISM

- 10:25-10:55 L. E. Nyquist\* and C.-Y. Shih - INVITED  
*The History of Lunar Volcanism*
- 10:55-11:15 C. R. Neal\* and L. A. Taylor  
*Cyclical AFC at Apollo 14: Sr Isotope Evidence from High-Alumina Basalts*
- 11:15-11:35 C. R. Neal\*, L. A. Taylor, J. B. Paces, and A. N. Halliday  
*Identification & Origin of Source Heterogeneities for Apollo 17 Basalts  
Using Isotopic Tracers*
- 11:35-11:55 C. M. Pieters\*  
*The Probable Continuum Between Emplacement of Plutons and Mare Volcanism in  
Lunar Crustal Evolution*
- 11:55-12:15 SUMMARY



# Contents

---

<b>Summary of Technical Sessions</b>	1
<b>Abstracts</b>	7
The Violent Side of Mare Volcanism C. R. Coombs, D. S. McKay, and B. R. Hawke	9
Formation of Apollo 14 Aluminous Mare Basalts by Replenishment Fractional Crystallization and Assimilation of Precursor Crust T. L. Dickinson and D. O. Nelson	11
Ancient Mare Volcanism B. R. Hawke, P. G. Lucey, J. F. Bell, and P. D. Spudis	13
Geological Setting and Morphology of Mare Volcanic Deposits: Implications for Chronology, Petrogenesis, and Eruption Conditions J. W. Head	15
Pristine Mare Glasses: Primary Magmas? P. C. Hess	17
Mare Serenitatis/Mare Tranquillitatis Shelf Region: Identification of Basalt Types from Multispectral Reflectance Measurements R. Jaumann, G. Neukum, and H. Hoffmann	19
Exploration of Relationships Between Low-Ti and High-Ti Pristine Lunar Glasses Using an Armalcolite Assimilation Model J. H. Jones and J. W. Delano	21
Dynamical Melting Models of Mare Basalts J. Longhi	23
Remelting Mechanisms for Shallow Source Regions of Mare Basalts M. Manga and J. Arkani-Hamed	25
REE Distribution Coefficients for Pigeonite: Constraints on the Origin of the Mare Basalt Europium Anomaly, III G. McKay, J. Wagstaff, and L. Le	27
Cyclical AFC at Apollo 14: Sr Isotope Evidence from High-Alumina Basalts C. R. Neal and L. A. Taylor	29
Models for Mare Basalt Petrogenesis Developed over the Last 20 Years C. R. Neal and L. A. Taylor	31
Identification & Origin of Source Heterogeneities for Apollo 17 Basalts Using Isotopic Tracers C. R. Neal, L. A. Taylor, J. B. Paces, and A. N. Halliday	36
The History of Lunar Volcanism L. E. Nyquist and C.-Y. Shih	39
The Probable Continuum Between Emplacement of Plutons and Mare Volcanism in Lunar Crustal Evolution C. M. Pieters	43

The Moon: Dead or Alive <i>P. H. Schultz</i>	45
The Relevance of Picritic Glasses to Mare Basalt Volcanism <i>C. K. Shearer, J. J. Papike, and N. Shimizu</i>	47
Lunar Mare Volcanism: Recent Advances in Petrogenesis <i>J. W. Shervais and S. K. Vetter</i>	49
Geochemical Constraints (and Pitfalls) on Remelting of Lunar Magma Ocean Cumulates for the Generation of High-Ti Mare Basalts <i>G. A. Snyder, L. A. Taylor, and C. R. Neal</i>	51
The Sources of Mare Basalts: A Model Involving Lunar Magma Ocean Crystallization, Plagioclase Flotation, and Trapped Instantaneous Residual Liquid <i>G. A. Snyder, L. A. Taylor, and C. R. Neal</i>	53
Lunar Magma Transport Phenomena <i>F. J. Spera</i>	55
Titanium-rich Basalts Within the Flamsteed-P Region of Oceanus Procellarum: New Results from High Spatial Resolution CCD Data <i>J. M. Sunshine and C. M. Pieters</i>	59
Apollo 15 Olivine-Normative and Quartz-Normative Mare Basalts: A Common Origin by Dynamic Melting <i>S. K. Vetter and J. W. Shervais</i>	61
Lunar Mare Meteorites <i>P. H. Warren and G. W. Kallemeyn</i>	63
A Spinifex-Textured Mare Basalt: Comparison with Komatiites <i>P. H. Warren, E. A. Jerde, and G. W. Kallemeyn</i>	65
<b>List of Workshop Participants</b>	67

# Summary of Technical Sessions

---

## GEOLOGICAL SETTING

Summarized by B. Ray Hawke

J. W. Head presented a very thorough review of the geological setting and morphology of mare volcanic deposits. He noted that developments in the past 15 years were highlighted by (1) an improved understanding of the extent and stratigraphy of mare units; (2) a more thorough understanding of the basic physical principles of lunar basaltic magma ascent and eruption; (3) increased knowledge of the implications of volcanic landform and deposit morphology for eruption conditions; and (4) convergence of sample research on problems related to processes of ascent and emplacement of basaltic magma.

At the conclusion of his presentation, Head discussed a number of unresolved questions or poorly understood issues that should be the subject of future research. These include (1) the distinctiveness of mantle source regions represented by different spectral units and implications for diversity in space and time, (2) the establishment of a Moonwide basalt stratigraphy, (3) the age range of mare volcanism and its significance, (4) the relationship of mare volcanism to possible highland volcanic deposits, (5) the relationship of extrusion to intrusion and the total volume of basalt intruded in the crust, (6) the link of mare volcanism to impact basin formation, (7) the presence and role of shallow magma chambers, and (8) the nature and compositional affinities of farside mare basalts.

The extensive discussion following this talk raised many interesting points. The asymmetry in distribution of mare basalts was of concern to several attendees. It was generally agreed that this nearside/farside asymmetry was poorly understood and that it should be the subject of future research. Other discussion centered around a model for the accumulation and eruption of large magma batches. Some suggested a "staging area" in the lower crust. Head pointed out that the high effusion rates associated with the Imbrium flows are compatible with magma coming directly from the mantle. Attendees expressed interest in the thermal erosion model for lunar sinuous rille formation. Most agreed that additional studies of lunar rilles and their terrestrial analogues are needed to confirm this hypothesis. Finally, it was noted that there was a growing body of evidence that the lunar pyroclastic glasses are not compositionally related to the sampled mare basalts. This point was raised in other sessions and became one of the themes of the workshop. It is clear that additional work is needed to investigate this issue.

The results of multispectral reflectance measurements of the Mare Serenitatis/Mare Tranquillitatis shelf region were presented by R. Jaumann and co-workers. Jaumann used

a new spectral-chemical model that describes the quantitative relationships between the spectral signatures of lunar samples and the chemical composition of these samples. Jaumann maintained that the concentrations of the chemical end members  $\text{TiO}_2$ ,  $\text{FeO}$ ,  $\text{SiO}_2$ ,  $\text{Al}_2\text{O}_3$ ,  $\text{MgO}$ , and  $\text{CaO}$ , which exhibit abundances  $>1.0$  wt% in lunar soils, and the agglutinate content can be estimated with confidence by using the spectral-chemical model. It was agreed that this was an exciting technique that offered great promise for producing chemical and lithologic maps from Galileo and Earth-based multispectral imagery. However, several attendees expressed concern about the errors associated with the model, and caution was urged. It was suggested that the technique be used to search for compositional changes along the length of lunar basalt flows.

New results from high-spatial-resolution CCD imagery of the Flamsteed-P ring in southern Oceanus Procellarum were presented by J. M. Sunshine and C. M. Pieters. In lower-resolution multispectral images of the Flamsteed-P ring, the basalt appeared to be one unit with a relatively high titanium content. However, the new high-resolution CCD data indicate that the mare in this region is actually composed of at least three distinct units that differ in titanium content. Sunshine noted that continued analysis of these data will concentrate on determining whether these units represent distinct homogeneous flows or compositional variation within a single flow, which would be indicative of *in situ* differentiation. The workshop participants indicated that this was very important work. However, several attendees urged caution in the selection of the minerals used in the laboratory spectral studies that are being conducted to aid in the calibration and interpretation of the CCD images.

P. Warren presented an excellent summary of our current knowledge of lunar meteorites. He noted that while a total of 11 pieces of the Moon have been found as meteorites in Antarctica, if an adjustment is made for obvious "pairing" of samples, the number of apparently distinct Antarctic Moon rocks is reduced to 8. It was emphasized that these eight apparently distinct lunar meteorites do not necessarily represent eight separate impact sites. However, there is very strong evidence that at least two and probably several distinct impact events were involved. Warren noted that it was very curious that four of the eight lunar meteorites are composed of or dominated by mare material. This is unusual because five-sixths of the lunar surface appears to be highlands material and the maria are believed to be relatively thin in many areas. Probability theory indicates that the chances of finding four out of eight instances of predominantly mare material, through random sampling of a pop-

ulation that is one-sixth mare, is only 0.031. Warren also pointed out that unless the four dominantly mare meteorites were ejected during a single lunar impact event, it is remarkable that they are so completely dominated by VLT basalts. In addition, the minor mare components in the highlands-dominated meteorites are largely VLT basalts! The extensive discussion following this talk centered around the abundance of VLT basalts in the lunar meteorites. It was pointed out that since the first lunar samples were rich in titanium, VLT basalts were thought to be very unusual. Others mentioned that we should expect VLT magmas to be produced by partial melting of the lunar mantle.

One of the major developments in the last 15 years has been the recognition that mare volcanism is as old as 4.3 Ga. At the time of the last mare basalt workshop (1975), the prevailing view was that the onset of mare volcanism occurred at about 3.9 Ga. B. R. Hawke reviewed the large amount of evidence that has been amassed from lunar sample, geologic, and remote sensing studies that strongly indicates that mare-type volcanism commenced very early ( $>>3.9$  Ga) in lunar history. Hawke emphasized that this determination has extremely important implications for several areas of lunar science. These include (1) the composition and thermal evolution of the lunar interior, (2) the composition of the crust, (3) the global asymmetry in basalt distribution, and (4) the origin of light plains deposits. The discussion following this talk was focused on the extent of the ancient mare deposits. Questions were also raised concerning the composition of the ancient volcanic deposits.

In the past 15 years, it has become increasingly evident that lunar pyroclastic volcanism played an important role in the formation and resurfacing of portions of the Moon. C. R. Coombs presented a summary of our current understanding of lunar explosive volcanism. Geologic and remote sensing data have allowed the identification of two genetically distinct types of pyroclastic mantling deposits: regional and localized. The composition, geometry, and source vent morphology of the pyroclastic deposits have been used to infer the eruption mechanisms and emplacement styles for both localized and regional deposits.

The discussion of explosive volcanism that followed this presentation centered around the nature and origin of the volatiles associated with lunar explosive eruptions. The source of the surface-correlated volatile elements associated with lunar pyroclastic glasses was considered by most participants to be a very important issue. It was also clear that additional studies of the compositional relationships between regional dark mantle deposits and the lunar pyroclastic samples are needed.

The final talk of this session addressed the critical question of whether the Moon is dead or alive. P. H. Schultz noted that the lack of evidence for basalts younger than  $\sim 3.2$  Ga among the returned lunar samples has established the para-

digim that the Moon is dead; that is, internal processes ceased long ago. Schultz presented a summary of the evidence that mare volcanism extended beyond the nominal age indicated by the youngest mare samples (3.0–3.2 Ga). In addition, he described unusual endogenic features along features radial to Imbrium Basin that may be the sites of late-stage activity. It is clear that this is an extremely important question and that additional work is needed.

## MAGMA EVOLUTION AND SOURCE REGIONS

*Summarized by John Longhi*

Speakers in this session discussed geochemical models of mare basalt petrogenesis. The emphasis was on determining whether observed chemical variations were the products of low-pressure fractionation and assimilation or source region heterogeneity. Where fractionation and assimilation were believed to operate, the major effort was to identify the assimilant and the least contaminated parent; where source regional heterogeneity was believed to control chemical variation, the major effort was put into determining the proportions of cumulus minerals, trapped liquid, and KREEP from the hypothetical lunar magma ocean.

C. Neal reviewed chemical evidence for distinguishing at least 18 distinct magma compositions. If one allows crystallization ages as an additional criteria, then four more magmas can be separated from the continuum in composition among the Apollo 14 aluminous basalts. T. Dickinson proposed a process of replenishment/fractional crystallization to explain how the Apollo 14 basalts with different ages might lie on the same fractionation trend. C. Shearer used trace-element data obtained from picritic volcanic glasses with the ion-microprobe to demonstrate that in only one or two cases are mare basalts permissible differentiates of the 24 known picritic magmas. The connection or lack thereof between mare basalts and the picritic magmas remains one of the important unanswered questions in lunar science.

J. Shervais introduced the concept of a mare basalt source region produced by mechanical mixing of dense, high-level, late-stage cumulates and liquids with underlying, less dense, earlier cumulates of the magma ocean. He based this concept on strong correlations of mare basalt compositions in various two-element plots with two distinct continua extending from primitive mare compositions and converging at KREEP. However, several members of the audience objected on the basis that the correlations included evolved as well as primitive compositions and, therefore, it was not possible to distinguish KREEP in the source from assimilated KREEP.

S. Vetter discussed a series of models relating the Apollo 15 olivine- and quartz-normative basalt (ONB and QNB) suites by dynamic melting of a common source. In these models the source, a combination of cumulate minerals and trapped liquid, partially melts to produce a magma parental

to the QNBs, but the magma is only partially drained from the source region. Remelting of the source produces the ONB parent magma. G. Snyder presented model calculations that began with the formation of a series of cumulates during fractional crystallization of the lunar magma ocean and proceeded to remelting of the cumulates plus trapped liquid and entrained plagioclase to produce parent magmas of the high-Ti basalts. The trapped liquid component in his model is the key to producing sufficiently high concentrations of REE and sufficiently strong Eu anomalies. Some members of the audience objected to the details of the calculations, which included the onset of ilmenite crystallization when  $\text{TiO}_2$  concentration in the magma ocean reached only 2 wt% and an increase in Mg/Fe in the liquid following ilmenite crystallization. Indeed, the entire concept of a simply stratified LMO is questionable based on density/viscosity considerations.

There was a brief discussion of G. McKay's abstract, which dealt with the need for plagioclase fractionation to produce the observed Eu-anomalies in mare basalts. His calculations showed that models involving simple remelting of cumulates required prior separation of plagioclase from the magma that produced the cumulates in order to produce the necessary enrichments in REE and slopes of the pattern. However, it is also possible to produce the REE patterns of the mare basalts by melting mixtures of primitive cumulates (no plagioclase fractionation) and KREEP. J. Papike reiterated the general principle that melting of clinopyroxene cumulates from plagioclase-undepleted magmas can produce melts with substantial negative Eu-anomalies.

J. Jones presented a novel model that relates Apollo 15 green glass to those of the high-Ti picritic glasses by assimilation of armalcolite coupled with fractional crystallization. One obstacle for this model, however, is the origin of the armalcolite: most evidence points to ilmenite, not armalcolite, crystallizing from the late stages of the magma ocean.

If one theme emerged from this session, it is that there still does not seem to be a unique explanation for the trace-element compositions of the mare basalts; much work still needs to be done in drawing distinctions between sources composed of cumulates and trapped liquid from those formed by mechanical mixtures of early- and late-stage magma ocean components.

## MAGMA SOURCES AND ASCENT PROCESSES

*Summarized by Michael J. Drake*

This session included four presentations and was focused on the question of the physical environment within which mare basalt genesis occurred. Of particular interest was the convective state of the Moon following the termination of the global "magma ocean" epoch and the reorganization of cumulates produced during that period to gravitationally

more stable configurations. The felicity with which the so-called pristine mare glasses record processes and conditions at depths of several hundred kilometers within the Moon was also discussed. In a nutshell, how can basalts get from as deep as 500 km to the surface without interacting with their "plumbing system," a requirement if they are to carry information about the lunar interior that can be interpreted unambiguously.

F. Spera opened the session with a discussion of the fluid dynamics of the Moon during and in the few hundred million years following the magma ocean epoch. He reviewed evidence that the magma ocean had characteristics more akin to a dusty atmosphere than to the viscous ooze we more generally associate with magmas. The balance of convective vs. resistive forces (the Rayleigh number) involves the term  $D^3$  in the numerator, where  $D$  = depth of the magma ocean. This cube dependency of depth scale strongly favors the convective forces, and leads to most of the magma ocean being in a turbulent convective regime. This turbulent region declines in volume with loss of heat through the passage of time. During the turbulent phase of most of the ocean, crystal fractionation may be impeded, but eventually a cumulate pile will be built up characterized by more Fe-rich (and hence, denser) mafic phases at progressively shallower depths.

Although this gravitational instability is unlikely to persist in reality until complete solidification, it is useful to consider the solid-state reorganization of such a gravitationally unstable mass after solidification. Spera did so by means of numerical experiment, and showed that the denser overlying cumulates would overturn on a timescale of a few million years, and that rising and descending plumes of mantle material would continue in convective motion for several hundred million years. Hess reached similar conclusions on the basis of an analytical approach to deducing timescales of processes. It seems probable that the physical environment for mare basalt genesis was the isentropic melting of rising mantle plumes. Because the solid-state redistribution of the cumulates results in complex mixing, a variety of magma types might be expected to be produced from similar depths in the Moon.

Spera and Hess also considered the physical requirements for pristine magmas to erupt virtually unchanged after transiting 500 km of the lunar mantle. The exact mechanism of extraction of magma from the crystalline matrix is uncertain. Leading candidate mechanisms are percolation theory, in which the matrix is regarded as a deformable porous matrix, and the vein theory, in which melt accumulates in veins and drains rapidly from the source region once three-dimensional connectivity is established. In order to extract unfractionated magmas from such depths, the product  $h^2u$  ( $h$  = fissure width,  $u$  = magma velocity) must exceed about  $10^4$  in MKS units. This constraint implies

fissure widths on the order of tens of meters and magma velocities on the order of meters per second are required to avoid "heat death."

J. Longhi continued this discussion by considering the ability of dynamical melting of convecting mantle to produce the pristine mare basalt glasses. He considered two possibilities. In one case, melting began at depth and proceeded in steps of progressively decreasing pressure while the source composition remains constant due to continuous replenishment from below, with the melt being accumulated at an arbitrary shallow depth. The second case involved fractional fusion, with complete extraction of the melt and no replenishment from below. He showed that melting processes at 500 km or below approaching the idealized fractional fusion could produce many of the major-element properties of the pristine mare basalt glasses. An implication of Longhi's calculations is that the Moon may be more refractory-rich (e.g., 40 ppm U) than is generally assumed.

Finally, M. Manga and J. Arkani-Hamed discussed remelting mechanisms for shallow source regions of mare basalts. They considered a radioactive heating model and a thermal insulation model. In the former, remelting is due to lateral variations in heat source distribution resulting from the earlier magma ocean event. In the latter, remelting is due to increased insulation resulting from the deposition of ejecta blankets in basin-forming impact events. Heat transfer is by conduction in both cases. The radioactive heating mechanism could be responsible for prebasin mare basalts, but not later mare basalts because the heat-producing elements would be extracted from the mantle into the basalts. The thermal blanketing mechanism could explain the delay between impact and volcanism observed for some mare basalt-filled basins, but could not account for earlier basalts. However, there is no clear evidence that remelting at shallow depths is required to account for mare basaltic volcanism.

The conclusions drawn from this session are that significant progress in understanding mare basaltic volcanism is likely to involve thoughtful integration of models for the physical environment of melting with more traditional phase equilibrium and geochemical considerations. It remains problematical whether magmas can be extracted from depths of many hundreds of kilometers in the Moon and arrive at the surface without undergoing chemical modification due to assimilating of wall rock from the "plumbing system" and partial or complete "heat death" due to crystallization during ascent.

## TIMING OF IGNEOUS ACTIVITY ON THE MOON

*Summarized by E. Julius Dasch*

Absolute dating of lunar magmatism and volcanism has recently produced new insights on the origin and development of the Moon and its major features. Such renewed interest and understanding result from a greatly enhanced

sensitivity and precision in the measurement of isotopic ratios, especially from very small samples, owing to improved mass spectrometric instrumentation and chemical techniques; development of new parent-daughter systems, with the resulting clarity provided by these chronologic and isotope composition studies; and new theories of lunar origin and petrogenesis that the chronologic and isotopic composition data can help to constrain. Fifteen years after the Apollo era, the excitement of the Moon remains, with many significant problems to be addressed. Experiments will continue to be performed with existing Apollo samples (and lunar meteorites), though we keenly await the more widely distributed and more geologically oriented materials that will result from the Space Exploration Initiative and excursions from a lunar base.

Productive avenues for the continued study of lunar chronology may be summarized as follows:

**1. Better definition of the beginning and end of lunar igneous activity.** Additional dating of ferroan anorthosites will help to constrain the timing of formation of the earliest lunar crust and further test the concept of a global lunar magma ocean. Whether or not isotopic "freezing-in" dates differ significantly from each other and from emplacement (geologic) ages has not been established unequivocally. Precise chronologic relations between the Mg suite of rocks and the ferroan anorthosites have yet to be fixed; these data are integral to an understanding of early lunar petrogenesis. Perhaps a "super pristine" category for lunar magmatic samples should be established. In addition to the several constraints devised for "pristine" samples, these rocks additionally would be limited to those samples that showed no significant degree of isotopic irregularity.

Additional analyses of Apollo 14 highland volcanic rocks, recently found to be the most ancient from the Moon, should be performed; though there are several precise dates in the range from 4.0–4.3 Ga, the data are sparse and some samples exhibit large analytical uncertainty.

Although significant volcanism younger than about 3.2 Ga may not have occurred on the Moon, photogeologic and remote sensing studies suggest that much younger (less than 2.6 Ga, perhaps even less than 1.0 Ga) volcanic rocks occur, awaiting sampling and analysis. Aside from a return sampling mission, the best hopes of determining younger volcanic events rest with continued analysis of existing Apollo collections (for example, A12) or a fortunate lunar meteorite find.

**2. Chronologic and chemical testing of the giant impact hypothesis for Moon's origin.** A Mars-sized impact into early Earth and the accretion of the Moon from the resulting orbiting debris, sometime near 4.5 Ga, may be discernable from isotopic study of lunar rocks and perhaps from models of terrestrial processes. Samarium-neodymium and Nd isotopic composition studies of chondritic meteorites

and the earliest lunar magmatic rocks suggest that constraints on the giant impact theory may be established. Less quantitatively, Pb isotopic modeling of early Earth has suggested to some workers that a significant "event" may have occurred near 4.5 Ga.

**3. Better chronologic definition of the lunar "cataclysmic event."** Although many believe that early lunar bombardment reached cataclysmic intensity near 3.8–4.0 Ga, evidence for such an event is not well demarked. Additional, careful dating of glasses from major impact structures, especially by the  $^{39}\text{Ar}$ - $^{40}\text{Ar}$  dating technique, should provide the required database for further testing of this theory. Like the other studies described herein, geologic mapping and collecting from a lunar base will provide the definitive dataset for this test.

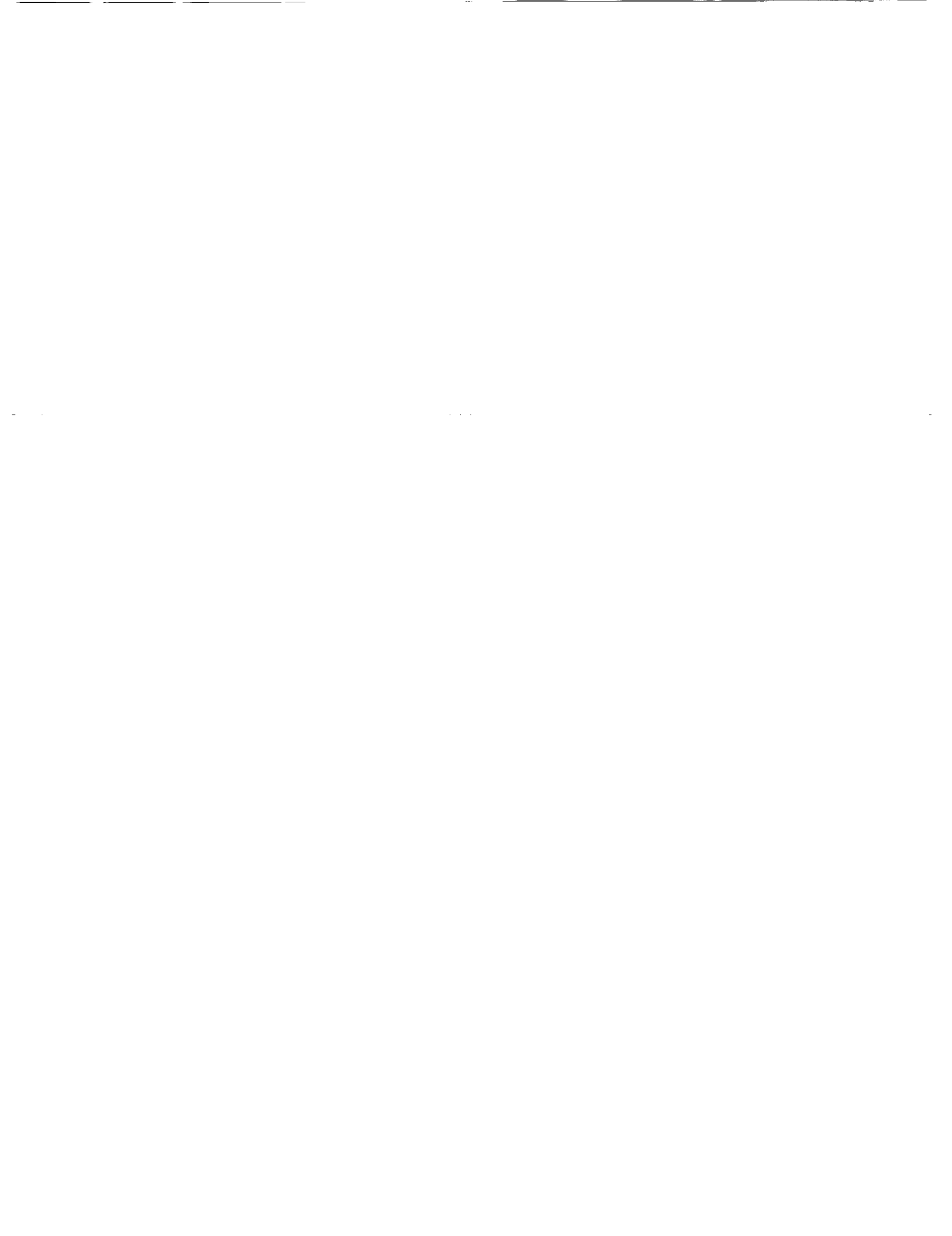
**4. Age and isotopic composition studies of pristine lunar volcanic glasses.** Physically and chemically defined sets of volcanic spherules of glass are thought to represent samples of the least "contaminated" of lunar volcanic materials. Thus, age and isotopic tracer studies of these unique samples should aid significantly in a better understanding of lunar petrogenesis. Though they represent a difficult analytical task, owing to their small size, recent advances in chemical and mass spectrometric techniques present an opportunity for extending these important experiments.

**5. Isotopic tracer studies of various lunar processes.** Continuing advances in analytical techniques, development of new isotopic systems for study, and developing theories in lunar petrogenesis have opened up promising avenues

of study of selected petrogenetic theories. For example, do the ancient A14 volcanic rocks represent partial melts from a simple, whole-Moon-type reservoir, or, did assimilation and perhaps other processes affect their composition? Are ancient mare basalts related to some of the members of the Mg suite of lunar rocks?

Continued additions to and refinement of the initial isotopic composition of lunar rock suites should help to determine better the relation of age, composition, and geologic setting. Such an improved dataset will help in establishing the relative importance of provenance composition, partial melting, magma mixing, assimilation, and crystal settling in establishing the composition of lunar rocks.

**6. Better comparison of the results from the several dating techniques.** Additional work is required for a more definitive comparison of the results of isotopic analysis of the several parent-daughter techniques. Differences in the measured time of formation of the same carefully chosen and analyzed sample, for example, commonly are only partly explainable. A variety of possible mechanisms (varying certainties in the decay rates of the several radioactive nuclides, varying analytical uncertainties in measurement, and varying diffusion rates of parent and daughter nuclides, primarily as a function of temperature), all may contribute to this problem. A better understanding of these variations will improve especially our understanding of the earliest lunar igneous activity that resulted in the ferroan anorthosites and the Mg suite of rocks.



# ABSTRACTS



N 9 2 - 1 0 9 6 2

9

**THE VIOLENT SIDE OF MARE VOLCANISM** C.R. Coombs, D. S. McKay,  
SN2, NASA, Johnson Space Center, Houston, TX 77058; B.R. Hawke, Planetary Geosciences  
Division, Hawaii Institute of Geophysics, 2525 Correa Road, Honolulu, HI, 96822.

### Introduction

In the past fifteen years it has become increasingly evident that lunar pyroclastic volcanism played an important role in the formation and resurfacing of portions of the Moon. Located on mare/highland boundaries, many of these deposits formed in association with mare volcanism. Based on recently acquired geologic and remote sensing data two genetically distinct types of pyroclastic mantling deposits have been identified: regional and localized. Both the regional dark mantling deposits (RDMD) and localized dark mantling deposits (LDMD) are widely distributed across the lunar nearside (Figs. 1 and 2). The larger RDMD are typically located in lunar highland areas adjacent to many of the major lunar maria, while the smaller LDMD are found on the floors of pre-Imbrian and Imbrian craters. Both deposits are basaltic in composition and are presumed to have originated at great depth (~300 km). The composition, geometry, and source vent morphology of the pyroclastic deposits have been used to infer the eruption mechanisms and emplacement styles for both types of deposits.

### Lunar Dark Mantle Deposits

**Regional** These extensive deposits cover tens of thousands of km<sup>2</sup>. Characteristically, the RDMD have low albedoes (0.079-0.096) and are relatively fine textured with a smooth, velvety appearance. These mantling deposits formed as products of strombolian-type (continuous) fire-fountaining in association with basaltic eruptions.<sup>(e.g.,1,2,3)</sup> Irregular depressions at the head of associated sinuous rilles are the probable source vents for these deposits.<sup>4</sup>

While all of the RDMD are basaltic in nature, returned sample and telescopic remote sensing data indicate that several of the RDMD contain a significant amount of Fe<sup>2+</sup>-bearing glass. Volcanic green, orange and black glass spherules returned by the Apollo 15 and 17 missions are believed to be relatively unfractionated samples of the deep lunar interior. These glasses are thought to have originated from a depth of approximately 300 km or greater.<sup>1</sup> Volatile-rich coatings on the surfaces of these spherules strongly suggest the existence of a gaseous phase in their source magmas. The fire-fountain origin of the volatile-coated pyroclastic glasses stands in striking contrast to the massive outpouring of the low-viscosity, volatile-depleted magma which formed the lunar maria. It has been suggested that the RDMD eruptions are analogous to terrestrial strombolian-type eruption activity and, as such, are likely to disperse and sort the pyroclasts over thousands of 1000's km<sup>2(5)</sup>. In these deposits the coarser material is concentrated in a zone peripheral to the vent while the finer debris is scattered over much greater distances.

**Localized** Localized dark mantling deposits (LDMD) are characterized as small, low albedo pyroclastic units. These deposits are generally associated with small (<3 km) endogenic dark halo craters. Typically, the LDMD are smooth, relatively block free deposits surrounding vents aligned along crater floor fractures or rilles. The endogenic source craters for the LDMD may be distinguished from the other exogenic or impact craters in that they lack obvious crater rays and are generally non-circular in shape.<sup>5</sup>

An eruption mechanism similar to terrestrial vulcanian eruptions is suggested to be the origin for these deposits.<sup>5</sup> In a vulcanian-style eruption, the accumulation of gas in a capped magma chamber leads to explosive decompression, and the subsequent emplacement of a "small" (<80 km<sup>2</sup>) pyroclastic deposit around an endogenic source crater. For these types of eruptions on the Moon, the maximum dispersion range of pyroclasts larger than 1 cm is about 4 km, while the smaller clasts may be ejected up to tens of kms. Magma source depths for these deposits are thought to be relatively deep also although material from different levels in the conduit is often entrained in the body of magma erupted.

Recent near-infrared and infrared reflectance data<sup>6,7</sup> of various LDMD has shown that although they may be genetically and morphologically similar, they are spectrally, and thus compositionally, distinct. Three types or classes of LDMD have been identified thus far based on the depth, center and overall shape of the ~1 μm band. Group 1 contains highland-type

material with minor amounts of olivine and/or volcanic glass. Group 2 spectra resemble mature mare basalts and Group 3 have olivine and pyroxene as the dominant mafic constituent.

### Lunar Volcanic Constraints

Lunar basaltic eruptions differ from their terrestrial counterparts in that the tremendous volumes of magmas originated at great depths and were relatively dense compared to the upper lunar crust. Effectively, this contrast is similar to the actual density contrast that drives terrestrial basaltic eruptions.<sup>e.g.,5</sup> Contrary to terrestrial eruptions however, the main volatile released during lunar eruptions is CO.<sup>8</sup> Because a gas decompresses to the near-zero ambient lunar atmospheric pressure and undergoes both vertical and horizontal expansion as they rise, a gas such as CO would provide much more efficient eruptive energy on the Moon than under comparable terrestrial conditions. On both the Earth and Moon gas exsolution and bubble coalescence commonly occur at depths of less than 2 km. Also, similar to the Earth, bubble coalescence on the Moon will occur in near surface magmas if the rate of ascent is sufficiently slow or the viscosity and yield strength are sufficiently small (<.5-1 m/s), otherwise relatively steady fire-fountaining will occur.

### How long did lunar pyroclastic eruptions last?

It is difficult to constrain the actual eruption time frame for the pyroclastic deposits. They could have occurred at any one location as one single event, or in numerous cycles of slow intrusion, surface cooling, gas build-up and explosion. Based on their size, it is thought that the RDMD were emplaced over a longer period of time than the LDMD and probably did not occur all at once. Fire-fountaining may have occurred concurrent with the outpouring of lava, at intervals, or just near the end of the eruption. For example, the Aristarchus RDMD was formed by activity at Cobra Head and several other similar vents, and at least part of it was emplaced following the eruption of the "red" mare material.<sup>9</sup> On a smaller scale, theoretical modelling of the eruption that formed Rima Mozart and the LDMD associated with it indicate that approximately 6400 km<sup>3</sup> of lava was erupted over a period of 950 days at a rate of 8 x 10<sup>4</sup> m<sup>3</sup>s<sup>-1</sup>, and approximately 10 km<sup>3</sup> of pyroclastic material was deposited about the two source vents. The return and analysis of more samples from the different pyroclastic mantling units will help constrain these ages and further define the nature of these deposits.

### References

- (1) Heiken G.H. et al. (1974) *Geochm. Cosmo. Acta*, 38, 1703-1718. (2) Howard K.A. et al. (1973) NASA SP-330, pp. 29-1 to 29-12. (3) Head J.W. (1974) *PLPSC 5th*, pp. 207-222. (4) Gaddis L.R. et al. (1985) *Icarus*, 61, 461-489. (5) Wilson L. and Head J.W. (1981) *JGR*, 78, 2971-3000. (6) Coombs C.R. and Hawke B.R. (1989) *Proc. Kagoshima Int'l Conf. on Volc.*, 416-419. (7) Hawke B.R. et al. (1989) *PLPSC 19th*, 255-268. (8) Housley R.M. (1978) *PLPSC 9th*, 1473-1484. (9) Whitford-Stark J..L. (1977) *PLSC 8th*, 2705-2724. (10) Coombs C.R. et al. (1987) *PLPSC 18th*, 339-353.



Figure 1: Locations of major RDMD.



Figure 2: Locations of major LDMD.

**FORMATION OF APOLLO 14 ALUMINOUS MARE BASALTS BY REPLENISHMENT FRACTIONAL CRYSTALLIZATION and ASSIMILATION OF PRECURSOR CRUST;** Tammy L. Dickinson<sup>1</sup> and Dennis O. Nelson<sup>2</sup>, (1) SN2 NASA Johnson Space Center, Houston, TX. 77058, (2) Drinking Water Section, Health Division, PO Box 231, Portland, OR. 97207.

Apollo 14 aluminous mare basalts (AMB) have been the subject of considerable controversy (1-7). These basalts were divided into 5 distinct groups on the basis of RE and HFS element abundances (1,2). The groups are similar in major element compositions, but display an 8-fold variation in REE abundances. (1) and (2) concluded that varying degrees of partial melting of a single source could not produce the observed compositional range of these basalts. They suggested an evolution dominated by assimilation of a KREEPy component. The acquisition of more data has indicated a continuum in AMB compositions rather than distinct groups (3-7). These authors have modeled the AMB by the combined processes of fractional crystallization and assimilation (AFC) of a KREEPy component.

Sr isotopic ages and initial ratios have been determined for several Apollo 14 AMB (8,9). On a plot of age vs. initial Sr ratio, 3 distinct eruption events are indicated: 4.3 (Group 5), 4.1 (Group 1 & 2) and 3.95 GA (Group 3). No data have been obtained for Group 4 basalts. (6) suggested that Group 5 magmas, the most primitive, were produced at several different times during this interval and subsequently followed the same AFC path to yield the more evolved compositions. The Apollo 14 AMB lie on a single radiogenic growth curve for source regions having time-averaged Rb/Sr=0.021 evolving from a primitive initial of LUNI at 4.56 GA ago (10). The magmas display, however, a range of incompatible trace element ratios. Further, the major element models of (7) can't produce the trace element variation within the F values indicated by the major elements (ie the major and trace elements are decoupled).

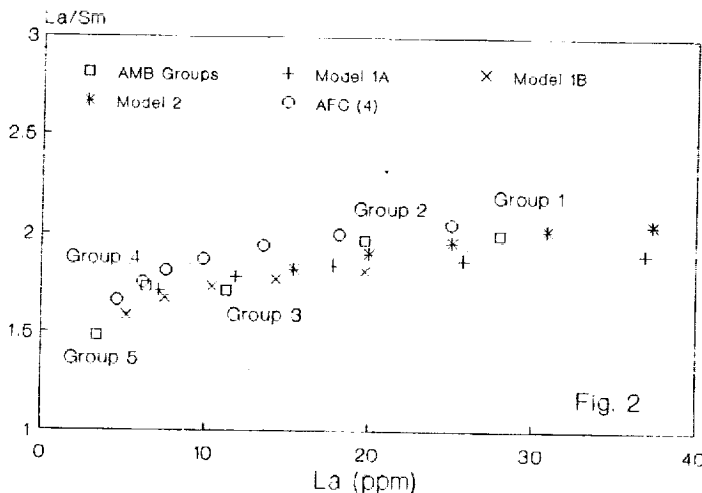
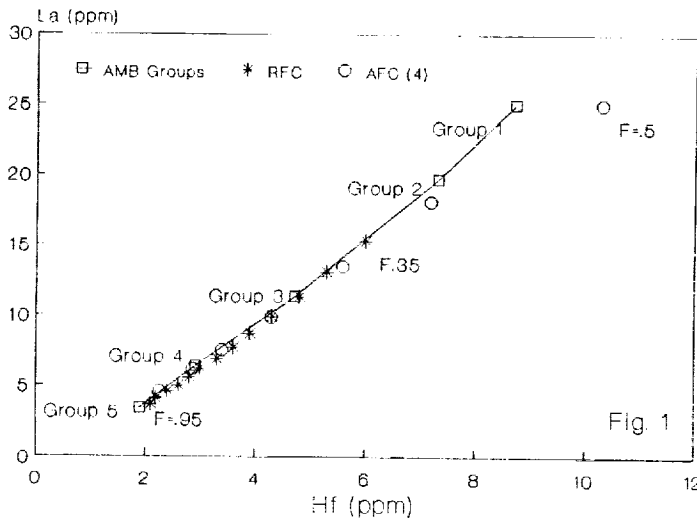
We have explored open-system processes common on earth (11): (A) combined replenishment-fractional crystallization (RFC) and (B) assimilation-fractional crystallization (AFC), where the assimilant is a partial melt of precursor crust. RFC often produces decoupled major and trace element variations (12), while AFC can produce significant variation in incompatible trace element ratios (4). We envision a model by which magmas of Group 5 composition were emplaced in shallow chambers. Given the suggestion that this Group was periodically erupted (6), it is possible that these chambers were within previously emplaced mare basalt flows. Periodic pulses of new magma into the chamber during crystallization lead to RFC: contemporaneous partial melting of the basaltic crust and subsequent incorporation of this melt by the crystallizing magma lead to AFC. The trajectory of AFC is influenced by (A) the composition of the assimilant, itself a function of source rock composition and degree of melting, (B) mass assimilated/mass of cumulate (Ma/Mc), a function of temperature of the crust, and (C) Kd values. Obviously, a wide range of variables are possible. We wish to demonstrate that a geologically reasonable set of

RFC/AFC conditions could produce variations in trace element content and ratios similar to those observed in the Apollo 14 magmas. An advantage to this model is that no preexisting evolved crustal reservoir (ie KREEP) is necessary to account for the contaminant. Experimental (13) and field (14) evidence suggest that partial melt of basaltic rocks yield tonalitic compositions. If equilibrium is reached, the liquid will be enriched in incompatible trace elements.

We have modeled the Apollo 14 AMB by RFC using a parental magma of Group 5 composition with the fractionating assemblage consisting of 60% Px, 30% Plag, and 3% Il (after 4). Groups 3 and 4 can be produced with  $F = 0.95-0.35$  and  $Mr/Mc = .5$  (Fig. 1). Even though RFC can produce the observed variations in incompatible trace element abundances, it can't produce the observed variations in incompatible element ratios. Thus, some assimilation appears to be needed to explain the Apollo 14 AMB.

Fig. 2 illustrates that for La vs La/Sm, an original Group 5 basalt can evolve to Group 3 with  $Ma/Mc = 0.5$  (Model 1A) or 0.3 (Model 1B) and the assimilant being a 25% partial melt of Group 3, or to Group 1 with  $Ma/Mc = 0.5$  (Model 2) and 25% partial melt of Group 1 as the assimilant. As seen in Fig. 2, our models give results similar to those of (3-7).

We do not believe that the age data necessarily reflect the production sequence. Just as (6) suggest that Group 5 was episodically produced, we suggest that the other groups may evolve episodically by RFC and AFC. Additional isotopic work is needed to further constrain the petrogenesis of the Apollo 14 AMB.



REFERENCES (1) Dickinson et al. (1985) PLPSC 15, C365-C374. (2) Shervais et al. (1985) PLPSC 15, C375-C395. (3) Neal et al. (1987) LPSC XVIII, 706-707. (4) Neal et al. (1988) PLPSC 18, 139-153. (5) Neal and Taylor (1989) LPSC XX, 768-769. (6) Neal and Taylor (1990) PLPSC 20, 101-108. (7) Neal et al. (1989) PLPSC 19, 147-161. (8) Papanastassiou and Wasserburg (1971) EPSL 12, 36-48. (9) Dasch et al. (1987) GCA 51, 3241-3254. (10) Shi and Nyquist (1989) LPSC XX, 1002-1003. (11) O'Hara and Matthews (1981) JGSL 138, 237-278. (12) Nelson et al. (1990) CJES. (13) Beard and Lofgren (1989) Science 244, 195-197. (14) Nelson et al. (1990) LPSC XXI, 867-868.

**ANCIENT MARE VOLCANISM.** B. Ray Hawke, Paul G. Lucey, and Jeffrey F. Bell, Planetary Geosciences Division, University of Hawaii, Honolulu, HI 96822; Paul D. Spudis, U.S. Geological Survey, Flagstaff, AZ 86001

**INTRODUCTION:** One of the major developments in the last fifteen years has been the recognition that mare volcanism is as old as 4.3 Ga. At the time of the last mare basalt workshop (1975), the prevailing view was that the onset of mare volcanism occurred at about 3.9 Ga.<sup>1</sup> Since that time, a large amount of evidence has been amassed from lunar sample, geologic, and remote sensing studies that strongly indicates that mare-type volcanism commenced very early (>3.9 Ga) in lunar history. e.g.,<sup>2,3,4,5,6,7,8,9</sup> This determination has extremely important implications for several areas of lunar science. These include: 1) the composition and thermal evolution of the lunar interior, 2) the composition of the crust, 3) the global asymmetry in basalt distribution, and 4) the origin of light plains deposits. The purposes of this paper are to summarize the results of previous geologic and remote sensing investigations of ancient mare basalts and to present the preliminary results of new studies of key areas.

**REVIEW OF PREVIOUS INVESTIGATIONS:** In the post-Apollo era, Ryder and Taylor<sup>2</sup> were the first to present arguments that mare-type volcanism was initiated far earlier than 3.9 Ga and cited evidence provided by rare mare-type basaltic lithic and mineral fragments in highland breccias. Hawke and Head<sup>10</sup> concluded that high-alumina mare basalts were emplaced in the Fra Mauro region prior to the Imbrium impact event.

Schultz and Spudis<sup>3,11</sup> studied the nature, origin, and distribution of dark-haloed impact craters and concluded that most are due to excavation of dark mare basalt from beneath a surface layer of light highlands material. They suggested that the onset of basaltic volcanism pre-dated the last major basin-forming impacts, that early farside volcanism may have been widespread, and that some lunar "light plains" are early volcanic deposits which were subsequently buried by varying thicknesses of impact ejecta. The apparent concentration of dark-haloed impact craters in particular regions and the presence of mafic anomalies in the Apollo orbital geochemistry data sets obtained for many of these regions<sup>3,8,9</sup> support this interpretation.

Interest in the possibility of ancient mare volcanism (> 3.8 Ga) greatly increased in 1983 with the discovery of mare-like basalt fragments in an Apollo 14 breccia (14305), one of which has been conclusively dated at  $4.23 \pm 0.05$  Ga.<sup>6,7</sup> Taylor and co-workers<sup>6</sup> suggested that mare-type volcanism commenced at least as early as 4.2 Ga in the Fra Mauro region and probably across much of the lunar surface.

In light of the above findings, Bell and Hawke<sup>4,12</sup> conducted a detailed remote sensing analysis of lunar dark-haloed impact craters. Near-infrared reflectance spectra were obtained for numerous exogenic dark-haloed craters located on either the ejecta blankets of large craters or Imbrian and Nectarian age light plains deposits. Spectral, thermal, radar, and photogeologic data conclusively demonstrated that dark-haloed craters on the ejecta blankets of Copernicus and other large impact structures excavated mare basalts from beneath lighter surface deposits rich in highlands material. Analyses of near-infrared reflectance spectra obtained for dark-haloed craters on light plains indicate that in every instance these craters exposed mare basalt which had previously been covered by varying thicknesses of highlands debris. Bell and Hawke<sup>4</sup> concluded mare volcanism was a significant process during much of the pre-Imbrian and may have been initiated as early as 4.2 - 4.3 Ga.

**RESULTS OF CURRENT STUDIES:** In order to better understand ancient mare volcanism, we are conducting additional remote sensing and geologic studies of selected areas on the lunar surface. In this section, we present the preliminary results of this effort.

1. Terrain Northwest of Humorum Basin: A portion of the highlands terrain northwest of Humorum basin exhibits anomalous characteristics in several remote sensing data sets. Gaddis *et al.*<sup>12</sup> first noted the unusual nature of this highlands terrain. They pointed out that an area (45,000 km<sup>2</sup>) west of Gassendi crater exhibited relatively low depolarized 3.8-cm radar returns in the radar images presented by Zisk *et al.*<sup>13</sup> This area, which is centered at 43° W, 15° S, also exhibits unusually low values in 70-cm radar images.

ANCIENT MARE VOLCANISM: Hawke, B.R. et al.

Lucey and co-workers<sup>14</sup> have recently presented the results of imaging spectroscopy of the Humorum basin region. They identified a spectral unit in the highlands northwest of Humorum which appeared to represent a mixture of highlands debris with lesser amounts of mare material. An episode of mare volcanism may have emplaced basaltic units in this region after the formation of the Humorum basin. Subsequently, large impacts in the vicinity, such as those which formed Gassendi, Letronne, and Mersenius craters, emplaced a veneer of highlands debris atop the basalt flows. The mare material could have been mixed with highlands debris either by "local mixing" during ejecta emplacement or by vertical mixing due to small impact craters in the area. Other interpretations are possible, and additional spectral studies will be required to confirm the existence of buried mare basalts in this region.

2. Schiller - Schickard Region: Based on their study of dark-haloed impact craters, Bell and Hawke<sup>4,5</sup> concluded that pre-Oriente mare volcanism not only occurred but also was pervasive in the Schiller-Schickard region. They suggested that the resulting mare deposits were extensive but discontinuous with numerous crater rims and other topographically high areas rising above the basalt surface.

The preliminary results of our remote sensing and geologic studies of this region are consistent with those of previous workers.<sup>3,4,5,11</sup> However the geology of this region is extremely complex. It exhibits anomalies in the radar, thermal, and multispectral data sets. This is at least in part due to the presence of previously unrecognized post-Oriente mare basalt deposits in the area southwest of Schiller crater.

3. Byrgius Region: Pre-Oriente mare volcanism may have occurred in the region south of Byrgius crater. Lagrange C is an Imbrian-aged crater (D=23 km, 65° W, 30° S) located south of Byrgius on the Oriente ejecta deposit. Much of the ejecta and wall of Lagrange C exhibits a very low albedo. While the low albedo of these features may be due to post-Oriente pyroclastic volcanism, it is also possible that these dark deposits were created by the excavation of mare material from beneath Oriente ejecta. The question will be resolved by the analysis of spectra obtained in August, 1990.

REFERENCES: 1) S.R.Taylor (1975) Lunar Science: A Post-Apollo View. 2) G.Ryder and G.J.Taylor (1976) PLSC 7, 1741. 3) P. Schultz and P.Spudis (1979) PLPSC 10, 2899. 4) J.Bell and B.Hawke (1984) JGR 89, 6899. 5) B.Hawke and J.Bell (1981) PLPSC 12, 665. 6) L.Taylor et al. (1983) LPS XIV, 777. 7) J. Shervais et al. (1983) JGR 88, B177. 8) B.Hawke and P.Spudis (1980) PCLHC 9, 467. 9) B.Hawke et al. (1985) EMP 32, 257. 10) B.Hawke and J. Head (1978) PLPSC 9, 3285. 11) P.Schultz and P.Spudis (1983) Nature 302, 233. 12) L.Gaddis et al. (1985) Icarus 61, 461. 13) S.Zisk et al. (1974) Moon 10, 17. 14) P.Lucey et al. (1990) PLPSC 21, submitted.

GEOLOGICAL SETTING AND MORPHOLOGY OF MARE VOLCANIC DEPOSITS: IMPLICATIONS FOR CHRONOLOGY, PETROGENESIS, AND ERUPTION CONDITIONS; James W. Head, Dept. of Geological Sci., Brown University, Providence, RI 02912

Developments in the last 15 years are highlighted by: 1) documentation of the distribution and stratigraphy of mare units, 2) a more thorough understanding of the principles of ascent and eruption of lunar magmas, 3) increased knowledge of the implications of volcanic landform and deposit morphology for eruption conditions, and 4) convergence of sample analysis research on problems linked to processes of ascent and eruption of magma.

**General Setting, Stratigraphy, and Timing:** Fifteen years ago it was known that the total area of exposed mare deposits is about  $6.3 \times 10^6 \text{ km}^2$ , that there is a major nearside-farside heterogeneity in distribution, that they cover only about 17% of the total surface area of the Moon, that on the basis of stratigraphic evidence the total volume of surface mare deposits is about  $1 \times 10^7 \text{ km}^3$ , and that this volume corresponds to less than 1% of the total volume of the lunar crust<sup>1,2</sup>. At this point and in subsequent studies it was also known from remote sensing data<sup>3</sup> that mare deposits were heterogeneous in composition and there was evidence for systematic variations of basalt types in space and time<sup>2,4</sup>. Mare deposits occur preferentially in topographic lows (basins and craters), and have a variety of modes of occurrence and styles of emplacement<sup>5</sup>. Studies of mare stratigraphy in individual basins began to provide evidence for sequence and modes of emplacement<sup>6,7,8</sup>, and the location of sources for various mare units, with evidence accumulating for high-volume early fill of basin interiors, and low-volume late flow units often from sources along the basin edges<sup>9</sup>. Insight into limb and farside compositions was provided by Apollo orbital geochemical data<sup>10</sup>. Additional geological evidence expanded the likely range of ages of mare units on the Moon to both earlier<sup>11</sup> and later times, with the latest activity in Procellarum of possible Copernican age. These latest deposits notwithstanding, lunar mare volcanism has apparently not been a volumetrically significant process since around the late Archean. Important syntheses of the lunar mare studies were published in 1981<sup>12</sup> and 1987<sup>13</sup> and references to a range of significant studies are found therein.

**Morphology, Style, and Eruption Conditions:** The basic physical principles of lunar basaltic magma ascent and eruption<sup>14</sup> permit a better understanding of the implications of mare landforms and deposits for the range of eruption conditions. In general, the differences between lunar and terrestrial magma rheologies should not lead to significant differences in effusion rates and flow lengths. Rather, the really extensive flow deposits and locally great flow lengths imply relatively greater fissure widths on the Moon (<10 m) than the Earth; these fissures may be linked to crustal fractures associated with impact craters and basins. The location, morphology, and lengths of sinuous rilles suggests that they represent thermal erosion caused by turbulent flow in lava flows of very high effusion rate<sup>15,16</sup>; thermal erosion of highland and mare material will contaminate lavas, but the volume is likely to be less than a few percent of the total flow volume<sup>17</sup>. A variety of volcanic sources and associated edifices are observed<sup>13</sup>. However, large shield volcanoes comparable to Hawaii in lateral or vertical scale, and built up of many flows whose lengths average less than the volcano radius, are noticeably lacking. This, combined with evidence for large volume, high effusion rate flows, implies that the source for some lavas was deep and that ascent and extrusion was rapid; such magma bodies are unlikely to produce shallow magma chambers. In addition, caldera-like craters are not common in and adjacent to the maria, which may mean that magma chambers are rare or deep. An understanding of the role of volatile exsolution in lunar magmas<sup>14</sup> has provided insight into a

range of features and deposits. Magmas containing even very small amounts of volatiles will undergo near-surface exsolution and the marked decompression and vertical and horizontal gas expansion guarantees that pyroclasts are spread away from the eruption site to produce deposits of pyroclastic beads<sup>18</sup>. The wide variety of glass beads of probable pyroclastic origin in Apollo and Luna samples is testimony to this. More widespread dark-mantling deposits, such as those seen at the Apollo 17 site, are likely to be the result of sustained effusive eruptions in which continuous gas exsolution causes pyroclasts to be spread to ranges<sup>18</sup> of tens to hundreds of km and emplaced in mantling deposits. A wide variety of compositions are inferred for lunar dark mantling deposits<sup>19</sup>. Individual dark halo craters such as those seen in Alphonsus are interpreted to be the result of vulcanian eruptions<sup>20</sup> and evidence has been presented for the presence of such deposits in many parts of the Moon<sup>21</sup>.

Tectonic Associations and Thermal Evolution: Relationships of mare basalt emplacement and tectonic structure<sup>22</sup> together with flexural studies and thermal evolution models<sup>23</sup> indicated that global horizontal thermal stresses changed from net extension to net compression about 3.6 b.y. ago, as the Moon shifted to overall cooling and contraction. Subsidence and flexure favored local extension and late eruption sites along the edges of the mare basins. The change from expansion to contraction inhibited the ascent and eruption of magma, and this factor, combined with less magma production as the Moon cooled, accounts for the decrease in volcanic flux and eventual cessation of mare basalt emplacement.

Outstanding Questions: Among the many unresolved questions or poorly understood issues are the relationship of mare volcanism to low albedo highland volcanic deposits<sup>24</sup>, the establishment of a lunar-wide mare basalt stratigraphy, the distinctiveness of source regions represented by different spectral units and implications for diversity in space and time, the link of mare volcanism to impact basin formation, the relationship of extrusion to intrusion and the volume of basalt intruded in the crust, the presence and role of shallow magma chambers, a model for the accumulation and eruption of large magma batches, and the nature and affinities of farside maria.

#### References:

- 1) J. Head (1975) *Origins of Mare Basalts*, 66. 2) J. Head (1976) *Rev. Geophys. Space Phys.*, 14, 265. 3) C. Pieters (1978) *LPSCP* 9, 2825. 4) J. Boyce (1976) *LSCP* 7, 2717. 5) J. Head (1975) *Origins of Mare Basalts*, 61. 6) C. Pieters et al. (1975) *LSCP* 6, 2689. 7) C. Pieters et al. (1980) *JGR*, 85, 3513. 8) J. Whitford-Stark and J. Head (1980) *JGR*, 85, 6579. 9) G. Schaber (1973) *LSCP* 4, 73. 10) I. Adler and J. Trombka (1977) *Phys. and Chem. of Earth*, 10, 17. 11) P. Schultz and P. Spudis (1979) *LPSCP* 10, 2899.
- 12) *Basaltic Volcanism Study Project* (1981) Pergamon, 1286p. 13) D. Wilhelms (1987) *The Geologic History of the Moon*, USGS PP-1348. 14) L. Wilson and J. Head (1981) *JGR*, 86, 2971. 15) M. Carr (1974) *Icarus*, 22, 1. 16) L. Wilson and J. Head (1980) *LPS* 11, 1260.
- 17) J. Head and L. Wilson (1980) *LPS* 11, 426. 18) L. Wilson and J. Head (1983) *Nature*, 302, 663. 19) L. Gaddis et al. (1985) *Icarus*, 61, 461. 20) J. Head and L. Wilson (1979) *PLPSC* 10, 2861. 21) B. Hawke et al. (1989) *PLPSC* 19, 255. 22) B. Lucchitta and J. Watkins (1978) *LPS* 9, 666. 23) S. Solomon and J. Head (1979) *JGR*, 84, 1667. 24) J. Head and T. McCord (1978) *Science*, 199, 1433.

PRISTINE MARE GLASSES: PRIMARY MAGMAS?; P. C. Hess, Dept. Geological Sciences, Brown University, Providence, RI 02912

Pristine mare glasses are among the most primitive liquid compositions yet discovered on the moon; they are the best candidates for primary magmas (1,2). The primary nature of these magmas is therefore accepted as a working hypothesis, and serves as a paradigm against which models of petrogenesis are tested. Questions of particular interest concern how mare basalts are produced, transported from their source mantle and erupted onto the lunar surface.

A widely accepted model requires that the primitive mare glasses are partial melts of cumulate minerals that crystallized from the lunar magma ocean. The lack of correlation of  $\text{TiO}_2$  abundances with  $\text{Mg}^*$  ratios, however, requires a complex petrogenesis appealing to magma mixing, hybridization of cumulate source regions and/or assimilation of mantle and anorthositic crust. Hughes et al. (3,4), for example, modelled the source regions as a mixture of cumulate olivine  $\pm$  orthopyroxene fertilized by the addition of late crystallizing and highly evolved cumulate minerals (calcic clinopyroxene, pigeonite, plagioclase and ilmenite) and KREEP-like residual liquid. Source hybridization occurs because the cumulate pile, which is gravitationally unstable, overturns, mixing both late and early cumulates (5). This heterogeneous mantle is eventually melted by the heat produced from the decay of radioactive elements in the deeper primordial interior.

An important constraint to mare petrogenesis is provided by experimental phase relations which show that pristine mare glasses are multiply saturated with olivine + orthopyroxene at pressures between 20 to 25 kb but have only olivine on the liquidus at lower pressures (6,7,8,9). The (assumed) primary mare glasses were derived at  $P=20-25$  if olivine + orthopyroxene were left in the source or pressures lower than this if only olivine coexisted with primary basalts. The strongest evidence that the higher pressures prevail is the requirement that Sm/Nd is fractionated at the time of melting (10,11). This fractionation is consistent with relatively low degrees of melting of an olivine cumulate containing orthopyroxene (3).

These arguments support the notion of a cumulate source region, 400 or more km deep, that gives rise to both high Ti and low Ti mare basalts. The physical problems of satisfying this model are not trivial, however. First, how are liquids isolated from the mantle at such great depths and erupted unmodified onto the moon's surface? Heating and melting of the cumulates by the build-up of radioactive heat would typically result in the adiabatic ascent of mantle, resulting in additional melt production by pressure release melt. Melt production would be continuous, and the melt composition(s) reflects the local equilibrium of melt with the olivine + orthopyroxene residue. Since the olivine + orthopyroxene cotectic migrates away from olivine with decreasing pressure, a series of liquids with lower normative olivine but higher  $\text{Mg}^*$  ratios are produced as the diapir rises towards the lunar crust. High  $\text{Mg}^*$  mare basalts with such low pressure signatures have not yet been found on the moon.

Adiabatic upwelling of heated mantle and convection, in general, is inhibited however, if a stable density distribution existed within the cumulate pile. Such a stable density distribution and the absence of convective mixing is consistent with source heterogeneities implied by the pristine mare glasses (1). The stable density distribution results from the overturning of the gravitationally unstable cumulate layer. Bouyant diapirs developed in the primitive, undifferentiated moon are either hot enough or contain enough melt to rise through the upper mantle and produce the magmas parental to the  $\text{Mg}^*$  suite.

The question remains how the mare basalts are extracted from and shielded from the mantle. It is likely that the melts form an interconnected network within an olivine dominated cumulate down to very small degrees of melting (12,13). Provided that the melts are bouyant and of low viscosity, they will escape by porous flow as the matrix compacts to fill the space that is left (14). This mode of transport cannot persist for very long distances because equilibrium between liquid and matrix is quickly reestablished at lower pressures. The expansion of the olivine liquidus with decreasing pressure causes olivine to crystallize from the melt and orthopyroxene from the matrix to melt, forcing the melt to the local olivine-orthopyroxene boundary curve. The melt must escape the harzburgite matrix in order to preserve its deep-seated signature.

The transition from porous flow to channelled flow (i.e., flow through dikes or veins) cannot be modelled satisfactorily. If it occurs, such flow can effectively isolate the melt from additional interaction with the mantle. Nevertheless, it is not easy to get such melts to the surface. First, the melts will cool by adiabatic decompression at approximately  $4^\circ\text{C}$  per kb or about  $80^\circ\text{C}$  over 20 kb. Second, the ascent is non-adiabatic since convective-conductive heat transfer and fusion of wall rock will also cool the melt (15). Even if the melt has enough "superheat" to avoid crystallization (approximately  $100^\circ\text{C}$  after adiabatic cooling), the upward progress of the mare basalt must be slowed by the low density plagioclase-rich lunar crust (and perhaps the liquid-KREEP sandwich layer). The mare liquids should tend to collect and pond at this level, giving ample opportunity for

## PRIMARY MAGMAS: Hess, P.C.

magma mixing and assimilation of the lower noritic crust. Given this plausible scenario, it is very difficult to conclude that even the pristine mare glasses are primary magmas.

There is also an important chemical paradox that raises problems for all mare cumulate remelting models. It has been argued that the similarity of  $Mg^*$  values of high and low  $TiO_2$  mare basalts and the estimated depths of melting support the re-equilibration of high level ilmenite-bearing cumulates with a large mass of olivine-rich mantle. It is difficult to reconcile this with the observation that high Ti mare glasses typically have low Ni contents (< 60 ppm), whereas low Ti mare glasses have high Ni contents (usually > 100 ppm) (1). If both equilibrated with the same mantle, why do they have different Ni values? Ringwood and Kesson (5) argued that high Ti mare basalts fractionated a metal phase and thereby lost Ni. The ratio of incompatible siderophile to lithophile elements (e.g., W/U), however, is the same in all mare basalts (e.g., 16), eliminating this explanation. Sulfide fractionation in high Ti mare basalts but not in low Ti mare basalts is inconsistent with solubility measurements (17), which show that high  $TiO_2$  mare basalts are 50% undersaturated with sulfide at the time of eruption.

There is no simple way out of this paradox except to conclude that high Ti and low Ti mare basalt cannot be produced from the same olivine-orthopyroxene cumulate zone notwithstanding the similarity of  $Mg^*$  values. If correct, this conclusion makes the cumulate redistribution model unnecessary. Moreover, if the primitive mare glasses are adulterated liquids, then the 20 kb pressures implied by the phase equilibria are less relevant. Perhaps we should return to models which prevent  $Mg^*$  values from evolving significantly during the magma ocean phase.

References: (1) Delano, J.W. (1986) JGR, V19: D201-213. (2) Delano, J.W. and Livi, K. (1981) *Geochimica Cosmochimica Acta*, 45: 2137-2149. (3) Hughes et al., (1988) *Geochimica Cosmochimica Acta*, 52: 2379-2393. (4) Hughes et al., (1989) Proc. 19th Lunar and Plan. Conf., 175-184. (5) Ringwood, A.E. and Kesson, S.E. (1976) Proc. Lunar Sci. 7th, 1697-1722. (6) Chen et al., (1982) JGR, 87: A171-181. (7) Delano, J.W. (1980) Proc. Lunar Sci. Conf. 6th, 871-893. (8) Stolper, E.M. (1974) Thesis, Harvard Univ. (9) Nyquist et al., (1979) Proc. Lunar Sci. Conf. 10th, 77-114. (10) Lugmair, G.W. and Marti, K. (1978) EPSL 39: 349-357. (11) Toramaru, A. and Fuji, N. (1986) JGR, 91: 9239-9252. (12) Waff, H.S. and Bulua, J.R. (1979) JGR, 84: 6109-6114. (13) McKenzie, O.F. (1984) J Petrol., 25: 713-765. (14) Marsh, B.D. (1978) Phil. Tran. R. Soc. Lond., A288: 611-625. (15) Newson, H.E. (1986) Origin of the Moon, Ed. Hartmann et al., Lunar Plan. Inst. 203-230. (16) Danckwerth et al., (1979) Proc. Lunar Plan. Sci. 10th, 517-530.

MARE SERENITATIS/MARE TRANQUILLITATIS SHELF REGION:  
IDENTIFICATION OF BASALT TYPES FROM MULTISPECTRAL REFLEC-  
TANCE MEASUREMENTS; R. Jaumann, G. Neukum, and H. Hoffmann, Planet.  
Remote Sensing Section, Inst. for Optoelectronics, DLR, D-8031 Oberpaffenhofen,  
FRG

The Mare Serenitatis/Mare Tranquillitatis shelf region is expected to expose basaltic materials which are highly different in composition and age. As we know from photogeological mapping (1), a number of surface units can be identified in this region. The goal of the presented study is the chemical identification of basaltic surface units as well as the determination of their areal distribution. Hence, lunar samples are only available for the adjacent small area of the Apollo 17 landing site and multispectral reflectance measurements have to be used for this purpose.

In order to derive quantitative information from multispectral reflectance measurements the correlation between the spectral characteristic and the chemical composition of lunar sample materials was investigated (2, 3, 4). These studies demonstrate that the VIS to NIR spectral range is highly indicative for chemical analyses (4, 5). The result of the investigations is a spectral-chemical model which describes the quantitative relationships between the spectral signatures of lunar samples and the concentration of chemical endmembers of the same samples (4). The spectral-chemical model is based on a principal component analysis which describes spectral signatures and on a multiple regression which defines the spectral-chemical correlation. The concentrations of the chemical endmembers which exhibit abundances  $> 1.0$  wt% in lunar soils such as FeO, TiO<sub>2</sub>, SiO<sub>2</sub>, Al<sub>2</sub>O<sub>3</sub>, MgO and CaO as well as the agglutinate content can be estimated with confidence by using the spectral-chemical model (4).

Encouraged by the results we applied the spectral-chemical model to earth-based multispectral measurements of the Apollo 17 landing site (3). The comparison of chemical concentrations calculated based on the spectral-chemical analysis of remote sensing measurements of the Apollo 17 landing site with the result of the chemical laboratory analyses of Apollo 17 samples yields a coincidence better than 9% between both chemical data sets. Thus, the concentration of chemical endmembers can be estimated within an acceptable error range if the spectral-chemical model is applied to earth-based spectral measurements of the lunar surface.

The analysis of multispectral measurements in the wavelength range 0.4  $\mu\text{m}$  to 2.5  $\mu\text{m}$  acquired by a CCD camera and a NIR spectrometer in combination with the spectral-chemical model results in the generation of chemical concentration maps. These maps reproduce the FeO, TiO<sub>2</sub>, and Al<sub>2</sub>O<sub>3</sub> abundances in the soils of the Mare Serenitatis/Mare Tranquillitatis shelf region. As mentioned above the adjacent Apollo 17 area was used to verify the confidence of the calculated concentration values.

In a first order approximation lunar materials can be discriminated on the basis of their iron, titanium and aluminium content. For this reason a ternary system TiO<sub>2</sub> - FeO - Al<sub>2</sub>O<sub>3</sub> is used for the identification of lunar rock types. This system can be simplified by introducing TiO<sub>2</sub>/FeO and FeO/Al<sub>2</sub>O<sub>3</sub> concentration ratios. Applying these ratios to lunar samples of all landing sites results in the differentiation of the following lithological units: anorthositic units, noritic or gabbroid units, mare basalts,

ilmenite basalts, titanium basalts, VLT basalts and VHT basalts. Mare basalts are characterized by moderate  $\text{TiO}_2/\text{FeO}$  ratios and  $\text{FeO}/\text{Al}_2\text{O}_3$  ratios  $> 1.2$ . The mare basalt unit includes the following lunar basalt types: olivine- and pigeonite-basalts which cannot be discriminated on the basis of the used lithological model, and high-Al basalts. Ilmenite-basalts have simultaneously high  $\text{TiO}_2/\text{FeO}$  ratios  $> 0.2$  and  $\text{FeO}/\text{Al}_2\text{O}_3$  ratios  $> 1.5$  while titanium-basalts are characterized by high  $\text{TiO}_2/\text{FeO}$  ratios  $> 0.33$  which correspond to  $\text{TiO}_2$  concentrations  $> 6.0$  wt.%.

The calculated  $\text{TiO}_2$  and  $\text{Al}_2\text{O}_3$  concentrations as derived from the spectral-chemical model were used to transform the chemical maps of the Mare Serenitatis/Mare Tranquillitatis shelf region into a lithological surface map of different lunar basalts as well as of the adjacent highland units. The advantage of this classification scheme is its simplicity.

Chemically and lithologically, three basalt units can be distinguished within the Mare Serenitatis/Mare Tranquillitatis shelf region: mare basalts, ilmenite basalts and titanium basalts. If additional information such as age determination (6) from crater statistics, mineralogical evidence from qualitative interpretation of reflectance spectra and photogeological interpretations (1) are combined with the chemical data the basalt units can further be discriminated into the following subunits:

undivided mare basalts of Mare Serenitatis,  
 olivine basalts of the Montes Haemus shelf (defined as mare-plateau-basalts by Wilhelms and McCauley (1)),  
 Mare Serenitatis ilmenite-basalts which are younger than the Mare Tranquillitatis ilmenite-basalts,  
 titanium-basalts of Mare Tranquillitatis and  
 dark mantle deposits of the Mare Serenitatis shelf.

In conclusion, the above approach provides a technique for the identification of lunar surface units which can also be applied to the imaging data of the Galileo SSI experiment.

#### References:

- (1)Wilhelms D.E. and McCauley J.F. (1971) U.S. Geol. Surv., Map I-703
- (2)Jaumann R., Kamp L. and Neukum G. (1988) Lunar and Planet. Sci. XIX, p.551-552
- (3)Jaumann R., Neukum G. and Hawke B.R. (1988) Lunar and Planet. Sci. XIX, p.553-554
- (4)Jaumann R. (1989) DLR-FB 89-40
- (5)Hoffmann H., Jaumann R. and Neukum G. (1990) Lunar and Planet. Sci XXI, p.520-521
- (6)Wilhelms D.E. (1987) U.S. Geol. Surv. Professional Paper 1348

EXPLORATION OF RELATIONSHIPS BETWEEN LOW-Ti AND HIGH-Ti PRISTINE LUNAR GLASSES USING AN ARMALCOLITE ASSIMILATION MODEL. J.H. Jones\* and J.W. Delano\*\*. \*SN2, NASA Johnson Space Center, Houston, TX 77058. \*\* Dept. of Geological Sciences, SUNY Albany, Albany NY 12222.

The pristine glasses of Delano [1] are the most primitive lunar basaltic magma compositions discovered to date. They are grouped into two (and possibly three) Arrays — a low-alumina Array (I) and a high-alumina Array (II). These glasses are very olivine normative and are multiply saturated at pressures of ~20 kbar, implying a depth of origin of 400-500 km in the Moon. Thus, these glasses appear to be our best candidates for primitive partial melts of the upper lunar mantle.

Some relationships between these glasses remain obscure. For example, Jones and Delano [2] pointed out that much of the compositional variation within an Array is minimized when the glass compositions are projected from ilmenite,  $\text{FeTiO}_3$ . Standard projections from  $\text{TiO}_2$  and DI onto an OL-PL-SI diagram indicate wide compositional diversity within and between Arrays, but projection from DI and IL greatly reduces the spread in the projected compositions. Even with this simplification, problems still exist. For example, the timing of the addition of this high-Ti component and the provenance of that component are unknown. Also, even though the pristine glass compositions may have been chemically similar prior to becoming enriched in Ti, we have argued previously, on the basis of Ni-Mg systematics, that these glasses could not have come from a single source region. In short, there was enough concern over our ignorance of how the high-Ti glasses were generated that Jones and Delano [2] based their reconstructions of the bulk composition of the Moon on low-Ti glasses only.

One of the most perplexing characteristics of the pristine glasses is a positive correlation between Ni and  $\text{SiO}_2$  within each Array. This is contrary to our terrestrial experience, where Ni is observed to positively correlate with MgO and negatively correlate with  $\text{SiO}_2$ . These systematics are believed to be due to the depletion of Ni by olivine fractionation.

The difference between the lunar and terrestrial Ni vs.  $\text{SiO}_2$  trends may be partially ascribed to the Ti-rich component. In the case of the pristine glasses,  $\text{SiO}_2$  increases, not because of olivine fractionation, but because they contain less of the high-Ti component. We have attempted to model this variation in Ni and  $\text{SiO}_2$  with a simple assimilation-fractional crystallization (AFC) model, where OL crystallizes as IL is assimilated. The results of this exercise were encouraging. Silica and Ni both decreased dramatically as the AFC process proceeded. Only 15-20% AFC was necessary to produce the observed variation, and the  $\text{SiO}_2$  vs. Ni variation was modeled quite well.  $D(\text{Ni})$  for olivine/liquid in this model was taken to be 10 and the olivine was assumed to be  $\text{Fo}_{80}$ . However, the results of this model for Ti and Mg were less than satisfactory. It seemed difficult to achieve the high  $\text{TiO}_2$  contents of some glasses (16-17 wt.%) by this method. Continual addition of ilmenite by AFC could indeed raise the titania concentrations to the necessary levels, but only by enriching the magma in FeO and greatly depleting the magma in MgO.

We have attempted to circumvent this problem by using armalcolite,  $(\text{Fe,Mg})\text{Ti}_2\text{O}_5$ , in the AFC model. The results for Ni,  $\text{SiO}_2$ ,  $\text{TiO}_2$  and MgO are shown for the Array I glasses in Figure 1. The starting composition for the models of Figure 1 was the A15 Green Glass E. The armalcolite was assumed to have an Mg# of 50 (idealized armalcolite),  $D(\text{Ni})$  was 10, and the olivine was again  $\text{Fo}_{80}$ . An assumption of the model was that the mass of armalcolite that could be assimilated by the crystallization of a gram of olivine was the same as that for ilmenite. Because the heat of fusion of armalcolite is unknown, this was a necessary assumption. In the case of olivine and ilmenite the heats of fusion (cal/g) are subequal.

As can be seen from Figure 1, the fit to the Ni vs.  $\text{SiO}_2$  data is quite good and the model has no difficulty generating both high-Ti compositions and reasonable MgO contents. Although not shown, results for the less-populated Array II are similar. Further, the high-Ti compositions can be generated without an inordinate increase in FeO, unlike the ilmenite models. If correct, these results strongly imply that the Arrays of Delano [1] were generated by AFC, with olivine and armalcolite as the principal players in this process.

Some other inferences from these data seem warranted. First, the addition of the armalcolite component must have occurred in a low-Ni setting. If the AFC model is correct, the armalcolite

itself contained little or no Ni and the Ni contents of the magmas generated by AFC were not buffered by a large olivine reservoir. Either such a reservoir was not in proximity or there was no opportunity for equilibration during/after the AFC process. Geologically permissible regions of the Moon that might have these characteristics are the uppermost mantle and the lower crust. Both these regions might be expected to be enriched in incompatible elements (e.g., Ti) and to be depleted in compatibles (e.g., Ni). This observation is contrary to the inference that multiple saturation at high pressure indicates a 400-500 km depth of origin. However, it is possible that descending diapirs of armalcolite-rich materials interacted with the pristine glass magmas [3], which then rapidly rose to the surface, without a chance to re-equilibrate with lower mantle materials. In either case, if the AFC model is correct, the experimental determinations of high-Ti magma phase relations at pressure may not accurately represent the phase assemblage at 20 kbar within the Moon. We note as an aside that armalcolite becomes unstable relative to ilmenite and rutile with increasing pressure [4]. Thus, our AFC model should be most viable at low pressure.

We have not yet explored the implication of our AFC model for either the trace element or isotopic characteristics of high-Ti glasses. If adequate data exist, we would welcome these tests of our models. However, we presently question whether simple partial melting of mantle sources (even "hybridized" sources [5]) is sufficient to explain the correlation between Ni and SiO<sub>2</sub>.

Given the apparent success of the armalcolite assimilation model, why do we still have reservations about the origin of high-Ti glasses? Principally, we are concerned because we have lost our ability to reduce compositional spread in our OL-SI-PL projections. Because ilmenite and armalcolite have different chemical compositions, it seemed unlikely that, if the ilmenite projection produced clustering, that the armalcolite projection would as well, and this is indeed the case. There is also uncertainty as to the meaning of the high-pressure experiments on high-Ti compositions. If armalcolite is a low pressure phase, did armalcolite assimilation occur at low pressure or did armalcolite/ilmenite diapirs sink to the depth of the pristine glass source regions? These issues must be resolved before there can be a substantive understanding of the high-Ti glasses in particular and high-Ti mare basalts in general.

Figure 1

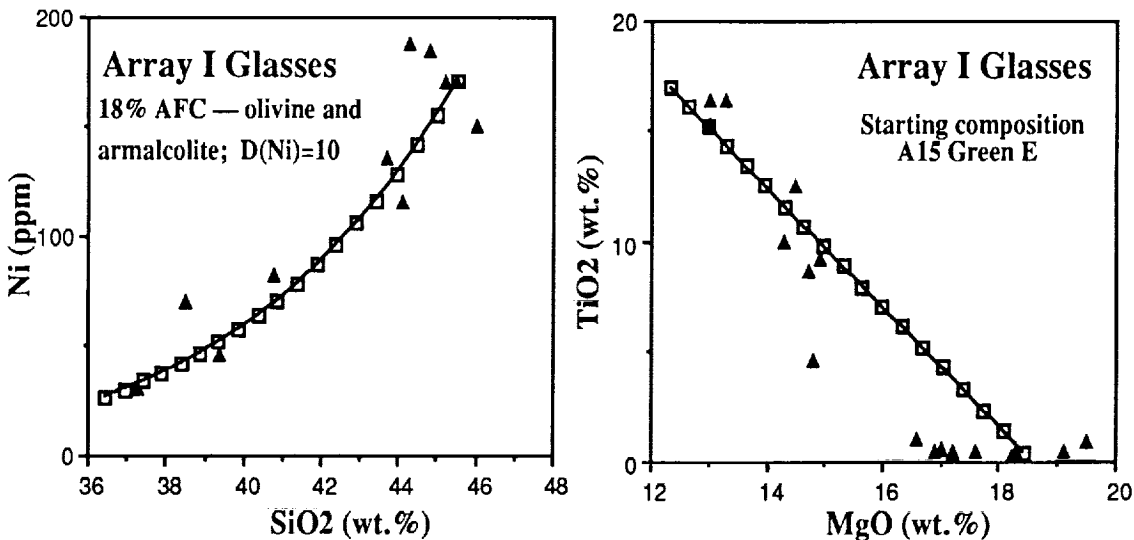


Figure 1. AFC model for production of high-Ti glasses. Triangles are glass compositions and squares are the range of AFC model calculations.

References. [1] Delano J.W. (1986) *Proc. Lunar Planet. Sci. Conf. 16th.* D201-D213. [2] Jones J.H. and Delano J.W. (1989) *Geochim. Cosmochim. Acta* **53**, 513-527. [3] Ringwood A.E. and Kesson S.E. (1976) *Proc. Lunar Sci. Conf. 7th.*, pp. 1697-1722. [4] Lindsley D.H. et al. (1974) *Proc. Lunar Sci. Conf. 5th.*, pp. 521-534. [5] Shearer C.K. et al. (1990) *Geochim. Cosmochim. Acta* **54**, 851-867.

DYNAMICAL MELTING MODELS OF MARE BASALTS; J. Longhi, Lamont-Doherty Geological Observatory of Columbia University, Palisades, NY 10964

There has been relatively little attention in recent years given to the processes through which the mare basalts and associated volcanic glasses acquired their major element compositions. Throughout the 1970's petrologists interpreted the point of olivine + pyroxene multiple saturation on the high-pressure liquidus of mare compositions (Fig. 1) as the pressure of melt segregation (e.g. 1,2,3). Although they issued caveats about the assumed primary nature of the compositions they investigated, they did not discuss in any detail the processes of melting or transport to the surface. This latter process has remained something of a mystery because many mare basalts and glasses have implied pressures of segregation  $> 10$  kb corresponding to depths  $> 200$  km. How magma could retain its primary composition through such extended transits to the surface except by kimberlitic eruption from depth has never been clear.

In the 1980's terrestrial geophysicists developed quantitative models for melt migration by porous flow, segregation, and compaction of the crystalline residua in a convecting mantle (4,5,6). These models typically portray a pool of melt consisting of contributions from a range of pressures collected at the top of the ascending mantle column and often ponded at the base of the crust or lithosphere. These treatments have incorporated terms for trace elements with constant partition coefficients, but do not readily lend themselves to major elements whose partition coefficients typically depend on composition. The one attempt to model major elements during polybaric porous flow approximated the process as one in which extraction of melt produced no change in the composition of the continuously melting source (7). This process may be described as total replenishment (TR).

Porous flow models may have some applicability to mare basalt petrogenesis. Mare basalts were produced by partial melting of low-Al mafic to ultramafic sources. During the time of mare petrogenesis the Moon had a thin, but growing elastic lithosphere that eventually supported the loading of mare basalts in the great basins to form mascons: stress modeling suggests elastic lithosphere thicknesses of  $\sim 50$  km at 3.6-3.8 b.y., and increasing to  $\sim 100$  km afterwards (8). Beneath the base of the lithosphere was the mare basalt source region, partially molten in places and probably convecting. In such a physical regime mare basalt magmas would pool at the base of the lithosphere and possibly would rise to the surface along fractures caused by impacts. A major test of the applicability of the porous flow model is its ability to generate composite melts ponded at 100 km or less ( $< 5$  kb) that appear to be multi-saturated at higher pressure and hence to be derived from greater depths. Fig. 2 illustrates this situation: the field of the picritic green volcanic glasses (9) sits astride the 20 kb olivine + orthopyroxene liquidus boundary -- well below the position of the boundary at 5 kb.

To test the porous flow model, I have carried out two variations of polybaric partial melting of lunar compositions and some of the results are shown in Fig. 2. In each case melting begins at some initial pressure and proceeds in a series of steps at progressively decreasing pressure with the melt pooling at some arbitrary lower pressure. One set of calculations involves extraction and accumulation of melt but no change in source composition analogous to (7); these results are labeled TR. The other set involves fractional fusion, i.e. complete extraction of the melt without replenishment; these results are labeled FF. Major element variation during true porous flow, which entails continuous interaction between melt and matrix and hence is difficult to calculate, lies somewhere between these tractable extremes. In these calculations I employed the value of 1.2% melt/kb adopted by (7) and based upon the thermal modeling of (10); melting began at pressures indicated in Fig. 2 (25 or 40 kb); melt extraction began at 2.4% (a pressure drop of 2 kb) and continued in 1 or 2 kb steps until 5 kb (or in the case of the 40 kb fractional fusion, until 10kb where  $Al_2O_3$  dropped below 0.2 wt% in the source). In the TR model the amount of melting increases with each 1 kb step (2.4, 3.6, 4.8, etc.); in the FF model the amount of melting remains constant (2.4% per 2 kb step). I derived the model source composition (Table 1) by subtracting 15 wt% Highland Crust from Primitive Mantle (11, Table 8.4). More aluminous compositions shift the FF and TR curves to the right; less aluminous and more ferroan compositions shift these curves to the left.

At first inspection results of these calculations suggest that compositions similar to those of the green glasses may be generated by fractional fusion of an ascending low-Al source that began to melt at great depth ( $\sim 800$  km) in the Moon. However, these particular results (FF, 40 kb) do not satisfy the model because pooled melt is too magnesian (Table 1) and the source becomes barren at 200 km. More importantly, the calculations require that the temperature actually increases at pressures less than 30 kb, which is an implausible situation in a convecting mantle. Although this modeling is still at a preliminary stage, it appears that models involving more ferroan source compositions, greater depths for the onset of melting, and a small component of replenishment may satisfy both the compositional and thermal constraints. If such models prove successful, then melting at great depths would correspond more closely to the thermal model of (12) based on 40 ppb of U for the bulk Moon, rather than the model of (13) based on 20 ppb of U, thus implying that the Moon is enriched in refractory elements by a factor of  $\sim 2$  over chondrites.

## REFERENCES

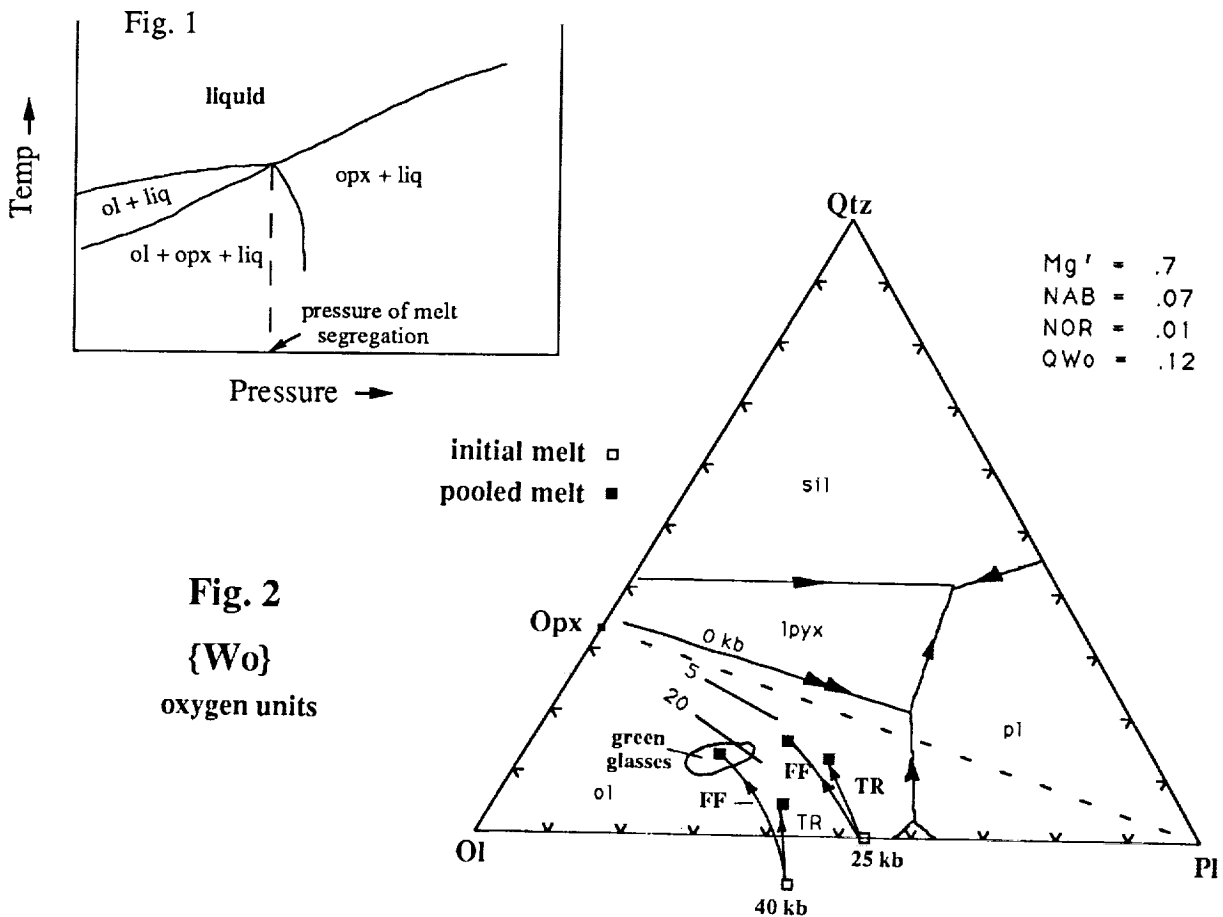
- (1) Green D.H., Ware N.G., Hibberson W.O., and Major A. (1971) *Earth Planet. Sci. Lett.* 13, 85-96. (2) Walker D., Longhi J., Stolper E.M., Grove T.L., and Hays J.F. (1976) *Geochim. Cosmochim. Acta* 39, 1219-1235. (3) Delano J.W. (1980) *Proc. Lunar Planet. Sci. Conf. 11th*, p. 251-288. (4) McKenzie D. (1984) *J. Petrol.* 25, 713-765. (5) McKenzie D. (1985) *Earth Planet. Sci. Lett.* 74, 81-91. (6) McKenzie D. and Richter F. M. (1984) *J. Geol.* 92, 729-740. (7) Klein E.M. and Langmuir C.H. (1987) *J. Geophys. Res.* 92, 8089-8115. (8) Solomon S.C. and Head J.W. (1979) *J. Geophys. Res.* 84, 1667-1682. (9) Delano J.W. (1986) *J. Geophys. Res.* 91, D201-D213. (10) Ahearn J.L. and Turcotte D.L. (1979) *Earth Planet. Sci. Lett.* 45, 115-122. (11) Taylor S.R. *Planetary Science: A Lunar Perspective*, The Lunar and Planetary Institute, Houston. (12) Solomon S.C. and Longhi J. (1977) *Proc. Lunar Sci. Conf. 8th*, p. 583-599. (13) Hubbard N.J. and Minear J.W. (1975) *Proc. Lunar Sci. Conf. 6th*, p. 1057-1085. (13) Longhi J. and Pan V. (1988) *Proc. Lunar Planet. Sci. Conf. 18th*, p. 459-470.

TABLE 1 (wt%)

	SiO <sub>2</sub>	TiO <sub>2</sub>	Al <sub>2</sub> O <sub>3</sub>	Cr <sub>2</sub> O <sub>3</sub>	FeO	MgO	MnO	CaO	K <sub>2</sub> O	Na <sub>2</sub> O	Mg'
model mantle	44.3	0.26	2.88	0.71	11.7	37.3	0.17	2.62	0.002	0.05	0.85
pooled melt 40 kb -FF	45.6	0.77	8.15	0.61	16.6	20.2	0.26	7.74	0.01	0.09	0.68
Ap 15 green glass A (9)	45.5	0.38	7.75	0.56	19.7	17.2	0.22	8.65	0.02	0.16	0.61

## FIGURE CAPTIONS

Fig. 1. Schematic high-pressure melting relations of low-Ti mare compositions. Fig. 2. Comparison of green glass compositions (9) and calculated polybaric, pooled melt compositions. Phase boundaries are appropriate for low pressure and compositional parameters shown in upper right: Mg' = MgO/(MgO+FeO); NAB and NOR are albite and orthoclase fractions of the normative feldspar; QWo is the Wo coordinate of the Ol-Pl-Wo-Qtz system in mole units (13). FF = fractional fusion model; TR = total replenishment model.



**REMELTING MECHANISMS FOR SHALLOW SOURCE REGIONS OF MARE BASALTS;** M. Manga and J. Arkani-Hamed, Department of Geological Sciences, McGill University, 3450 University Street, Montreal Quebec H3A 2A7, Canada.

## INTRODUCTION

Two remelting mechanisms are studied which could induce remelting at shallow depths: a radioactive heating model in which remelting is due to lateral variations of heat source distribution emplaced by the end of the initial differentiation event, and a thermal insulation model in which remelting is induced by lateral variations of near-surface thermal conductivity due to a high porosity ejecta blanket created by basin forming impacts. The effect of these perturbations is studied by evaluating the thermal evolution of an otherwise radially symmetric lunar model.

## RADIOACTIVE HEATING MODEL

Heat producing element anomalies emplaced by the end of the initial differentiation event may be related to convection patterns in the magma ocean [1], trapped interstitial late-stage residual liquid [2], or the late accretion of large planetessimals [3]. Later enrichments might be due to diapirism or melt migration from deep previously undifferentiated regions [4,5], or the sinking of cumulates and convective overturn due to a possible inverted density structure produced by fractional crystallization [6].

The geometry of the radioactive heating model is shown in figure 1. The region of enrichment (U anomaly) is a disc-shaped region with a thickness of 20 km and a diameter of 175 km at depths from 60-80 km for a shallow enrichment, and from 180-200 km for a deep enrichment. The concentration of heat producing elements is 3 times (shallow enrichment model) and 5 times (deep enrichment model) the concentration of the radially symmetric model at that depth. The moon is assumed to be covered by a uniform megaregolith 1 km thick [7] with a conductivity about one order of magnitude less than the underlying rock [8].

## THERMAL INSULATION MODEL

The important effect of megaregolith insulation on thermal evolution is the basis of the thermal insulation model [8-11]. The geometry of the thermal insulation model for an Imbrium-size impact is shown in figure 2. A basin forming impact creates a 5 km thick low thermal conductivity ejecta blanket surrounding the basin, with a conductivity identical to the megaregolith. The surface layer above the basin has a higher thermal conductivity due to temperature induced scintering. The instantaneous basin rebound following impact is accounted for by the rise of a 40 km mantle plug. This model relates the spatial distribution of the maria to the cause of melting.

## RESULTS

For both models studied here, heat transfer is by conduction. The distribution of heat producing elements and initial temperature conditions are based on the cumulate source model [12]. The distribution of melt is shown for the radioactive heating model with a shallow (figure 3a) and deep (figure 3b) region

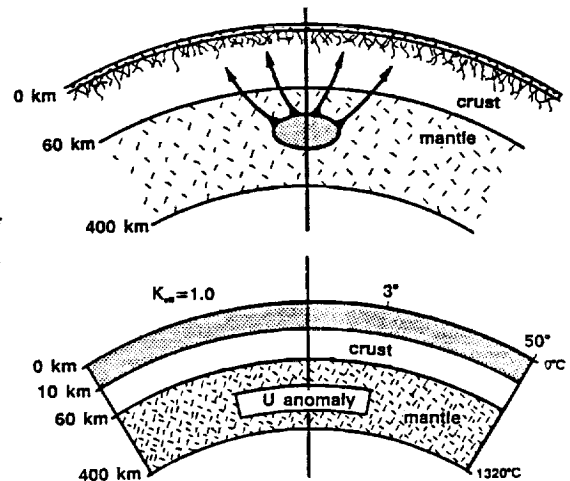


Figure 1. Radioactive heating model

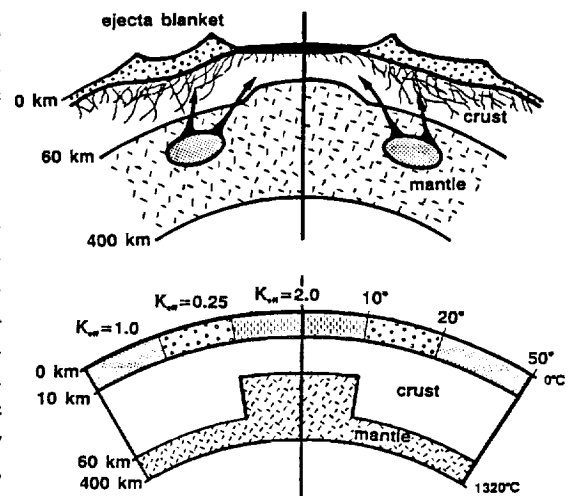
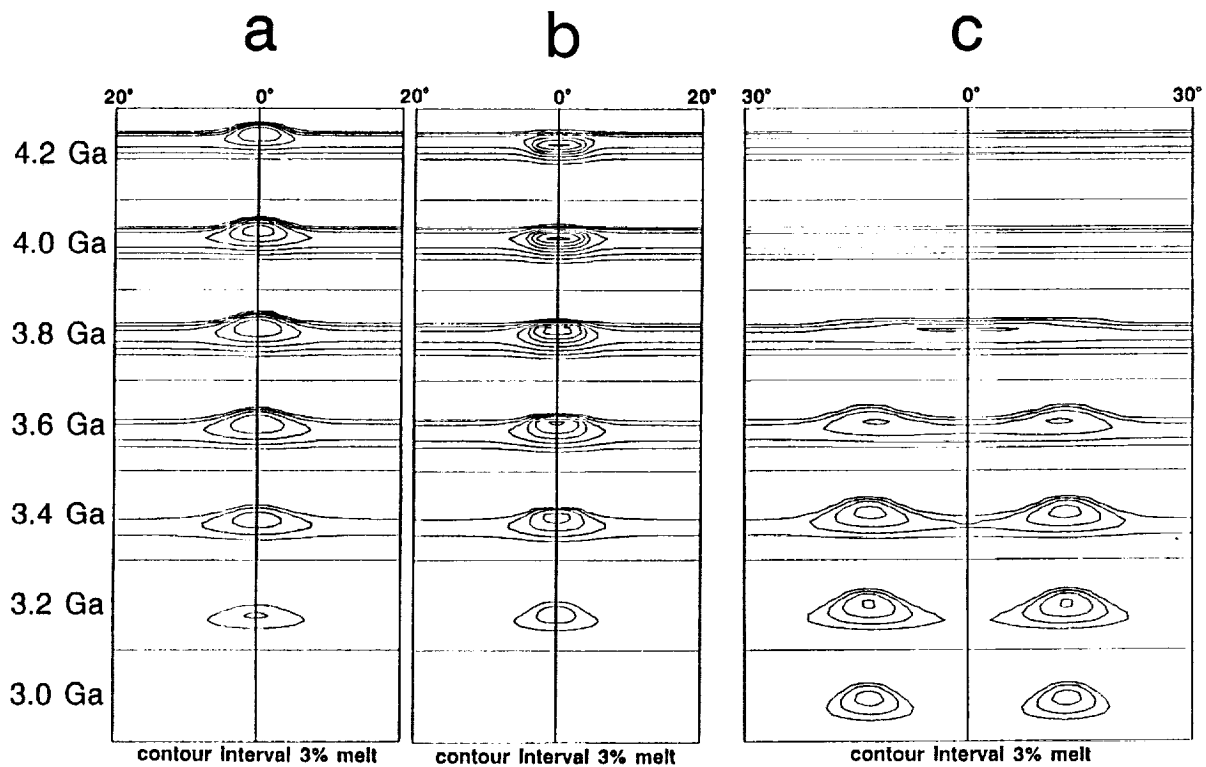


Figure 2. Thermal insulation model

of enrichment. These models predict extensive pre-basin volcanism, which would probably remove from the source region much of the heat producing elements responsible for melting. Therefore, uranium anomalies emplaced early would most likely not be heat sources for the basin filling mare basalts, however, they are plausible heat sources for pre-basin mare basalts [13].

The distribution of melt for the thermal insulation model is shown in figure 3c. The model predicts a delay of about 200 m.y. between impact and volcanism. It may also allow for the persistence of source regions at shallow depths to account for young basalts. If older basin ages, 4.2 to 3.9 b.y. [14,15], are correct and most mare volcanism occurred between 3.8 and 3.6 Ga [16], then the thermal insulation model may explain the delay. If on the other hand, the basins formed during a terminal cataclysmic event 3.9 Ga [17] then the earliest stages of basin filling about 3.8 Ga may have been a result of melting beneath the basin due to mantle uplift and impact heating [18]. Basin filling is characterized by a migration of the source region from beneath the basin as it cools to beneath the adjacent highlands as this region warms up (figure 3c). Cooling of the top 200 km beneath the basin after 200 m.y. due to its high surface conductivity is consistent with the mascon support requirement [19].



**Figure 3.** Distribution of melt in the upper mantle and crust for the radioactive heating model with a shallow (a) and deep (b) region of enrichment, and the thermal insulation model for an impact at 4.0 Ga (c). Each figure consists of 7 panels at different times in the thermal evolution, beginning at 4.2 Ga and then at every 200 my until 3.0 Ga. The horizontal dimension of each panel is 1200 km for (a) and (b) and 1800 km for (c). The top of each panel corresponds to the surface of the moon, and the bottom to a depth of 400 km.

#### REFERENCES

- [1] Brown G.M. (1977) *Phil. Trans. R. Soc. Lond. A* 285, 169-176. [2] Taylor S.R. (1978) *PLSC* 9, 15-23. [3] Hartmann (1980) *Proc. Conf. Lunar Highlands Crust*, 155-171. [4] Ringwood A.E. and Kesson S.E. (1976) *PLSC* 7, 1697-1722. [5] Turcotte D.L. and Ahern J.L. (1978) *PLSC* 9, 307-318. [6] Herbert F. (1982) *PLSC* 11, 2015-2030. [7] Warren N. and Trice R. (1977) *Phil. Trans. R. Soc. Lond. A* 285, 469-473. [8] Warren P.H. and Rasmussen K.L. (1987) *J. Geophys. Res.* 92, 3453-3465. [9] Haack H. et al. (1990) *J. Geophys. Res.* 95, 5111-5124. [10] Arkani-Hamed J. (1974) *Moon* 9, 183-209. [11] Arkani-Hamed J. (1973) *PLSC* 4, 2673-2684. [12] Taylor S.R. and Jakes P. (1974) *PLSC* 5, 1287-1305. [13] Taylor A.T. et al. (1983) *EPSL* 66, 33-47. [14] Baldwin R.B. (1987) *Icarus* 71, 1-18. [15] Baldwin R.B. (1987) *Icarus* 71, 19-29. [16] Head J.W. (1976) *Rev. Geophys. Space Phys.* 14, 265-300. [17] Ryder G. (1990) *EOS* 71, 313-323. [18] Bratt S.R. et al. (1985) *J. Geophys. Res.* 90, 12415-12433. [19] Arkani-Hamed J. (1973) *Moon* 6, 380-383.

**REE DISTRIBUTION COEFFICIENTS FOR PIGEONITE: CONSTRAINTS ON THE ORIGIN OF THE MARE BASALT EUROPIUM ANOMALY, III.** G. McKay (SN4, NASA-JSC, Houston, TX, 77058) J. Wagstaff, and L. Le (Lockheed ESCO, 2400 NASA Rd. 1, Houston, TX 77058)

**Introduction.** A long-held paradigm of lunar science is that the complementary REE patterns and Eu anomalies of the lunar crust and mare basalt source regions reflect an early differentiation event of global scale resulting from the crystallization of a lunar magma ocean (MO) [e.g. 1,2,3]. The positive Eu anomaly of the crust is generally thought to result from plagioclase enrichment, while the negative Eu anomaly in mare basalts is thought to be inherited by the source region from an evolved MO in which prior plagioclase removal had produced a negative Eu anomaly [e.g. 2].

The need for plagioclase removal has recently been reexamined [4,5]. These authors explicitly addressed the question of whether prior plagioclase removal is required to produce Eu anomalies of the magnitude observed in mare basalts, and arrived at opposite conclusions.

Part of the uncertainty in this issue is a result of inadequate mineral/melt partition coefficient data, especially for Eu at lunar oxygen fugacities. The situation is most critical for low-Ca pyroxene (a major carrier of REE among MO crystallization products throughout much of the MO crystallization sequence), but less so for olivine and high-Ca pyroxene. Olivine distribution coefficients are so low [6] that even a small proportion of pyroxene in the source region will dominate REE abundances in both cumulates and their partial melts. High-Ca pyroxene distribution coefficients have been studied by several workers [e.g. 7,8,9] under near-lunar oxygen fugacities, and indicate a significant Eu anomaly.

The magnitude of the Eu anomaly for Low-Ca PX is less well constrained. OPX distribution coefficients [10] indicate only a very minor anomaly. However, those results were obtained before the difficulty of measuring very low distribution coefficients on small crystals was appreciated [6], so the magnitude of the anomaly is likely to be unreliable. The goal of our current study is to provide reliable values for the partitioning of REE and Sr between low-Ca pyroxene and melt at near-lunar  $fO_2$  so that the origin of the mare basalt Eu anomaly can be better constrained. This abstract reports additional results obtained since our previous reports on this topic [11,12,13].

**Experiments.** McKay [11] reported distribution coefficients for trivalent REE between pigeonite and a melt produced by 15-20% crystallization of a synthetic basalt resembling 12015, but did not study partitioning of Eu. For the present study, we prepared a similar starting composition containing about 1 wt% each of Gd, Eu, and Sr. Pellets (125mg) of this starting material were suspended on wire loops in a controlled atmosphere ( $CO/CO_2$ ) furnace at oxygen fugacities near IW, held at 1300°C for four hours, cooled to 1200° in 2 hours, then to 1175° at 0.3°/hr, held for 24 hours, and then air quenched. This multi-stage cooling history permitted growth of large (>200  $\mu m$  wide) pigeonite crystals for which even very low partition coefficients could be measured without interference from adjacent glass [6]. Resulting charges were sectioned, polished and analyzed with the JSC Cameca microprobe, with no analyzed spot being closer than 100  $\mu m$  from the nearest glass, to ensure absence of analytical interference.

**Results.** We previously [12,13] reported  $D(Pig/L)$  for Gd, Eu, and Sr, but to provide a complete set of REE coefficients for use in modelling the petrogenesis of mare basalts, we were forced to combine the new data for these three elements with our earlier values [11] for the other REE. This was not straightforward because the average  $D(Gd)$  value from the current series of experiments [13] is only about 60% as large as that from our 1981 study [11], making direct comparison of current average Eu values with earlier results suspect. We demonstrated [13] that the discrepancy with our 1981 Gd value was the result of differences in average WO content ( $Ca/Ca+Fe+Mg$ ) and Na content between the two series of experiments. Our latest results confirm this hypothesis for Yb, Nd, and Sm. Pigeonite/melt REE partition coefficients are clearly correlated with the WO content of the

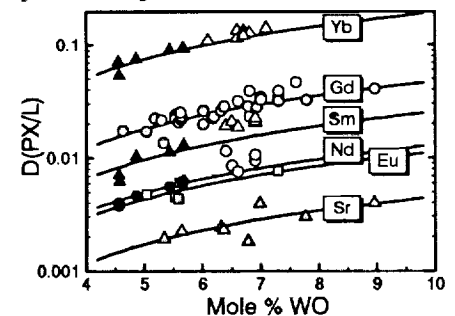


Figure 1. Variation of  $D$  with WO content of pigeonite. Filled symbols are new data points. Shaded symbols are from [13]. Open symbols are from Na-bearing experiments [11]. Eu data are for  $fO_2 = IW/10$ .

crystal (Fig. 1). Samples from our 1981 study (open symbols in Fig. 1) have higher WO contents than most of the samples from our recent experiments (filled symbols, Fig. 1), and hence higher D values. When the correlation with WO is considered, agreement between the 1981 experiments and the current ones is much better than a simple comparison of averages would suggest. We have not investigated the effect of Na for Sm, Nd, and Yb, but there is no reason to expect that it would be significantly different than the effect we reported for Gd [13].

Table 1 gives REE and Sr partition coefficients interpolated to WO of 5.5, the average composition of liquidus pyroxenes in multiply-saturated high pressure experiments on VLT ultramafic glasses [14]. We assume the

appropriate oxygen fugacity for lunar petrogenesis is IW. The resulting distribution coefficient pattern is shown in Figure 4, along with the OPX values of [10] for comparison. It is clear from these results that low-Ca pyroxene has a much larger capacity to develop Eu and Sr anomalies than the earlier data suggest. These results are in qualitative agreement with partition coefficients derived by [15] from ion probe analyses of  $Wo_{12}$  pyroxenes from lunar mare basalt, but suggest an even larger Eu anomaly for pyroxenes with lower Ca content, in agreement with arguments based on crystal chemistry [5].

**Discussion.** A major question in lunar science is whether the magnitude of the Eu anomaly in the low-Ca pyroxene partition coefficient pattern is sufficient to permit derivation mare basalts or ultramafic volcanic glasses from a lunar mantle formed without prior crystallization of plagioclase from the lunar magma ocean. We are currently studying this question using models similar to those of [4], [5], and [16] but our models differ because they include a trapped liquid component in the mafic cumulates. Shaffer *et al.* [16] found that they could not simultaneously match Eu/Sm and Sm/Ce ratios in primitive ultramafic glasses. Models producing a sufficiently large Eu anomaly resulted in Sm/Ce ratios higher than observed. Our calculations indicate that addition of a trapped liquid component lessens the magnitude of this problem, but does not eliminate it. We have been unsuccessful in matching REE in the A15 green glass, without resorting to either prior plagioclase removal or assimilation of a Eu-depleted component. Less primitive basalts or glasses are even more difficult to match with simple models.

**References:** [1] Walker *et al.* (1975) PLSC 6th, 1103. [2] Taylor (1982) *Planetary Science: A Lunar Perspective*. [3] Wood (1975) PLSC 6th, 1087. [4] Brophy and Basu (1990) PLPSC 20th, in press. [5] Shearer and Papike (1989) GCA 53, 3331. [6] McKay (1986) GCA 50, 69. [7] Grutzeck *et al.* (1974) *Geophys. Res. Lett.* 1, 273. [8] McKay *et al.* (1988) *Meteoritics* 23, 289. [9] McKay *et al.* (1989) LPSC XX, 677. [10] Weill and McKay (1975) PLSC 6th, 1143. [11] McKay *et al.* (1989) Workshop on Lunar and Volcanic Glasses, LPI. [12] McKay *et al.* (1990) LPS XXI, 773. [13] McKay (1981) EOS, Trans. AGU 62, 1070. [14] Chen *et al.* (1981) PLPSC 13th, A171. [15] Shearer *et al.* (1989) GCA 53, 1041. [16] Shaffer *et al.* (1990) *Lunar Planet. Sci.* XXI, 1130.

Table 1. Pigeonite/liquid distribution coefficients for REE and Sr. Values are interpolated to pigeonite with 5 mole % Wollastonite.

Ce	Nd	Sm	Eu(IW)	Eu(IW/10)	Gd	Yb	Sr
.00172	.0058	.011	.0068	.0050	.021	.087	.0020

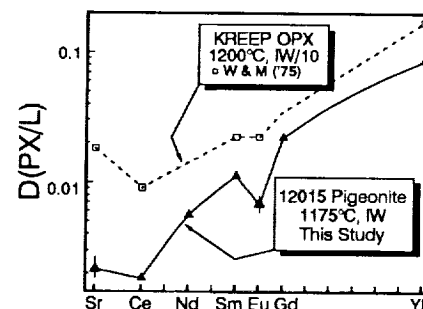


Figure 4. Distribution coefficient patterns for orthopyroxene [10] and  $Wo_5$  pigeonite.

## CYCLICAL AFC AT APOLLO 14: Sr ISOTOPE EVIDENCE FROM HIGH-ALUMINA BASALTS.

Clive R. NEAL\* and Lawrence A. TAYLOR, Department of Geological Sciences, University of Tennessee, Knoxville, TN 37996 (\* Now at: Dept. Earth Sciences, University of Notre Dame, Notre Dame, IN 45565).

Samples returned by the Apollo 14 mission have yielded a vast suite of high-alumina basalts. Most basalts have been found as breccia clasts, in particular from breccia 14321 (e.g., [1,2]). These authors reported groups of Apollo 14 high-alumina basalts. However, as more data have been collected from breccia pull-apart efforts, a continuum of high-alumina basalt compositions has become apparent [3-5]. For example, those samples with the highest MG# usually possess a LREE-depleted REE profile, whereas those with the lowest MG# possess a LREE-enriched, KREEP-like REE profile. Neal et al. [3-5] proposed an assimilation and fractional crystallization model to account for this compositional continuum. In this model, a fractionating high-MG#, low-SiO<sub>2</sub>, LREE-depleted magma assimilates a KREEPy component. The "r" value used was 0.22, and the proportions and composition of fractionating phases were estimated both from petrography and from considerations of the An-Q-Ol pseudoternary. Using these parameters, Neal et al. [3-5] demonstrated that major- and trace-element compositions can be adequately generated by an AFC process.

Although this AFC model can easily explain the major- and trace-element compositions of the high-alumina basalts, potential problems exist in the generation of major- versus trace-element plots and in the isotopic signatures by such a process. Dasch et al. [6] and Papanastassiou and Wasserburg [7] reported crystallization ages and initial <sup>87</sup>Sr/<sup>86</sup>Sr ratios for a total of six Apollo 14 high-alumina basalts. The Apollo 14 high-alumina basalts used in the study of Dasch et al. [6] were described in terms of "Groups", after Dickinson et al. [1]: Group 5 represents the most primitive or LREE-depleted basalts, whereas Group 1 represents the most evolved or LREE-enriched basalts. Crystallization ages range from 4.33 to 3.96 Ga, with the most primitive (LREE-depleted) basalt being the oldest.

Furthermore, the initial <sup>87</sup>Sr/<sup>86</sup>Sr ratio, Sr abundance, and Rb/Sr ratios increase as age decreases. An exception to this is the Group 3 basalt of Papanastassiou and Wasserburg [7], which is intermediate with regard to trace-element compositions (e.g., [3-8]), but is the youngest basalt analyzed and contains the highest initial <sup>87</sup>Sr/<sup>86</sup>Sr ratio.

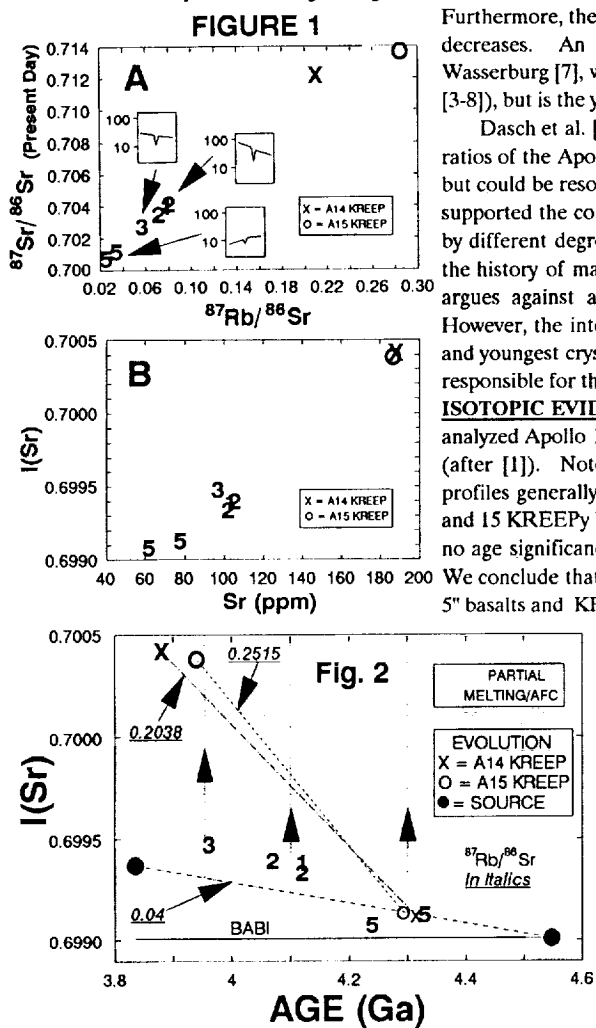
Dasch et al. [6] suggested that the range in crystallization ages and initial <sup>87</sup>Sr/<sup>86</sup>Sr ratios of the Apollo 14 high-alumina basalts negated a petrogenesis involving KREEP, but could be resolved by assimilating urKREEP residuals (after [9,10]). These authors supported the contention of Dickinson et al. [1] that the high-alumina basalts evolved by different degrees of partial melting of a common source at different times early in the history of mare volcanism. We acknowledge that the range of crystallization ages argues against a single-stage AFC process for the petrogenesis of these basalts. However, the intermediate Group 3 basalt possesses the highest initial <sup>87</sup>Sr/<sup>86</sup>Sr ratio and youngest crystallization age which suggests that simple source evolution is also not responsible for the generation of the Apollo 14 high-alumina basalts.

**ISOTOPIIC EVIDENCE FOR AFC** - An isochronous relationship exists between the 6 analyzed Apollo 14 high-alumina basalts (Fig. 1a). Numbers refer to the basalt Group (after [1]). Note that those basalts with the most evolved (LREE-enriched) REE profiles generally possess the most radiogenic <sup>87</sup>Sr/<sup>86</sup>Sr signature and that Apollo 14 and 15 KREEPy basalts plot at the upper end of Fig. 1a. However, these plots can have no age significance as the individual basalts have been erupted at different times [6].

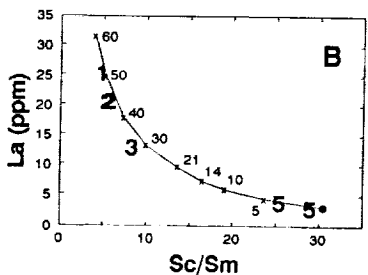
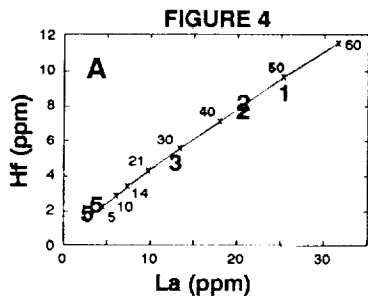
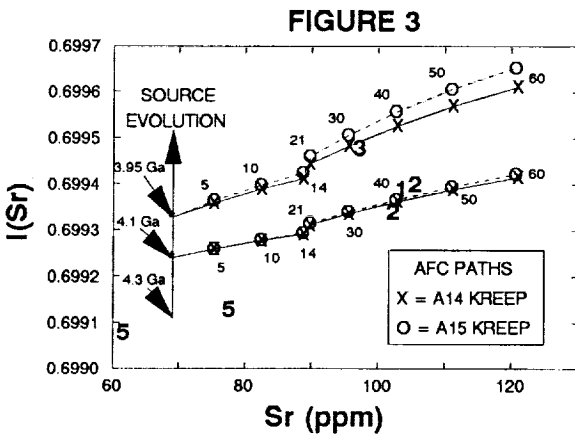
We conclude that this correlation represents a mixing line/AFC trend between "Group 5" basalts and KREEP. This borne out when initial <sup>87</sup>Sr/<sup>86</sup>Sr is plotted against Sr (ppm). The intermediate and evolved basalts contain progressively more radiogenic initial <sup>87</sup>Sr/<sup>86</sup>Sr ratios and a greater abundance of Sr. An exception to this is the intermediate "Group 3" basalt, which possesses the highest initial <sup>87</sup>Sr/<sup>86</sup>Sr, inconsistent with single-stage AFC trace element modelling. The significance of this observation will be discussed below.

**Sr ISOTOPE MODELLING** - Unlike the trace elements, modelling of the Sr isotopes requires that the age relationships be taken into account. The Apollo 14 high-alumina basalts have been represented on plot of initial <sup>87</sup>Sr/<sup>86</sup>Sr versus Age (Fig. 2); an AFC path will form a vertical trend on such a plot. We envisage the following scenario. The source of the basalts evolved along a path of Rb/Sr of 0.04, similar to Dasch et al. [6] and the bulk Moon value of Nyquist [11]. At various points along this evolution path, melt extraction occurred producing the primitive "Group 5" parental magma. From the isotope data, we envisage three partial melting and AFC events to have occurred (at 4.3, 4.1, and 3.95 Ga). With more data, we would expect to find the full range of Apollo 14 high-alumina basalt compositions to have been erupted during each of these AFC cycles. Furthermore, because the trace-element data suggest a single-stage AFC process, each cycle must have followed essentially the same path.

As the assimilant, we have used both Apollo 14 and 15 KREEP [7,12-15] as these both plot at the end of the positive correlations in Figure 1. We have calculated the isotopic compositions of these end-members from Figure 2 by assuming that their model ages



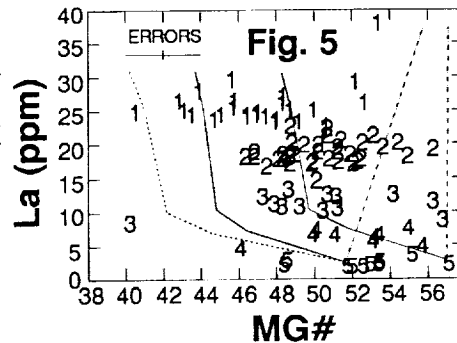
represent the time they departed from a bulk Moon evolution path [16]. By calculating the evolution path between the model and crystallization ages,  $^{87}\text{Sr}/^{86}\text{Sr}$  compositions of KREEP can be estimated at the times of the envisaged three AFC cycles. Furthermore, the Sr isotopic composition of the parental magma at these time intervals can also be estimated. We assume that Sr abundance did not change. We have calculated AFC paths using these parameters at 4.1 and 3.95 Ga. We did not calculate a path at 4.3 Ga because KREEP and the Apollo 14 high-alumina-basalt source had similar isotopic characteristics at this time. Proportions of crystallizing phases were the same as in the trace element modelling [3,4], and published partition coefficients were used (see [5] for details). Results are presented in Figure 3 and are similar to those of [18]. These are to be compared with the trace element modelling presented in Figure 4. The numbers on Figures 3 and 4 represent the amount of crystallization. There is good agreement between the isotope and trace-element modelling for the amount of



AFC required to generate each sample, assuming a  $r$  value of 0.22. However, the amount of AFC required to generate the "Group 1" basalt is somewhat higher for trace element-modelling than that for the Sr isotopes. This may be due to the fact that this sample is a mixture of 5 different "Group 1" basalt clasts [4]. The above discussion demonstrates that the Sr isotopes are consistent with an AFC petrogenesis for the Apollo 14 high-alumina basalts.

**MAJOR ELEMENT MODELLING** - Shih and Nyquist [17,18] used a plot of MG# versus La (Fig. 5) to demonstrate groupings rather than a continuum of Apollo 14 high-alumina basalt compositions. These authors demonstrated that the evolution path of Neal et al. [1] does not pass through the data on such a plot. However, in the construction of this AFC path, the major elements were modelled by fractional crystallization alone (after the method of [19]). In Figure 5, we have re-evaluated the AFC path, allowing for the effect of the assimilated (IKFM of [20]) upon the major-element compositions of the residual melt (solid lines). These curves are calculated from the parental composition defined by Neal et al. [3] and the "Group 5" basalt with the highest MG#. The original AFC curve is represented as the dotted line. Drawing more than one AFC curve is feasible due to the cyclical nature of the AFC process at the Apollo 14 site. Also shown on Fig. 5 are bulk mixing lines between the two parental "Group 5" basalts and our KREEP assimilant (dashed lines). These mixing lines miss the bulk of the data, but do not rule out the possibility of post-KREEP-assimilation olivine fractionation as proposed by Shih and Nyquist [17,18]. However, much of the scatter may be a function of the large errors associated with the MG# calculation (Fig. 5). When this effect and the cyclical nature of the AFC process at the Apollo 14 site are taken into account, this plot does not negate an AFC petrogenesis for the Apollo 14 high-alumina basalts.

REFERENCES - [1] Dickinson et al. (1985) *PLPSC 15*, in *JGR 90*, C365-C374; [2] Shervais et al. (1985) *PLPSC 15*, in *JGR 90*, C375-C395; [3] Neal et al. (1988) *PLPSC 18*, 139-153; [4] Neal et al. (1989) *PLPSC 19*, 147-161; [5] Neal & Taylor (1990) *PLPSC 20* (in press); [6] Dasch et al. (1987) *GCA 51*, 3241-3254; [7] Papanastassiou & Wasserbug (1971) *EPSL 12*, 36-48; [8] Neal et al. (1987) *LPS XVII*, 706-707; [9] Binder (1982) *PLPSC 13*, in *JGR 87*, A37-A53; [10] Binder (1985) *PLPSC 16*, in *JGR 90*, D19-D30; [11] Nyquist (1977) *Phys. Chem. Earth* 10, 103-142; [12] McKay et al. (1978) *PLPSC 9*, 661-687; [13] McKay et al. (1979) *PLPSC 10*, 181-205; [14] Nyquist et al. (1973) *PLSC 4*, 1823-1846; [15] Nyquist et al. (1975) *PLSC 6*, 1445-1465; [16] Dowty et al. (1976) *PLSC 7*, 1833-1844; [17] Shih & Nyquist (1989a) *Wkshp on Moon in Transition*, 128-136; [18] Shih & Nyquist (1989b) *LPS XX*, 1002-1003; [19] Depaolo (1981) *EPSL 53*, 189-202; [20] Vaniman & Papike (1980) *Proc. Conf. Lunar Highlands Crust*, 271-337.



**MODELS FOR MARE BASALT PETROGENESIS DEVELOPED OVER THE LAST 20 YEARS.** Clive R. NEAL\* & Lawrence A. TAYLOR, Dept. of Geological Sciences, University of Tennessee, Knoxville, TN 37996. (\* = Now at: Dept. of Earth Sciences, University of Notre Dame, Notre Dame, IN 45565).

During the Apollo years, the research on the returned mare basalts was intense, culminating in the 1975 Workshop on Mare Basalts and Volcanism. However, studies have continued, and many significant "post-Apollo" developments in mare basalt petrogenesis have resulted. The subject of this presentation is to review the progress made in our knowledge of mare basalt petrogenesis over the last 20 years. Each Apollo landing site where mare basalts have been found (except Apollo 16) will be discussed in turn, and those small samples returned by the Russian Luna missions will be evaluated, where applicable, within this framework.

**APOLLO 11:** Four different types of high-Ti basalts have been described from this site: A (high-K); B1, B2, and B3 (all low-K); and D (low-K, but high-La) [1,2]. These groups can be unambiguously resolved on a K vs. La plot (Fig. 1, after [1]). The within-group variations can be explained by fractionation of liquidus phases (e.g., B2 samples are related by ilmenite fractionation and B3 samples by olivine fractionation - [1]). However, none of these groups can be related to each other by post-magma generation processes, such as fractional crystallization [1,3,4]. Each group requires a distinct source as most igneous processes do not fractionate K from the REE. However, B2 and D basalts could have been derived from the same source region (with plagioclase in the residue) as both have high La/K ratios [1,3]. Hughes et al. [5] conducted source modeling for the A, B1, B2, and B3 magmas. In this model, the basalt sources for each basalt are comprised of an early and a late LMO cumulate component, with a proportion of trapped LMO residual liquid (<3.5%, Table 1). These LMO components are considered to be mixed by convective overturn late in the crystallization of the magma ocean (Hughes et al., 1989).

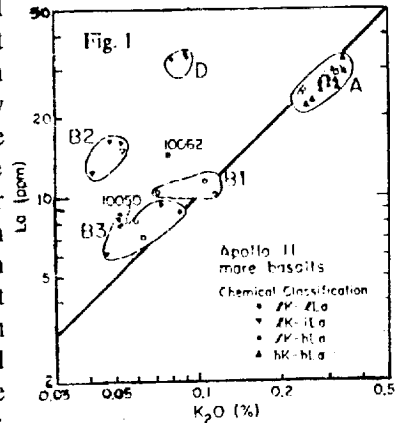
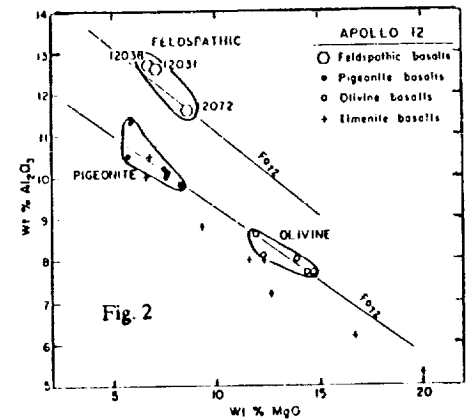


**TABLE 1**

F(%)	APOLLO 11			
	Low-K	Low/Int-K	Int-K	High-K
	10	7	20	10
		Early Cumulates		
Olivine	88.9	84.9	74.2	85.0
		Late Cumulates		
Augite	6.44	6.25	18.1	1.75
Pig		5.68		7.63
Plag	1.69	1.49	2.54	1.32
Ilm	2.37	0.90	2.04	2.01
Apatite	0.065	0.096	0.15	0.18
LMO evol	(97)	(97)	(97)	(98)
		Trapped LMO Liquid		
TL	0.53	0.72	3.0	3.1
LMO evol	(99)	(98)	(99)	(99)

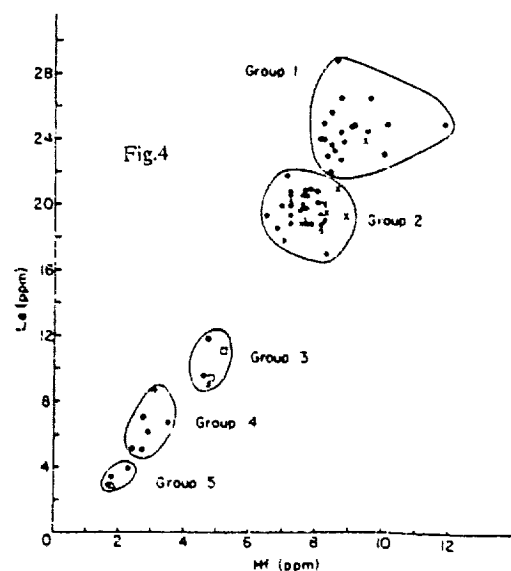
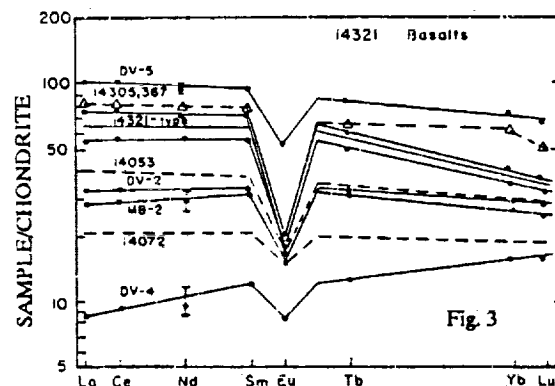
**APOLLO 12:** Rhodes et al. [6] reported whole-rock data for four types of Apollo 12 low-Ti mare basalts: 1) olivine; 2) pigeonite; 3) ilmenite; and 4) feldspathic. The olivine and pigeonite basalts are comagmatic and related by olivine fractionation (Fig. 2, after [7]), but no other relationships between these four basaltic groups were found. Rhodes et al. [6] concluded that the variation within the ilmenite and olivine-pigeonite basalt groups is caused by olivine-dominated (~30%) near-surface fractional crystallization. This fractionation occurred on the surface within thick (~40m) flows. Rhodes et al. [6] also concluded that parental compositions were close to the vitrophyres in each group, with the formation complimentary olivine cumulates and more evolved end-members. The feldspathic basalts are not as numerous as other types at the Apollo 12 site. These were described in detail by Beaty et al. [7] who argued for the presence of two types of feldspathic basalt on the basis of mineralogy, each requiring a distinct source region. Beaty et al. [7] suggested that one of these feldspathic basalt types was probably exotic to the Apollo 12 site. Furthermore, Nyquist et al. [8] argued, on the basis of Sr isotopes, one of the "feldspathic" basalts described by Beaty et al. [7] (12031) was in fact a plagioclase-rich pigeonite basalt, and that the pigeonite basalts could not have been derived from the olivine basalts by differentiation within a single flow.



**APOLLO 14:** Two basaltic types have been described from Apollo 14. The first, and more abundant, is the high-alumina suite (e.g., [9-11]). These basalts contain 11-14 wt% Al<sub>2</sub>O<sub>3</sub>, < 0.3 wt% K<sub>2</sub>O, and a K/La ratio of ~ 100. The second, and less common suite is that of very high potassium or VHKB basalts [12-15] which are

essentially the same composition as the high-alumina basalts, but contain  $> 0.3$  wt%  $K_2O$ , a  $K_2O/Na_2O$  ratio  $> 1$ , and a  $K/La$  ratios  $> 150$ .

Original studies defined 5 groups of high-alumina basalts at the Apollo 14 site [10,11] (Figs. 3, after [11], & 4, after [10]). Dickinson et al. [10] concluded that groups 1-5 could be generated by partial melting of a source proposed by Unruh et al. [16] for 12038 which contains trapped liquid (olivine 65.5%, cpx 20%, opx 9%, plagioclase 4%, ilmenite 0.5%, trapped liquid 1%). However, these authors also noted that groups 1-4 could also be generated by assimilation of 15386 KREEP by a group 5 magma. Shervais et al. [11] concluded that partial melting of a magma ocean cumulate containing 29% olivine, 29% opx, 33% cpx, 4% plagioclase, and 5% trapped liquid, could generate all groups of high-alumina basalts, except their "14321-type". The 14321-type basalts could be generated by KREEP assimilation by a trace-element-poor parental magma. Neal et al. [17,18] have

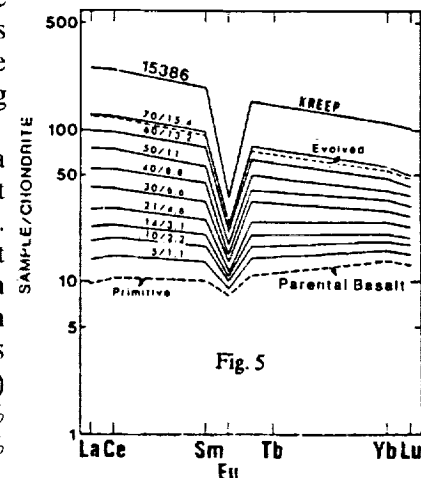


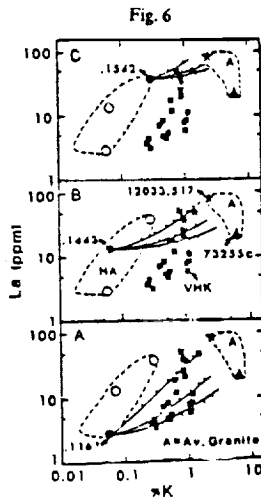
modelled the entire high-alumina suite with KREEP assimilation by a LREE-depleted ("Group 5") parental magma (Fig. 5, after [17,18]). This model was developed in response to further data which filled in the gaps between the various "groups" defined by Dickinson et al. [10] and Shervais et al. [11]. Approximately 15.5% of 15386 KREEP assimilation is required in this model, accompanied by  $\sim 70\%$  fractional crystallization of liquidus phases ( $r = 0.22$ ) in order to generate all observed high-alumina compositions.

The VHK suite was considered to be a high-alumina magma which had experienced contamination by lunar granite [12-15]. This accounts for the elevated  $K/La$  ratios of these basalts over the high-alumina varieties (Fig. 6, after [18]), yet still maintains essentially a high-alumina basalt major element signature. Neal et al. [17,18] refined this model by calculating AFC paths between high-alumina parent magmas and lunar granites. With new VHK basalt data it became obvious that no single parental magma could account for all VHK compositions reported from Apollo 14. The upshot of this was

that high-alumina basalts already contaminated by KREEP were required as parents for the more trace-element enriched VHK basalts (Fig. 6). This observation suggested some kind of KREEP-granite relationship in order to account for the change in assimilant during high-alumina basalt evolution.

The AFC model developed for the high-alumina basalts allowed a primitive (primary?), parental magma to be defined. This is equivalent to the LREE-depleted variants described by Dickinson et al. [10] ("group 5"), Shervais et al. [11], and Neal et al. [17,18]. Hughes et al. [19] took an average of all reported LREE-depleted high-alumina basalts and calculated the source required to generate such a magma. In a multi-faceted approach, Hughes et al. [19] described the source of this parental high-alumina magma as being dominated by olivine (91-97%) with additional late-stage LMO phases of: 1.4-2.0% cpx; 0.4-2.8% pigeonite; 0.9-3.3% plagioclase; 0.4-0.5% ilmenite; and 0.2-0.8% trapped liquid. These authors concluded that even though the parental magma was LREE-depleted, this model required a hybridized source containing a "KREEPy" component. Dickinson et al. [20] further suggested a metasomatized source for the Apollo 14 high-alumina basalts on the basis of Ge abundances.





**APOLLO 15:** Two types of mare basalt (not including the KREEPy basalts) have been described from Apollo 15 [21-23]. These are the olivine normative (ONB) and quartz normative (QNB) basalts. The ONBs are characterized by high FeO and TiO<sub>2</sub> concentrations, low SiO<sub>2</sub> and LIL elements (K, Ba, Sr, Rb), relative to the QNBs. Rhodes and Hubbard [21] concluded that the between group variation could not be accounted for by near-surface fractional crystallization (Fig. 7, after [21]), but is related to various degrees of partial melting of an inhomogeneous source (with respect to the trace elements). The within-group variation can be accounted for by moderate (< 15%) fractionation of olivine (for ONBs - also supported by Ryder and Steele [24]) and pigeonite (for QNBs). However, Ma et al. [25] stated that near-surface fractionation could not account for the observed trace element trends in the ONBs, but that mobilization of the residual liquid (filter pressing) during crystallization, or derivation from an inhomogeneous source were more likely processes. Butler [22] reported three groups, defined statistically, of Apollo 15 basalts, two of which were olivine normative. Vetter et al. [23] reported 3 types of ONB: 1) *low SiO<sub>2</sub> ONB* - low SiO<sub>2</sub> (44-46 wt%), high FeO (20-23 wt%) and TiO<sub>2</sub> (2.2-2.5%); 2) *high SiO<sub>2</sub> ONB* - high SiO<sub>2</sub> (47-48 wt%), high MgO (9.7-12.7 wt%), low TiO<sub>2</sub> (1.6-1.9 wt%) and FeO (19-20 wt%); and 3) *olivine-pyroxene cumulates* - highest MgO contents and lowest incompatible trace element abundances. Vetter et al. [23] concluded that the low-SiO<sub>2</sub> ONBs could not be parental

to the QNB suite, but it was possible that the high-SiO<sub>2</sub> ONBs could. This conclusion was based upon the similarity between the high-SiO<sub>2</sub> ONB composition reported by Vetter et al. [23] and the hypothetical QNB parental magma postulated by Chappell and White [26]. However, Vetter and Shervais [27] proposed a dynamic melting model to explain the similar REE patterns and abundances between the ONB and QNB suites (Fig. 8, after [23]). In this model, the high-SiO<sub>2</sub> ONBs are included in the QNB suite and the QNB suite is considered to have been generated before the ONB suite. The model assumes that 2-10% of the first melt is left behind in the residue as dikes. Three sources were postulated: 1) Cpx-rich source with late-stage LMO

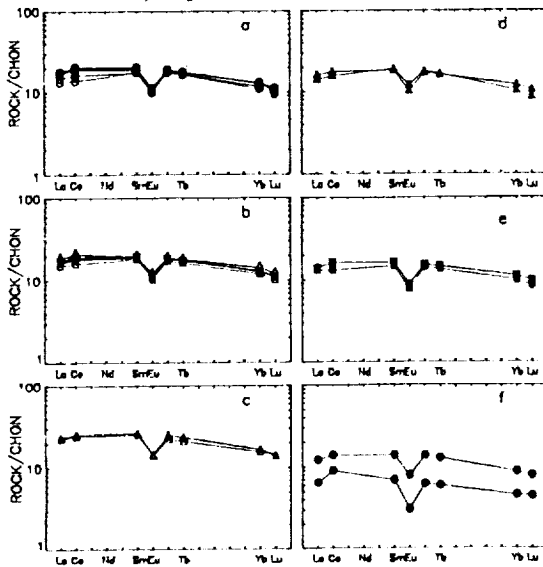
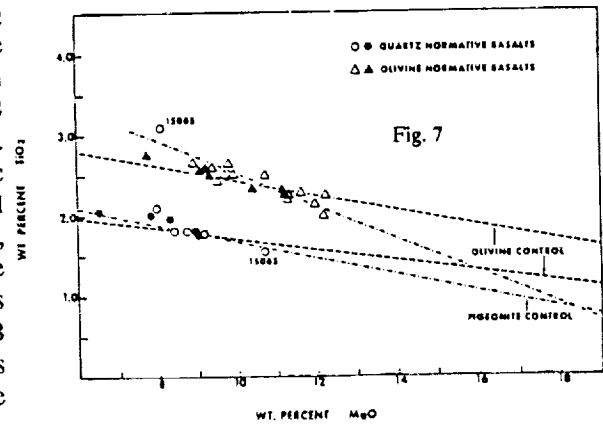
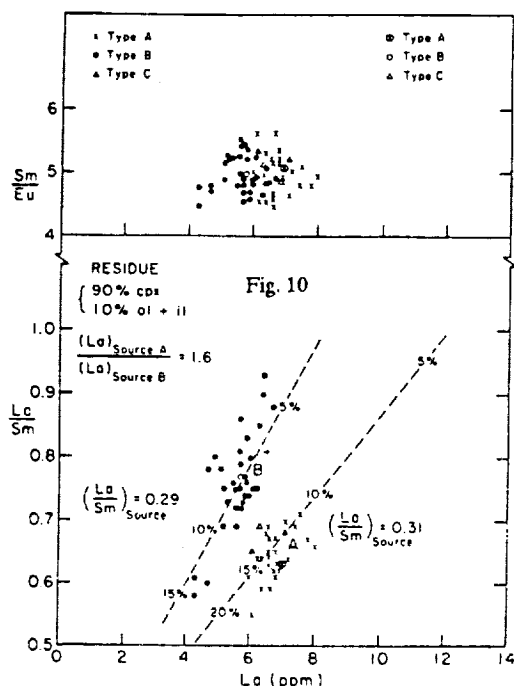
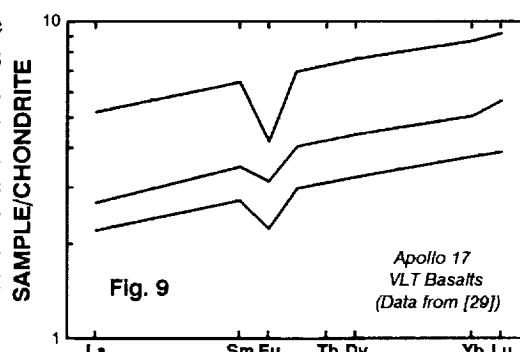


Fig. 8. Chondrite-normalized REE concentrations for 15498 basalts. (a) = primitive QNBs, (b) = intermediate-1 (boxes) and intermediate-2 (diamonds) QNBs, (c) = evolved QNBs, (d) = low-SiO<sub>2</sub> ONBs, (e) = high-SiO<sub>2</sub> ONBs, (f) = cumulate ONBs.

residual liquid (La = 30 x chondrites) produces the QNB parent after 25% partial melting: the ONB suite is produced after 20% melting of the residue (with 10% dikes); 2) olivine-rich source with late LMO trapped liquid (La = 30 x chondrites) - produces the QNB parent magma after 5-7% partial melting and the ONB suite are produced after 5-7% melting of the residue (with 5-9% dikes); and 3) olivine-rich source with early LMO trapped liquid (La = 10 x chondrites) produces the overall shape of the QNB parent after 4% partial melting, but abundances are low and 50% fractional crystallization is required to generate the absolute REE concentrations. Re-melting of this residue (with 5% dikes) produces the ONB, but again 50% fractional crystallization is required to generate REE abundances.

**APOLLO 17:** Two compositional types of mare basalt have been returned from the Apollo 17 site. The distinction is based upon TiO<sub>2</sub> content: 1) Very Low Ti (VLT) basalts (< 1 wt% TiO<sub>2</sub>; and 2) high-Ti basalts (> 7 wt% TiO<sub>2</sub>). The VLT basalts are rare at Apollo 17 [28-29], but

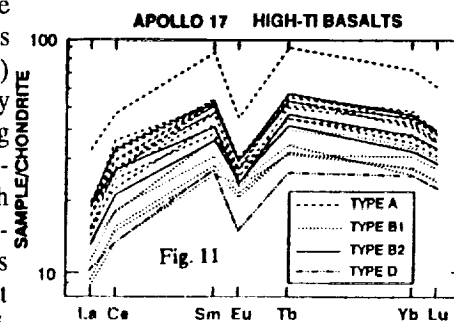
common at the Luna 24 (Mare Crisium) site [30-31]. These varieties are similar to the Apollo 12 and 15 low-Ti basalts but cannot be related to them by fractional crystallization [28]. The REE monotonically increase from La to Lu  $[(La/Lu)_N \sim 0.5]$  with a slight negative Eu anomaly [29] (Fig. 9). Although Wentworth et al. [29] stressed the problem of the small sample sizes of the VLTs yielding representative results, they demonstrated that the observed VLT liquid composition can be produced by 1-2% partial melting of a 90% olivine, 10% opx cumulate, assuming this cumulate crystallized from a melt with a flat REE pattern [29]. If this source cumulate formed from a



melt with a fractionated REE pattern [e.g.,  $(La/Lu)_N \sim 2$ ], then the VLT basalt REE pattern can be generated by  $\sim 4\%$  partial melting of a 70% olivine, 30% opx source [29].

The high-Ti basalts are common at Apollo 17 and have been extensively studied. The LIL elements resemble the Apollo 11 low-K (Type B) basalts. Longhi et al. [32] used experimental evidence to propose that the Apollo 17 high-Ti basalts were derived from an olivine, cpx, Fe-Ti oxide source at 100-150 km within the Moon. Shih et al. [33] noted the range of LIL element abundances in the Apollo 17 high-Ti basalts. These authors concluded that near-surface fractional crystallization was not important in the petrogenesis of these basalts, but multiple parental melts were required. These were derived from an inhomogeneous source of cpx, olivine, and ilmenite (Fig. 10), all of which remained in the residue. Rhodes et al. [34] defined three types of Apollo 17 high-Ti basalts - A, B, C. Type C is decidedly more primitive (e.g., higher MG#) than groups A and B. Rhodes et al. [34] concluded that within-group variation was produced by 4-22% fractional crystallization of olivine, armalcolite, ilmenite, and Cr-ulvöspinel. However, the chemical differences between the types was due to source heterogeneities. Warner et al. [35] also defined three types of high-Ti basalt (A, B, C). Types A and B

have similar major element compositions, suggesting similar source mineralogies - only the absolute abundances of trace elements in the respective sources differ. Differences in La/Sm vs. La (ppm) correlations suggested that Type A and B basalts were produced by multiple parents generated by varying degrees of partial melting (Fig. 10, after [35]). Ryder [36] described a Type D Apollo 17 high-Ti basalt, which is similar to the Type C's, but more primitive with lower REE abundances (Fig. 11, after [37]), but all are LREE-depleted. Ryder [36] went to great lengths to demonstrate that this Type D sample was a liquid, not a cumulate composition. Neal et al. [37] reported a further subdivision of the Apollo 17 high-Ti basalts. In this study, the Type B's were subdivided into B1 and B2 varieties (Fig. 12, after [37]) on the basis of trace element correlations. This dramatically reduced the range of La/Sm ratios of the Type B basalts. Neal et al. [37] concluded that, on the basis of whole-rock data, the Type A, B1, and B2 basalts were produced from distinct source regions, followed by closed-system fractional crystallization of olivine, Cr-ulvöspinel, armalcolite, ilmenite, and pyroxene. However, Paces et al. [38] used isotopic data to demonstrate that an open-system evolution (AFC???) was required for the Type B2 basalts. Source modeling for the Apollo 17 high-Ti basalts was undertaken by Hughes et al. [5], but these authors only took an average basaltic composition. According to the hybridization model proposed by Hughes et al. [5], the source required was

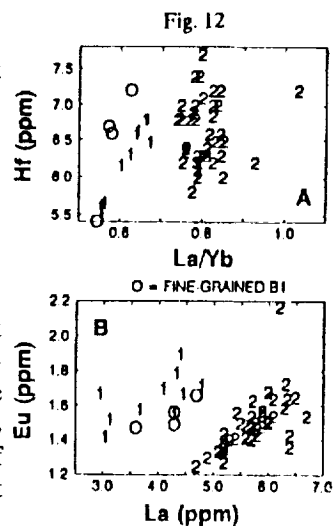


86.5% olivine, 6.47% augite, 3.07% plagioclase, 3.48% ilmenite, 0.052% apatite, and 0.44% trapped liquid with 15% partial melting. Paces et al. [38] and Neal et al. [39] used Rb/Sr ratios to demonstrate that the source regions of B2 and C basalts had been metasomatically enriched in the alkalis at  $\sim 4.1$  Ga. These authors suggested this metasomatic event may have been responsible for the trace-element diversity between Apollo 17 high-Ti basalts.

From the above review, it is evident that we have come along way to understanding the petrogenesis of mare basalts. One thing is noticeable from the above models and that is the problem of defining parental magma compositions. As petrogenetic models become more involved, it is evident that almost all basalts analyzed have experienced some degree of post-magma-generation modification. Therefore, the basaltic compositions used in source modeling must be carefully evaluated in order not to yield misleading results (see Snyder and Taylor [40], for discussion of this problem). It is this facet of mare basalt petrogenetic modeling which can be thoroughly evaluated now that primitive (primary?), parental magmas have been more adequately defined.

Previous source modeling must be re-evaluated in order to discard the misleading results produced by using basalts which have experienced modification since their generation. Ultimately, this will lead to a better understanding of the lunar mantle and allow a sturdy test of the LMO hypothesis.

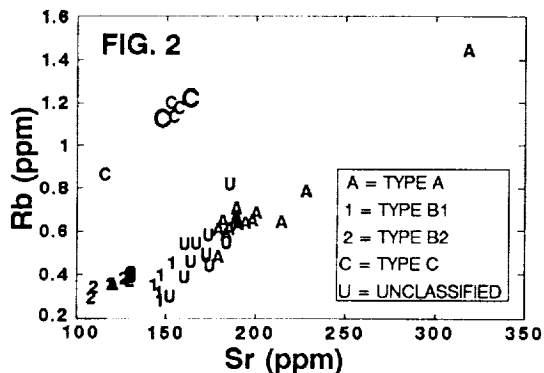
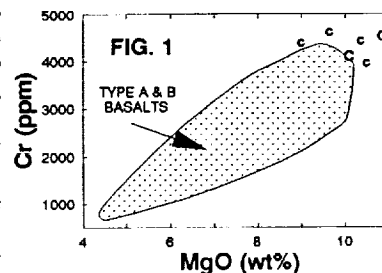
**REFERENCES** - [1] Beatty et al. (1979) *PLPSC 10th*, 41-75; [2] Beatty and Albee (1978) *PLPSC 9th*, 359-463; [3] Ma et al. (1980) *PLPSC 11th*, 37-47; [4] Rhodes and Blanchard (1980) *PLPSC 11th*, 49-66; [5] Hughes et al. (1989) *PLPSC 19th*, 175-188; [6] Rhodes et al. (1977) *PLSC 8th*, 1305-1338; [7] Beatty et al. (1979) *PLPSC 10th*, 115-139; [8] Nyquist et al. (1979) *PLPSC 10th*, 77-114; [9] Warner et al. (1980) *PLPSC 11th*, 87-104; [10] Dickinson et al. (1985) *PLPSC 15th*, in *JGR 90*, C365-C374; [11] Shervais et al. (1985) *PLPSC 15th*, in *JGR 90*, C375-C395; [12] Shervais et al. (1984) *LPS XV*, 768-769; [13] Shervais et al. (1985) *PLPSC 16th*, in *JGR 90*, D3-D18; [14] Goodrich et al. (1986) *PLPSC 16th*, in *JGR 91*, D305-D318; [15] Shih et al. (1986) *PLPSC 16th*, in *JGR 91*, D214-D228; [16] Unruh et al. (1984) *PLPSC 14th*, in *JGR 89*, B459-B477; [17] Neal et al. (1988) *PLPSC 18th*, 139-153; [18] Neal et al. (1989) *PLPSC 19th*, 147-161; [19] Hughes et al. (1990) *LPS XXI*, 540-541; [20] Dickinson et al. (1989) *PLPSC 19th*, 189-198; [21] Rhodes et al. (1973) *PLSC 4th*, 1127-1148; [22] Butler (1976) *PLSC 7th*, 1429-1447; [23] Vetter et al. (1988) *PLPSC 18th*, 255-271; [24] Ryder and Steele (1988) *PLPSC 18th*, 273-282; [25] Ma et al. (1978) *PLPSC 9th*, 523-533; [26] Chappell and Green (1973) *EPSL 18*, 237-246; [27] Vetter and Shervais (1989) *LPS XX*, 1152-1153; [28] Vaniman and Papike (1977) *PLSC 8th*, 1443-1471; [29] Wentworth et al. (1979) *PLPSC 10th*, 207-223; [30] Haskin (1978) *Mare Crisium: The View from Luna 24*, 593-611, Pergamon; [31] Taylor et al. (1978) *Mare Crisium: The View from Luna 24*, 357-370, Pergamon; [32] Longhi et al. (1974) *PLSC 5th*, 447-469; [33] Shih et al. (1975) *PLSC 6th*, 1255-1285; [34] Rhodes et al. (1976) *PLSC 7th*, 1467-1489; [35] Warner et al. (1979) *PLPSC 10th*, 225-247; [36] Ryder (1988) *LPS XIX*, 1013-1014; [37] Neal et al. (1990) *GCA 54*, 1817-1833; [38] Paces et al. (1990) *LPS XXI*, 926-927; [39] Neal et al. (1990) *LPS XXI*, 855-856; [40] Snyder and Taylor (this Workshop).



## IDENTIFICATION & ORIGIN OF SOURCE HETEROGENEITIES FOR APOLLO 17 BASALTS USING ISOTOPIC TRACERS.

Clive R. NEAL\* & Lawrence A. TAYLOR, Dept. of Geological Sciences, University of Tennessee, Knoxville, TN 37996; James B. PACES, USGS Isotope Branch, M.S. 963, Denver, CO 80225; Alex N. HALLIDAY, Dept. of Geological Sciences, University of Michigan, Ann Arbor, MI 48109. (\* Now at: Dept. of Earth Sciences, University of Notre Dame, Notre Dame, IN 45565).

The Apollo 17 mission returned a large quantity of high-Ti basaltic material which has permitted an in-depth evaluation of basalt petrogenesis and source evolution at this site. Two types of Apollo 17 high-Ti basalts (A and B) were originally defined on the basis of trace element abundances [1]. Three basaltic types (A, B, C) were subsequently defined on the basis of whole-rock chemistry using only fine-grained basalts to avoid sampling errors [2,3]. Type A basalts contain 50-60% higher abundances of incompatible trace elements than Type B basalts. Neal et al. [4,5] recently demonstrated that the Type B basalts can be split into two "Groups" (B1 and B2) on the basis of incompatible trace-element abundances. Type C basalts are rare, only being described from Station 4 at Shorty Crater. These basalts are distinct from the Type A, B1, and B2 variants as they contain elevated MgO and Cr<sub>2</sub>O<sub>3</sub> contents along with relatively high incompatible element abundances [2] (Fig. 1). In particular, Rb abundances and Rb/Sr ratios are elevated relative to the Type A, B1, and B2 basalts [6-8], and Type C basalts are mineralogically distinct as they contain olivines with the highest Fo contents (up to Fo<sub>80</sub> - [2,3]). Originally, Sr isotope data were not able to clearly resolve differences in age or initial <sup>87</sup>Sr/<sup>86</sup>Sr ratios between any of the different magma types [6,9,10]. This led to conclusions that large differences in Rb/Sr ratios between the basaltic types were caused during magma genesis [6], which in turn required CPX as a residual phase [6,11]. Data presented by Paces et al. [7,8] allowed the recognition of Sr and Nd isotopic differences between the previously defined chemical groups. These authors demonstrated closed-system evolution for all types of Apollo 17 basalt, except the Type B2's which appeared to have experienced a complex AFC petrogenesis.



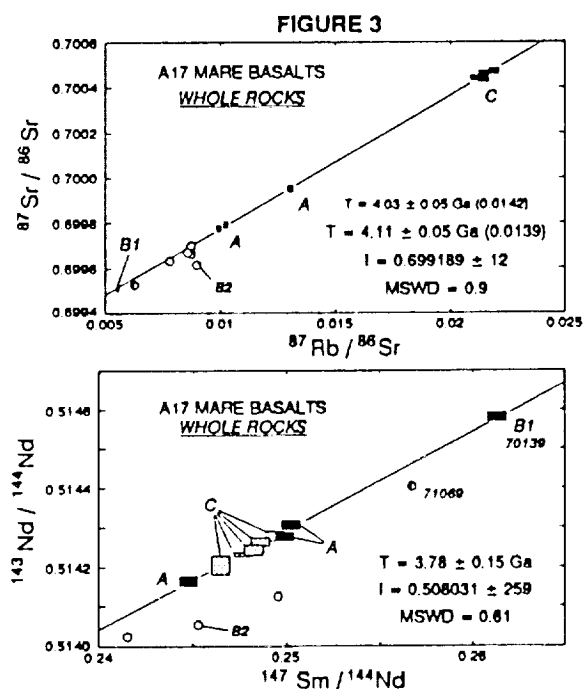
**RELATIONSHIPS BETWEEN TYPE A, B1, B2, AND C BASALTS:** If the primitive Type C magmas (Fig. 1) are parental to the more evolved Type A, B1, and B2 Apollo 17 high-Ti basalts, their incompatible trace-element abundances should be lower. However, Type C basalts contain higher REE contents than both Type B basalts and similar REE abundances and profiles to Type A basalts. Type C basalts also contain elevated alkali element abundances, in particular Rb, relative to all other types of Apollo 17 high-Ti basalts (Fig. 2), where only data obtained by isotope dilution techniques have been plotted. Although one of the most evolved Type A basalts (71095) contains a high Rb abundance, it possesses a typical Type A Rb/Sr ratio. Clearly, the higher Rb/Sr ratio of the Type C basalts cannot be generated from a Type A, B1, or B2 magma by fractionation of observed phenocryst phases. Such a conclusion is supported by the isotope data.

**WHOLE-ROCK ISOCHRONS:** Types A, B1, and C magmas form remarkably well-defined linear arrays on Sr and Nd isochron plots (Fig. 3). These relationships cannot be caused by two-component mixing since consistent end-members cannot be established. For example, Type C basalts contain the highest Rb/Sr ratios but only intermediated Sm/Nd ratios (Fig. 3). In addition, the samples do not form linear arrays on isotopic ratio versus elemental abundance plots [7]. Therefore, we interpret the linear arrays as isochrons with potential age significance. The resulting Sr whole-rock isochron age of  $4.11 \pm 0.05$  Ga (95% confidence;  $\lambda^{87}\text{Rb} = 0.0139$  b.y.<sup>-1</sup>) is very precise, but 350-450 Ma older than the eruptive ages of the basalts [6,8,11]. The less-precise Nd whole-rock isochron age is identical to the eruption age of Types A and C basalts and within error of the eruption age of Type B basalts. The Rb-Sr isochron suggests that the source regions for Apollo 17 high-Ti basalts had a homogeneous <sup>87</sup>Sr/<sup>86</sup>Sr composition of  $0.699189 \pm 12$  at 4.11 Ga. This age conflicts with the generally accepted crystallization age of magma ocean cumulates of approximately 4.4 Ga [12-14]. The possibility of Rb-Sr fractionation during magma generation will limit the significance of whole-rock isochron ages, and it has been argued that any such age will probably represent an *upper limit* to the age of source region formation [13]. Paces et al. [7,8] and Neal et al. [15] argued for the closed-system evolution of the Type A, B1, and C basalts which were derived from isotopically distinct source regions. This, combined with the arguments presented above and the high precision of the whole-rock isochron, offers a strong case for attaching significance to the 4.11 Ga age.

**ORIGIN OF THE SOURCE HETEROGENEITIES:** Although Type A, B1 and C basalts fall along well defined Rb-Sr and Sm-Nd whole-rock isochrons, Type C basalts exhibit distinctly higher <sup>87</sup>Sr/<sup>86</sup>Sr at the time of magma genesis. Tight clustering of whole-rock compositions and concordance on whole-rock isochron plots (Fig. 3), also suggest that Type C basalts did not experience post-magma-generation modifications similar to those affecting Type B2 magmas. Furthermore, there are significant age differences between Type A, B1, B2, and C magmas [8]. This evidence, along with arguments presented above indicates that the different magma types at Apollo 17 cannot be related to each other through a common parent magma fractionating in either a closed or open system.

Backward projection of average A, B1, and C isotopic compositions from present-day data (solid and dashed lines in Fig. 4) shows  $\epsilon_{\text{Nd}}$  paths converging near the age of Apollo 17 high-Ti magmatism, whereas the <sup>87</sup>Sr/<sup>86</sup>Sr paths converge on the more ancient, whole-rock T<sub>1</sub>(Sr) values. Further extrapolation of the B1 Sr path back to 4.4 Ga (assumed age of the formation of magma ocean cumulates)

## IDENTIFICATION AND ORIGIN OF SOURCE HETEROGENEITIES: Neal et al.



is nearly coincident with previous models of LUNI and Bulk Moon evolution [6,14,16]. The close agreement between present-day  $^{87}\text{Rb}/^{86}\text{Sr}$  and the 4.4-3.66 Ga model value is interpreted as additional evidence for the lack of Rb-Sr fractionation at the time of magma genesis. Previous Nd-Hf modelling requires that the A17 basalt source contained OPX:CPX:OLV:ILM in the proportions 30-65:8-18:59-14:3-3 with the basalts representing 10-15% partial melts [17]. We conclude that the isotopic arguments presented here are compatible with a melting model where all CPX enters the melt so that Rb/Sr in the melt retains its source composition, while Sm/Nd in the melt is substantially lowered (assuming OPX:OLV residue and partition coefficients from [16,17]). The high MgO, MG#, and  $\text{Cr}_2\text{O}_3$  contents of the Type C basalts (Fig. 1) can be generated by a source which contains relatively more opx and olivine (+ chromite?) and relatively less cpx than the Type A and B1 source regions. However, the Type C source maintained a LREE-depleted signature, and possessed REE abundances similar to those of the Type A source.

We further conclude that the source regions for the Type A, B1, and C had homogeneous  $^{87}\text{Sr}/^{86}\text{Sr}$  ratios at  $4.11 \pm 0.05$  Ga, suggesting that an originally homogeneous Apollo 17 high-Ti basalt source region was modified at  $\sim 4.1$  Ga by a process which affected at least the Rb-Sr systematics. Since Type B1 magmas contain  $^{87}\text{Rb}/^{86}\text{Sr}$  ( $\sim 0.005$ ) coincident with the hypothesized magma ocean cumulates [6], the elevated Type C  $^{87}\text{Rb}/^{86}\text{Sr}$  ratios ( $\sim 0.021$ ) are due to enrichment of a B1-like source, rather than the B1 source representing a depleted residue of a Type C source after melt extraction (Figs. 3 & 4). The Type C basalt source has experienced a four-fold increase in  $^{87}\text{Rb}/^{86}\text{Sr}$  ratio due to an influx of Rb (Fig. 4). This cannot be produced by varying the degree of partial melting relative to that required for Type A and B1 magma genesis as La/Sm ratios are similar, suggesting similar degrees of partial melting (see above). Furthermore, partial melting has not modified the Rb/Sr ratio of the Type A, B1, or C basalt source, as all cpx was removed during melting. This allows the recognition of the 4.11 Ga source-modification event.

The whole-rock Sm-Nd isochron, yielding an age close to the average crystallization age for these basalts ( $3.78 \pm 0.15$  Ga), suggests that Sm/Nd ratios have been modified by partial melting [7]. As Type A, B1, & C basalts have been produced by similar degrees of partial melting (above and Fig.3), modification of the REE at  $\sim 4.1$  Ga must have: (a) affected the REE of each source in a similar manner; or (b) did not affect the REE. This suggests that source regions for the Type A, B1, & C basalts possessed similar REE profiles, although the Type C source possessed higher REE abundances than in the Type B1 and similar to that of the Type A sources.

**NATURE OF SOURCE ENRICHMENT:** There are several candidates which can be used to enrich the Type C source region in alkalis: (a) KREEP; (b) lunar granite (the "K-Fraction" of [18]); and (c) volatile-rich fluids. Apollo 17 KREEPy basalts [19-21] were erupted at  $4.01 \pm 0.04$  Ga [17]. If these compositions are mixed into a Type B1 source to generate that for the Type C basalts, addition of 10-15% KREEP is required. While this can adequately generate the Rb and Sr abundances and ratios, such enrichment will radically alter the Sm-Nd systematics, for which we have no evidence, in addition to the REE ratios, for which we have contrary evidence. Also, addition of KREEP to the Type C source region will introduce radiogenic Sr, for which there is no evidence. Furthermore, the Sm-Nd and Rb-Sr whole-rock isochrons defined by Type A, B1, and C basalts (Fig. 3) should represent mixing lines, if KREEP progressively metasomatized the A and C source regions and such correlations would have no age significance. If so, the Type A, B1, and C basalts should plot in the same positions on each isochron although in the opposite sense (i.e., the most radiogenic Sr end-member should be the least radiogenic Nd end-member). This is not the case. Finally, if KREEP variably metasomatized the homogeneous source at  $\sim 4.1$  Ga, the intercept of  $^{87}\text{Sr}/^{86}\text{Sr}$  ratios would not be expected to lie on the magma ocean cumulate evolution path. Enrichment of the Type C source region by the "K-Fraction" (lunar granite) is possible, as it contains high Rb abundances [13]. However, it also contains up to 80 ppm Nd and 22 ppm Sm, with a Sm/Nd ratios of  $\sim 0.25-0.3$  [13] - Type C basalts possess a Sm/Nd ratio of  $\sim 0.4$ . Addition of this component to the homogeneous Apollo 17 high-Ti basalt source region at  $\sim 4.1$  Ga would lead to different Sm/Nd, La/Sm, and

$^{143}\text{Nd}/^{144}\text{Nd}$  ratios between the different sources at the time of magma genesis. Also, because of the viscous nature of this melt [22], it would be unable to percolate through and metasomatise the Type C basalt source.

*The most likely metasomatizing agent is an alkali-rich/REE-poor fluid.* Evidence for such fluids have been documented on the surface of Apollo 17 glasses, where the halogen-rich sublimates contain substantial quantities of alkalis. However, there are no reports of REE in these volatile-rich fluids [23-24]. Percolation of these fluids through a Type B1 source region at  $\sim 4.1$  Ga will modify the Rb/Sr ratio, while leaving the Sm/Nd and La/Sm ratios unaffected. Evidence for fluid/magma migration around 4.1 Ga is found in basalt and granite clasts from Apollo 14 breccias [25-27], and KREEP basalt clasts from Apollo 17 breccias [22].

References: [1] Warner et al. (1975) *PLSC 6th*, 193-220; [2] Rhodes et al. (1976) *PLSC 7th*, 1467-1489; [3] Warner et al. (1979) *PLPSC 10th*, 225-247; [4] Neal et al. (1990) *GCA* 1817-1833; [5] Neal et al. (1990) *LPS XXI* 857-858; [6] Nyquist et al. (1976) *PLSC 7th*, 1507-1528; [7] Paces et al. (1990) *LPS XXI* 926-927; [8] Paces et al. (1990) *LPS XXI* 924-925; [9] Nyquist et al. (1974) *PLSC 5th*, 1515-1539; [10] Nyquist et al. (1975) *PLSC 6th*, 1445-1465; [11] Shih et al. (1975) *PLSC 6th*, 1255-1285; [12] Carlson and Lugmair (1979) *EPSL* 45, 123-132; [13] Nyquist et al. (1979) *PLPSC 10th*, 77-114; [14] Nyquist et al. (1981) *EPSL* 55, 335-355; [15] Neal et al. (1990) *LPS XXI*, 855-856; [16] Nyquist et al. (1977) *PLSC 8th*, 1383-1415; [17] Unruh et al. (1984) *PLPSC 14th*, in *JGR* 89, B459-B477; [18] Neal et al. (1989) *GCA* 53, 529-542; [19] Ryder et al. (1975) *The Moon* 14, 327-358; [20] Ryder et al. (1977) *EPSL* 35, 1-13; [21] Salpas et al. (1987) *PLPSC 17th* in *JGR* 92, E340-E348; [22] Compston et al. (1975) *The Moon* 14, 445-462; [23] Butler and Meyer (1976) *PLSC 7th*, 1561-1582; [24] Cirlin and Houseley (1979) *PLPSC 10th*, 341-354; [25] Taylor et al. (1983) *EPSL* 66, 33-47; [26] Shih et al. (1985) *GCA* 49, 411-426; [27] Dasch et al. (1987) *GCA* 51, 3241-3254.

**THE HISTORY OF LUNAR VOLCANISM.** L. E. Nyquist, SN2, NASA Johnson Space Center, Houston, TX 77058 and C.-Y. Shih, C-23, Lockheed Engineering and Science Co., 2400 NASA Road 1, Houston, TX 77258.

The timing and extent of volcanism must have reflected the internal thermal evolution of the moon and a knowledge of the history of lunar volcanism is important for understanding the global evolution of the moon. Recent studies show that lunar volcanism began prior to formation of at least some of the major lunar basins, although the exact provenance of the earliest volcanism remains somewhat obscure.

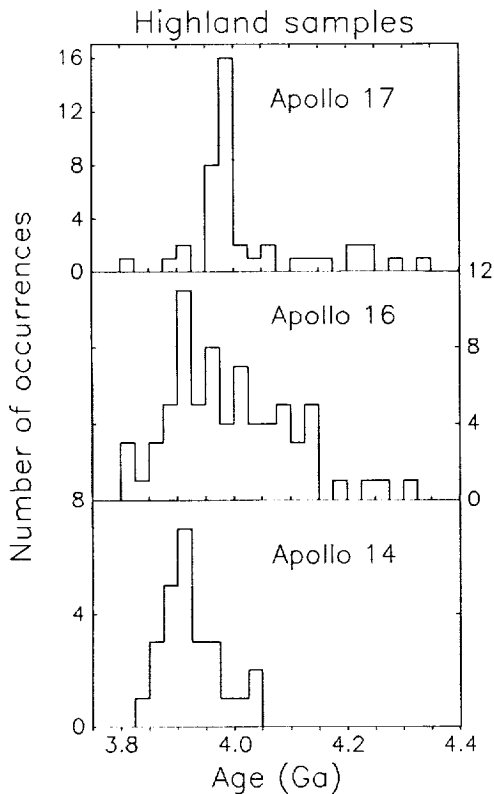


**Figure 1.**  $^{39}\text{Ar}$ - $^{40}\text{Ar}$  ages of lunar highlands samples. From Basaltic Volcanism Study Project (29).

The effects of the so-called "late, heavy bombardment", during which most of the major lunar basins are thought to have been formed, must be considered when evaluating the radiometric ages of lunar samples. The product of this bombardment was impact-lithified breccias, composed dominantly of fine-grained matrix material. Numerous  $^{39}\text{Ar}$ - $^{40}\text{Ar}$  studies of breccias collected at the highland landing sites have shown the predominance of ages in the interval  $\sim 3.85$  -  $\sim 4.0$  Ga (Figure 1). However, analyses of clastic materials also yielded higher ages and it is this clastic material which has received the most recent attention. The development of techniques for recognizing pristine clasts consisting of a single pre-impact lithology has been of vital importance for determining meaningful ages.

Figure 2 summarizes available age data for pristine clasts of lunar plutonic highland rocks as determined by the  $^{39}\text{Ar}$ - $^{40}\text{Ar}$ , Rb-Sr, Sm-Nd, and U-Pb methods. Multiple entries are shown for a single rock when its age has been determined by more than one method. Entries for individual rocks are not identified and thus age discordances are suppressed. (Rb-Sr ages would be reduced by 2% for the value recommended by (1), or 1% for the value found by (2) for a comparison of the Rb-Sr and U-Pb ages of chondrites). The central point of the figure is that each highland lithology is represented by a variety of ages, with the possible

exception of the ferroan anorthosites. Very old ( $>4.4$  Ga) ages have been postulated for ferroan anorthosites because of their very primitive  $^{87}\text{Sr}/^{86}\text{Sr}$  ratios. Carlson and Lugmair (3) and Hanan and Tilton (4) have confirmed this expectation by the Sm-Nd and U-Pb methods, respectively. Some of the younger ages determined by the  $^{39}\text{Ar}$ - $^{40}\text{Ar}$  method for the ferroan anorthosites could be biased towards low values because of Ar loss due to impact-associated reheating; a point requiring resolution since the ferroan anorthosites are the best candidates to be remnants of the postulated lunar magma ocean.

The Mg-suite rocks are the second major category of highland rocks. Very old ages  $\sim 4.5$ - $4.6$  Ga reported for a dunite and a troctolite (5,6) have been controversial because a discordant, lower age of  $4.26 \pm 0.06$  Ga was found for the troctolite by the Sm-Nd method (7). Carlson and Lugmair (8) found Sm-Nd ages of 4.2-4.3 Ga for a number of Mg-suite norites and gabbro-norites, and favored an age of  $\sim 4.33$  Ga for norite 78236. The Sm-Nd system of 78236 has been disturbed and Nyquist et al. (9) argued for

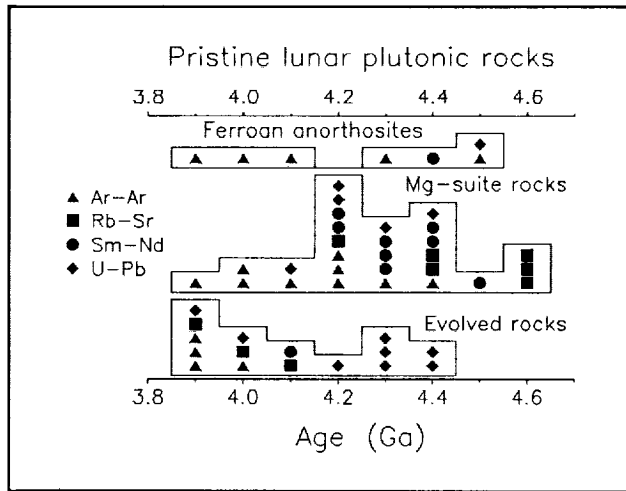


Figure 2. Ages of pristine lunar plutonic rocks. Rb-Sr ages are reported for  $\lambda(^{87}\text{Rb}) = 0.0139 \text{ Ga}^{-1}$ .

have been determined from U-Pb analyses of individual zircons (cf. 12). The ages of the evolved rocks are variable in the range ~3.9-4.4 Ga as also can be inferred from Rb-Sr and Sm-Nd mineral isochrons for granitic clasts from Apollo 14 and 17 breccias and the Rb-Sr model age of granitic breccia 12013.

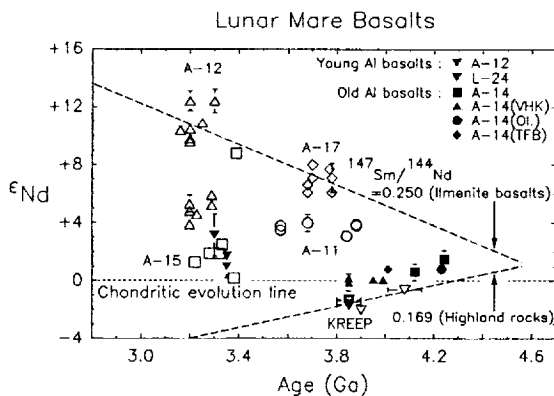


Figure 3.  $\epsilon_{\text{Nd}}$  vs. age for lunar basalts.

greatly and similarly depleted in LREE beneath the widely separated landing sites in Oceanus Procellarum, Mare Imbrium, and Mare Serenitatus, an observation supportive of a global process of differentiation. It also may be significant that those aluminous "mare" basalts which so far have been recognized only as clastic fragments in Apollo 14 highland breccias plot along or parallel to the lunar crustal growth curve for  $^{147}\text{Sm}/^{144}\text{Nd} \sim 0.17$  defined by highland rocks. The growth curves for highland rocks and highly LREE-depleted lunar mare basalt source regions intersect at ~4.45-4.55 Ga, consistent with the postulated early global differentiation of the moon.

Figure 4 reports ages of KREEPy basalts. Only the Apollo 15 samples and the three oldest Apollo 17 samples are pristine, igneous rocks. The other samples are impact melt rocks and have ages in the range ~3.8-3.9 Ga, typical of the late, heavy bombardment (Figure 1). The apparent close association of KREEPy impact melts with the formation of the large impact basins has led to considerable confusion about their

an older age of ~4.43 Ga from data for mineral phases retaining both old Sm-Nd and old Rb-Sr ages. Recent U-Pb analyses of the sister sample 78235 by Premo and Tatsumoto (10) confirm an old age of ~4.43 Ga for these norites. A Sm-Nd age of  $4.46 \pm 0.07$  Ga has also been found for norite 15445,17 and an old age of  $4.59 \pm 0.13$  Ga ( $\lambda(^{87}\text{Rb}) = 0.0139 \text{ Ga}^{-1}$ ) is indicated by Rb-Sr data for anorthositic norite clast 15455,228 (11). Thus, the evidence is strong that at least some Mg-suite rocks formed early in lunar history, whereas others formed significantly (~200-400 Ma) later.

Highly evolved granites and quartz-monzodiorites comprise a third suite of lunar highland rocks. The majority of ages for these types of rocks

The existence of ancient, highly evolved rocks was recognized early in the Apollo program as evidence for early differentiation of the moon. This conclusion has been confirmed by later isotopic studies, most notably Sm-Nd studies of both mare basalts and highland rocks. Figure 3 summarizes  $\epsilon_{\text{Nd}}$  values for lunar basalts as a function of age, landing site and composition. Common mare basalts have positive  $\epsilon_{\text{Nd}}$  bounded by the chondritic evolution line and a growth curve for  $^{147}\text{Sm}/^{144}\text{Nd} \sim 0.25$ . Significantly, basalts from the Apollo 12, 15, and 17 landing sites lie along this growth curve which corresponds to the maximum observed depletion of LREE for lunar mantle source regions. It can be inferred that the lunar mantle is



through the crust to the lunar surface.

Figure 5 also displays the well-known age relationships among the common mare basalts collected at the Apollo and Luna sites: "middle-aged" (3.6-3.9 Ga) high Ti basalts at the Apollo 11 and 17 sites, and "young" (3.2-3.4 Ga) low and very low Ti basalts at the Apollo 12, Apollo 15, and Luna 24 sites. The correlation between  $TiO_2$  contents and age may be only apparent since Pieters (24) concluded that only  $\sim 1/3$  of the lunar basalt units have been sampled and Boyce (25) concluded that some of the unsampled high-Ti basalts are also young. No correlation between age and composition is found for aluminous mare basalts, among which both old (Apollo 14) and young (Apollo 12 and Luna 16) examples can be found. An interesting observation is that none of the common mare basalts appear to carry the KREEP (or highland) signature in  $\epsilon_{Nd}$  (Figure 3), suggesting that if this signature is due to assimilation of a KREEP-rich component, the assimilant was isolated or stripped away during the formation of the basins into which the mare basalts later flowed.

Important features of the isotopic record of lunar volcanism are most simply explained by the "standard model": development of a lunar magma ocean, solidification of a plagioclase-rich crust accompanied by formation of a mantle enriched in the complementary mafic minerals, genesis of common mare basalts by remelting this mantle, etc. However, petrogenetic processes occurring between lunar formation and cessation of the late, heavy bombardment appear to have been complex and not directly explained by the standard model. The variable ages of most types of lunar crustal rocks are more consistent with petrogenesis via "serial magmatism" (26) than with solidification from a magma ocean. Pre-mare volcanics have different trace element and isotopic signatures than the common mare basalts and seem to be characterized by assimilation of pre-existing materials. Preservation of a LIL-element enriched residuum of the magma ocean just below the lunar crust and at a temperature near the solidus for  $\sim 350$  Ma, as predicted by several thermal models (27,28) seems to provide both an environment and an opportunity for complex petrogenetic processes in the "pre-cataclysm" time frame. Lunar volcanism may have continued to somewhat later times than the  $\sim 3.2$  Ga ago recorded in the lunar samples. Boyce (25) argues from photogeologic studies that volcanism persisted to at least  $2.6 \pm 0.3$  Ga ago in large areas of western Oceanus Procellarum, whereas the cratering team of the Basaltic Volcanism Study Project (29) estimated that mare volcanism may have extended to  $\sim 2.9$  ( $+0.6/-0.9$ ) Ga ago in inner Mare Serenitatis.

**REFERENCES:** (1) Steiger R.H. and Jaeger E. (1977) *Earth Planet. Sci. Lett.* **36**, 359-362. (2) Minster J.F., Birck J.L., and Allegre C.J. (1982) *Nature* **300**, 414-418. (3) Carlson R.W. and Lugmair G.W. (1988) *Earth and Planet. Sci. Lett.* **90**, 119-130. (4) Hanan B.B. and Tilton G.R. (1987) *Earth Planet. Sci. Lett.* **84**, 15-21. (5) Papanastassiou D.A. and Wasserburg G.W. (1975) *Proc. Lunar Sci. Conf.* **6th**, 1467-1489. (6) Papanastassiou D.A. and Wasserburg G.W. (1976) *Proc. Lunar Sci. Conf.* **7th**, 2035-2054. (7) Lugmair G.W., Marti K., Kurtz J.P., and Scheinen N.B. (1976) *Proc. Lunar Sci. Conf.* **7th**, 2009-2033. (8) Carlson R.W. and Lugmair G.W. (1981) *Earth and Planet. Sci. Lett.* **52**, 227-238. (9) Nyquist L.E., Reimold W.U., Bogard D.D., Wooden J.L., Bansal B.M., Wiesmann H., and Shih C.Y. (1981) *Proc. Lunar Sci. Conf.* **12th**, B67-B97. (10) Premo W.R. and Tatumoto M. (1990) *Lunar and Planet. Sci.* **XXI**, 977-978. (11) Shih C.-Y., Nyquist L.E., Dasch E.J., Bogard D.D., Bansal B.M., and Wiesmann H. (1990) to be submitted to *Geochim. Cosmochim. Acta*. (12) Meyer C. Jr., Williams I.S., and Compston W. (1988) *Workshop on Moon in Transition: Apollo 14, KREEP, and Evolved Lunar Rocks*, 39-42, Lunar and Planetary Institute, Houston. (13) Nyquist L.E. (1977) *Phys. Chem. Earth*, Vol. **10**, 103-142. (14) Leich D.A., Kahl S.B., Kirschbaum A.R., Niemeyer S., and Phinney D. (1975) *The Moon*, **14**, 407-444. (15) Compston W., Foster J.J., and Gray C.M. (1975) *The Moon*, **14**, 445-462. (16) Shih C.-Y., Nyquist L.E., Bansal B.M., and Wiesmann H. (1990) to be submitted to *Earth and Planet. Sci. Lett.* (17) Meyer C. (1977) *Phys. Chem. Earth* **10**, 239-260. (18) Taylor L.A., Shervais J.W., Hunter R.H., Shih C.-Y., Bansal B.M., Wooden J., Nyquist L.E., and Laul J.C. (1983) *Earth Planet. Sci. Lett.* **66**, 33-47. (19) Dasch E.J., Shih C.-Y., Bansal B.M., Wiesmann H., and Nyquist L.E. (1987) *Geochim. Cosmochim. Acta*, **51**, 3241-3254. (20) Dickinson T., Taylor G.J., Keil K., Schmitt R.A., Hughes S.S., and Smith M.R. (1985) *Proc. Lunar Sci. Conf.* **15th**, C365-C374. (21) Shervais J.W., Taylor L.A., and Lindstrom M.M. (1985) *Proc. Lunar Planet. Sci. Conf.* **15th**, C375-C395. (22) Shih C.-Y., Nyquist L.E., Bogard D.D., Dasch E.J., Bansal B.M., and Wiesmann H. (1987) *Geochim. Cosmochim. Acta*, **51**, 3255-3271. (23) Warren P.H. and Wasson J.T. (1980) *Proc. Conf. Lunar Highland Crust*, 81-99. (24) Pieters C.M. (1978) *Proc. Lunar Planet. Sci. Conf.* **9th**, 2825-2849. (25) Boyce J.M. (1976) *Proc. Lunar Sci. Conf.* **7th**, 2717-2728. (26) Walker D. (1983) *Proc. Lunar Planet. Sci. Conf.* **14th**, B17-B25. (27) Solomon S. and Longhi J. (1977) *Proc. Lunar Sci. Conf.* **8th**, 583-599. (28) Hubbard N.J. and Minear J.W. (1975) *Proc. Lunar Sci. Conf.* **6th**, 1057-1085. (29) Basaltic Volcanism Study Project (1981) Pergamon Press, 1286 pp. New York. (30) Neal C.R., Taylor L.A., and Lindstrom M.M. (1988) *Proc. Lunar Planet. Sci. Conf.* **18th**, 139-153.

**THE PROBABLE CONTINUUM BETWEEN EMPLACEMENT OF PLUTONS AND MARE VOLCANISM IN LUNAR CRUSTAL EVOLUTION** Carle M. Pieters, Brown University, Providence RI 02912

**Facts and generally accepted information**

- Ages of basaltic surface units sampled by the Apollo and Luna missions have been measured directly in the laboratory and range from around 3.2 to 3.9 Ga [1]. Crater degradation analyses indicate ages of unsampled basalt units can extend to about 2.0 Ga [2]. Superposition arguments for the Lichtenberg region suggest limited deposits with even younger ages [3].
- A great diversity of mare basalt types exist within the lunar sample collections [4]. Remote sensing studies show that only about 1/3 of basalts that exist as extensive surface units on the nearside have been directly sampled [5].
- "Pristine" samples of the original lunar crust that somehow escaped the brecciation transformation suffered by most highland materials continue to be identified [e.g. 6]. These pristine samples form two distinct suites with different chemical trends [7]: the ferroan anorthosites (hypothesized to be remnants from a magma ocean scale differentiation) and the Mg-rich suite (hypothesized to represent intrusions or plutons emplaced within the plagioclase-rich crust). Although compositional trends observed for the two suites of pristine materials are similar to those observed for materials found at the Stillwater, a classic layered mafic intrusion, these two lunar suites are not believed to be directly related based on other geochemical and isotopic properties [7, 8].
- As components of the original lunar crust, the pristine lunar samples are naturally old, clustering near 4.3 Ga, but with the oldest almost 4.5 Ga. There is no clear age relation between the Ferroan and the Mg-rich suites, although it is assumed the Mg-rich suite must be later [1, 7].

**Additional new information.**

- Fragments of mare basalts have been found in the sample collection with ages as old as 4.2 Ga [9]. The existence of ancient volcanism partially covered by subsequent lighter deposits has been argued on the basis of orbital chemistry, albedo, and reflectance spectroscopy [3, 10].
- A variety of surface compositions ranging from what is almost certain to be anorthosite to compositions consistent with several Mg-suite/KREEP rock types have been identified for areally extensive highland regions overflowed by the Apollo gamma ray experiment [11]. This variety is particularly important information about the farside highland crust, which is presumed to be thicker than the nearside and to contain only minor amounts of mare-like volcanism.
- A diversity of rock types reminiscent of layered mafic plutons have been identified at higher spatial resolution using large nearside craters as probes to the interior [12]. The classic example is at Copernicus, where the dunite-troctolite central mountains range about factor of three in olivine abundance [13]. Additional examples of deep-seated rock types distinct from the noritic anorthosite breccias that apparently dominate the nearside highland megaregolith [12] include the clinopyroxene-rich gabbro pervasive at Tycho [14, 12], the clinopyroxene-rich gabbro and troctolite mixtures at Aristarchus [12], and the variety of gabbros overlying crystalline norite at Bullialdus [16]. The age of these large craters is Eratosthenian or Copernican [17].

**Hypothesis**

Any one of these additional fragments of information can be viewed as unusual or simply interesting, but taken together they suggest there is no gap in magmatic evolution of the Moon. Only the form varies with time and random events as the crust evolves. The scale and variety of highland materials observed with remote observations is inconsistent with a compositionally

homogeneous crust to 25 - 60 km depth. The association of frequent "unusual" compositions at 5-10 km depth for nearside crustal areas excavated by late large impact events suggests extensive plutonism occurred in the nearside highland crust roughly contemporaneous with the mare basalts. Although our current data about the Moon are seriously incomplete and we are in desperate need of regional and global information, the following scenario appears to be consistent with these data and the leading hypothesis of formation of the Moon and is worthy of discussion and testing:

Ga b. p.	Event(s)
4.6 - 4.5	Proto-Earth forms, differentiates, and meets other large proto-planetary body in disruptive event creating a large mass of material in near-earth orbit.
4.5 - 4.45	Moon accretes and forms refractory An-rich crust [and mantle and core (?)]. Concentration of KREEP-rich zones must occur during the later stages.
<-->	Continued heavy bombardment
4.4 -->	Initiation of internal magmatism. Several (Mg-suite) plutons must have formed and cooled by 4.3.
4.3 - 3.8	Basin forming period (with rigid crust). These events mixed and delivered much of the highland material eventually to be sampled. They also fractured the crust to depths providing easier conduits for low density melts.
3.9 - 3.2	Major outflow of mare basalts on the nearside Plutonic activity continued within the highland crust.
3.2 - 2.0	Continued basaltic volcanism until conduits closed. Plutonic activity within crust paralleled mare volcanism.
2.0 - present	Random local activity (degassing, minor melt, etc.)

### Conclusion

Although the volume of mare basalts is estimated to be only 0.1% of the lunar total [1], this value should not be taken to represent the amount of partial melt produced within the lunar interior nor should the mare basalts be viewed to represent the only products of internal heating. The actual amount of magmatic activity is certain to be substantially larger, but cannot be estimated without a global assessment of lunar highland heterogeneity and the character, scale, and abundance of lunar plutons.

### References:

- [1] S. R. Taylor (1982) *Planetary Science: A Lunar Perspective*, pp. 481.
- [2] J. M. Boyce et al. (1974), *Proc. Lunar and Planet. Sci. Conf. 5th*, pp. 11-23.
- [3] P. H. Schultz and P. Spudis (1983), *Nature*, 302, 233-236.
- [4] J. J. Papike et al. (1976), *Rev. Geophys. Space Physics*, Vol. 14, No. 4, pp. 475-540.
- [5] C.M. Pieters (1978), *Proc. Lunar and Planet. Sci. Conf. 9th*, pp. 2825-2849.
- [6] J. W. Shervais (1988), *Moon in Transition*, pp. 82-91.
- [7] P. H. Warren (1985), *An. Revs. Earth Planet. Sci.*, 13, 201-240.
- [8] L.D. Raedeke and I.S. McCallum (1980), *Proc Conf. Lunar Highland Crust*, pp. 133-153.
- [9] L.A. Taylor, L.E. Nyquist, and J.C. Laul (1983), *Earth Planet. Sci. Lett.* 66, pp. 33-47.
- [10] B.R. Hawke and J.F. Bell (1981), *Proc. Lunar and Planet. Sci. Conf. 12B*, pp. 655-678.
- [11] P.A. Davis and P.D. Spudis (1985), *Proc. Lunar and Planet. Sci. Conf. 16, J. Geophys. Res.*, D61-D74.
- [12] C.M. Pieters (1986), *Revs. Geophys.*, Vol 24, No. 3. pp. 577-578.
- [13] C. M. Pieters (1990), *Lunar and Planetary Science XXI*, pp. 962-963.
- [14] B. R. Hawke et al. (1986), *Lunar and Planetary Science XVII*, pp. 999-1000.
- [15] P. Lucey et al. (1986), *Proc. Lunar Planet. Sci. Conf 16th, J. Geophys. Res.*, D344-D354.
- [16] C.M. Pieters (1989) *Lunar and Planetary Science XX*, pp. 848-849;  
----- (1990) *Remote Geochemical Analysis*, LPI and Cambridge Univ. Press, in press.
- [17] D.E. Wilhelms (1987) *The Geologic History of the Moon*, USGS-PP #1348, pp. 302.

**THE MOON: DEAD OR ALIVE;** P.H. Schultz, Department of Geological Sciences, Brown University, Providence, RI 02912

**INTRODUCTION:** One of the most significant results from the Apollo missions was the documentation that widespread lunar volcanism occurred between 3.2 and 4.0 AE (AE= billion years before present). The lack of evidence for younger lavas from returned samples established the present paradigm that the Moon is dead; that is, internal processes ceased long ago. Aside from impacts, the Dead Planet Paradigm is now well established in lunar science. This contribution reconsiders such a paradigm in terms of the geologic record and processes.

Four criteria can be used to constrain the *relative* age of lunar features: evolution of the photometric function (1); retention of the photometric contrast (1,2); preservation of relief and surface texture (1,3); and degradation of slopes (4,5). Determination of *absolute* age (and hence "recent"), however, further requires dated samples from the Apollo missions. The first criterion is perhaps the most sensitive. It principally depends on the physical structure of the uppermost regolith for a given unit. For example, crater rays and ejecta typically are poor forward scatterers of light due to surface roughness and blocks casting shadows (1). Repeated impacts rapidly (10 my) homogenize such differences in the photometric function. Photometric (i.e. the luminance) contrast, the second criterion, refers to the contrast in reflectivity integrated over different angles (and here, implicitly, over the visible spectrum). Bright filamentary crater rays eventually degrade to a diffuse ray pattern, then to a bright crater halo, and finally to the average background. Each stage reflects slightly different processes affecting the regolith and compositional contrasts created by ejecta. Three young impact craters dated by returned lunar samples illustrate this sequence in absolute terms. North Ray Crater (0.9 km in diameter) is 50 million years old (my) and retains only a faint, diffuse halo and ray system, whereas South Ray Crater (0.7 km in diameter and 2 my) exhibits a filamentary bright ray system (see 6). The third and fourth criteria reflect the degradation of surface relief by impact bombardment. Surface textures on the scale of 5 m associated with ejecta from North Ray Crater is nearly erased yet remains evident around South Ray Crater. Textures as small as 20 m associated with cooling impact melt remain visible in Copernicus crater, which has been interpreted as 1 AE. Studies of crater slope evolution (5) suggest that small craters 4-5 m in diameter superposed in North Ray ejecta would have wall slopes reduced to only 1 degree, while small craters superposed on Copernicus would have to be 100 m in diameter to reach a similar state of degradation.

These results can be generalized by calibrating the accumulated record of small craters on North Ray, Cone, South Ray, and Tycho to other young craters. Even though such craters span 100 my, the cumulative cratering record combined with the absolute sample ages clearly resolve the differences in age (7), thereby resolving the states of degradation. Consequently deposits exhibiting unusual photometric properties (e.g., strong forward scattering), abrupt changes in reflectivity, and small features (< 10 m) preserving subtle relief or steep slopes all indicate recent, if not ongoing, formation.

From such considerations, three lines of evidence indicate that mare volcanism extended beyond the nominal age indicated by the youngest sample lavas. First, degradation models of impact craters suggest that the last stages of widespread lava flooding occurred  $2.5 \pm 0.5$  AE (5) with minor outpourings as young as 1.7-2.0 AE (5). Second, the bright-rayed Copernican crater Lichtenberg (20 km in diameter) was embayed by a mare unit with well-defined surface flow textures (8). Although ambiguity can exist concerning the preservation of bright rays, particularly if a significant contrasting ejecta component is admixed, number densities of superimposed craters support the inferred stratigraphic age of about 1 AE. Third, the preservation of very small scale surface relief (5 m.) associated with the emplacement of several "blue" mare flows in western Oceanus Procellarum (3) and crater statistics (8) indicate that the young basalt flow near Lichtenberg is not unique (8). Consequently, the youngest lunar mare basalts remain to be sampled. It is possible that even younger flows could exist, particularly if emplaced as a unit with a thickness comparable to a youthful regolith (1-3 m).

Perhaps equally intriguing are recent endogenic features expressed as shallow, closed depressions identified in at least four locations (1,9). These depressions typically occur in clusters with individual depressions generally less than 500 m across, 3-6 m deep, and bounded by an irregular, highly reflective scarp which is abrupt down to the limit of resolution (5 m). The floors are invariably flat, reflective, and rubble-covered. Several examples occur as "dimple" craters, i.e., subdued craters with gently sloping walls forming a dimple-shaped profile but abruptly ending on a small, reflective floor. Two of the best examples occur within Huyginus (1) and as part of the complex Ina structure. Huyginus is a 10 km- diameter irregular rimless depression at the junction of three lunar rilles and most likely represents a collapse structure originally created at the time of peak mare volcanism (3 AE). On its floor, however, Lunar Orbiter V revealed numerous irregular depressions indicative of much more recent processes. Well-preserved

boulder trails (less than 10 m across) down the wall of Huyginus further document recent mass wasting. The Ina structure is a D-shaped depression about 2.9 km in diameter and 60 m deep and contains numerous mounds and plateaus of undisturbed material surrounded by bright material (see 10). It occurs near the summit of a broad rise flanked by outward-facing scarps radial to the Imbrium impact basin. Additionally, small isolated depressions along an extension of a tectonic rille in Mare Tranquilitatis (1) and in the low-albedo shelf region west of Mare Serenitatis (11) indicate that the Huyginus and Ina structures are not unique. All such structures are far removed from a recent impact. They all have, however, four common geologic contexts: b.) association with sites of past pyroclastic activity; c.) general correlation with dark, blue-colored units; d.) and fine-scale features (photometric, topographic, and morphologic) indicative of an age younger than 100 my.

Three origins have been proposed to the Huyginus/ Ina structures: Volcanic caldera collapse (10), seismically triggered collapse (1), or sites of recent outgassing (1,9). The first proposal did not explicitly consider the implications of such an origin, i.e., ongoing volcanic activity on the Moon without any other supporting evidence. The second proposal fails to account for the broad, flat floors, but must remain a viable working hypothesis. The last suggestion provides a mechanism to remove or freshen the regolith, is consistent with the tectonic and geologic setting, and does not require invoking ongoing volcanic eruptions.

In summary, mare volcanism may have extended well beyond the time span represented by collected lunar samples. Unusual endogenic features along fractures radial to Imbrium may provide sites for sampling the last gasps of this late-stage activity.

- REFERENCES:** 1) Schultz, P.H. (1976) Moon Morphology, University of Texas Press, Austin, Texas, 616 pp.
- 2) Wilhelms, D.E. and McCauley, J.F. (1971) Geologic map of the nearside of the moon. U.S. Geological Survey Misc. Inv. Map I-703.
- 3) Schultz, P.H., Greeley, R. and Gault, D.E. (1976) Degradation of small mare surface features. *Proc Lunar Sci Conf. 7th*, 985-1003.
- 4) Soderblom, L.A. (1970) A model for small-impact erosion applied to the lunar surface, *J. Geophys. Res.* 75, 2655-2661.
- 5) Boyce, J.M. and Johnson, D.A. (1978) Ages of flow units in the lunar nearside maria based on Lunar Orbiter V photographs, *Proc Lunar Planet. Sci. Conf. 7th*, 2717-2728.
- 6) Taylor, S.R. (1975) Lunar Science. Pergamon, New York.
- 7) Schultz, P.H. and Posin, S. (1988) Non-random cratering flux in recent time, *Global Catastrophes in Earth History*, LPI Contrib. No. 673, 168-169.
- 8) Schultz, P.H. and Spudis, P.D. (1983) Beginning and end of lunar mare volcanism. *Nature* 302, 233-236.
- 9) Schultz, P.H. (1988) Mare volcanism from 4.1 to 1.0 by, *Eos* 69, p.392.
- 10) Strain, P.L. and El-Baz, F. (1980) The geology and morphology of Ina. *Proc Lunar Planet Sci. Conf. 11th*, 2437-2446.
- 11) Howard, K.A. (1978) Apollo over the moon: A view from orbit (H. Masursky, G.W. Cotton and F. El-Baz, eds.) p.221 NASA SP-362.

THE RELEVANCE OF PICRITIC GLASSES TO MARE BASALT VOLCANISM. C.K. Shearer, J.J. Papike, Institute of Meteoritics, Dept. of Geology, University of New Mexico, Albuquerque, NM 87131 and N. Shimizu, Woods Hole Oceanographic Institute, Woods Hole, Massachusetts 02543.

## INTRODUCTION

The pertinency of picritic volcanic glasses within the framework of mare basalt petrogenesis is enigmatic. These volcanic glasses tend to have higher Mg/(Mg + Fe) than crystalline basalts [1] and therefore a logical assumption is that crystalline mare basalts were derived from primary magmas with compositions similar to the picritic glasses. However, calculated liquid lines of descent suggest that most mare basalts are not derived by simple, low-pressure fractionation from parental melts with compositions of the picritic glasses [2]. Unfortunately, these empirical models were based primarily upon various algorithms for major element basalt compositions because of the sparsity of trace element data for these minute glass beads. Using the empirical models of Longhi [2], we have calculated trace element variations along liquid lines of descent for 24 of the volcanic glasses tabulated by Delano [1] and additional preliminary, volcanic glass types [3]. This new trace element data were produced by secondary ion mass spectrometry (SIMS). The rationale for this exercise is to further elucidate the petrogenetic connection between the picritic glasses and crystalline mare basalts, the relationship among the picritic glass types and implications for mare basalt magmatism.

## SIMS ANALYSIS

The glass beads were identified and documented in selected polished thin sections using an electron microprobe. These chemically documented glass beads were then analyzed with a Cameca IMS-3f ion microprobe operated by the MIT-Brown-Harvard Consortium. The trace elements were analyzed using moderate (La, Ce, Nd, Sm, Eu, Dy, Er, Yb) to stringent (Sc, V, Co, Zr, Sr, Ba) energy filtering [4,5] and sensitivity factors derived from well-defined lunar glasses [6,7,8].

## TRACE ELEMENT CONNECTION BETWEEN PICRITIC GLASSES AND CRYSTALLINE MARE BASALTS.

In most of the empirical fractional crystallization major and trace element models, the calculated magma compositions derived from the picritic glass compositions show contrasting trace element concentrations and ratios compared to crystalline mare basalts with similar Mg, TiO<sub>2</sub> and Al<sub>2</sub>O<sub>3</sub>. This agrees with conclusions reached by Longhi [2] for the entire suite of picritic glasses and Shearer et. al [9] for the Apollo 14 picritic glasses. Only one suite of picritic glass and modeled compositions appear to approach crystalline mare basalt compositions. Fractional crystallization of olivine from A17 VLT glass will produce modeled major and trace element melts which approach A17 crystalline VLT (10% crystallization) and Luna 24 ferrobasalts (30% crystallization) (Table 1).

Table 1. Comparison of selected major and trace element characteristics of calculated melts modeled from A17VLT glass and crystalline basalts.

	Mg	TiO <sub>2</sub> %	Al <sub>2</sub> O <sub>3</sub> %	La	Sm	Ba	Zr	Sr	Co	Ni
A17 VLT glass	57	.66	9.6	1.6	1.0	21	35	63	54	150
10% olivine f.c.	52	.73	10.6	1.8	1.1	23	38	70	45	72
30% olivine f.c.	35	.92	13.6	2.5	1.6	34	49	100	26	6
A17 VLT	52-54	.69	10-11	1.3	1.1	-	226	-	44	-
L24 ferrobasalt	36-37	.89	12-14	2.8	2.1	40	50	110	36	20

The substantial deviations of Zr, Ni and CaO of the VLT basalts contrasts with the fractional crystallization model (10%). These deviations, however may be attributed to analytical error (Zr = 226 ppm) and selection of  $k_D^{Ni}$  [10]. Although major element modeling does not preclude that some types of high-Ti glasses (A17 orange) may be parental to the high Ti basalts, the trace element modeling appears to eliminate this possibility (Table 2).

Table 2. Comparison of selected major and trace element characteristics of calculated melts modeled from orange glass and crystalline basalts.

	Mg	TiO <sub>2</sub> %	Al <sub>2</sub> O <sub>3</sub> %	La	Sm	Ba	Zr	Sr	Co	Ni
A17 Orange	54	9.12	5.79	6	8	216	175	76	57	70
30% f.c.	38	10.62	8.30	10	13	343	244	120	28	3
A11 orange	52	10.0	5.7	4.5	6.4	174	206	56	64	30
30% f.c.	38	10.8	8.5	6	9	250	270	80	37	4
A11 high k	42	12.1	7.9	29	22	161	504	330	-	<2
A11 low k	42	10.5	9.9	8.1	9.4	150	224	77	14	<2

## PETROGENETIC RELATIONS AMONG GLASSES

Although most of the high-Ti glasses define distinct compositions and liquid lines of descent, implying distinct source regions or melting processes, the petrogenetic relations among several types of low-Ti picritic glasses (i.e., A15 green glass) are more ambiguous. Numerous studies have recognized the A15 green glasses are compositionally heterogeneous (11,12). These subtle variations have been attributed to crystal-liquid fractionation processes involving olivine  $\pm$  orthopyroxene  $\pm$  aluminous pyroxene  $\pm$  Fe-rich metallic phase  $\pm$  FeS-rich immiscible melt [11, 12, 13, 14, 15]. These processes fail to account for four important aspects of the chemical variation; SiO<sub>2</sub> increases with Mg', Ni inversely correlates with Mg' [1,12] positive correlations of strongly incompatible elements (Zr, Ba, Nd) with the highly compatible elements (Co) and distinct groups defined in compatible-incompatible element diagrams (i.e., Co vs Zr). The magmas represented by the high- (Group A and D) and low-Co (Groups B and C) trends are interpreted to have been erupted from two distinct but compositionally variable source regions. A third group (Group E) appears to have been erupted from a source with more limited chemical variability. Less subtle compositional distinctions in the picritic sources are implied by a comparison of glasses of similar major element compositions. The A14 and A12 (Black) glasses appear to have a distinct KREEP signature (Ba/Sr) relative to glasses from the other sites. If the incorporation of the KREEP signature is a result of hybridization in the source region, the KREEP component in the mantle source may range up to 2%.

## IMPLICATIONS CONCERNING MARE BASALT PETROGENESIS

The picritic glass bead data indicate that (1) In only a few cases can an argument be made (based on major and trace element liquid lines of descent) for a low pressure fractional crystallization linkage between a picritic glass and a mare basalt (e.g., A17VLT  $\rightarrow$  L24 ferrobasalt). (2) The wide range of primary magma compositions (greater than 25) and the lack of petrogenetic linkages (via crystal fractionation) to crystalline basalts indicate that either a wide compositional range of evolved mare basalts has not yet been sampled or a unique mechanism is selectively tapping these picritic magmas directly from their mantle source region. (3) The picritic magma source region (300-500 km [1, 16]) is chemically heterogeneous and capable of generating a wide range of picritic melt compositions (e.g., TiO<sub>2</sub>, Al<sub>2</sub>O<sub>3</sub>) with distinct trace element signatures. These heterogeneities may be attributed to hybridization type processes. In addition; the melting process and subsequent eruption preserved the subtle difference reflected in the source. (4) Two distinct models exist for the relationship between mare basalts and the picritic magmas: (a) Picritic magmas were generated below 300 km [1, 16] (assuming multiple saturation) and subsequently fractionated (at <300 km) to produce a wide compositional range of mare basalts and (b) Picritic magmas were generated below 300 km through small degrees of partial melting whereas mare basalts represent fractionation products of primary magmas generated at shallower depths and higher degrees of partial melting. The volatile-rich source for the picritic magmas in (b) provided an eruptive dynamic mechanism capable of delivering these melts to the lunar surface without fractionation (e.g., lunar kimberlites). Although this exercise and limited isotopic data [17] on glass beads suggests (b) is a more likely possibility, the limited sampling of the mare basalt populations limits any conclusions.

## REFERENCES

- [1] Delano, J.W. (1986) PLPSC 16th, D210-D213. [2] Longhi, T. (1987) PLPSC 17TH, E349-E360. [3] Papike J.J. et. al (1989) LPS XX, 818-819. [4] Shimizu, N. and le Roex, A.P. (1986) J. Volcan. Geotherm. Res. 29, 159-188. [5] Shimizu, N. et al. (1978) GCA, 42, 1321-1334. [6] Taylor, S.R. (1975) Lunar Science: A post-Apollo view. [7] Ryder, G. (1975) Catalog of Apollo 15 Rocks. [8] Basaltic Volcanism of the Terrestrial Planets. [9] Shearer, C.K. et al (1990) GCA 54, 851-867. [10] Hart, S.R. and Davis, K.E. (1978) EPSL 40, 203-219. [11] Stolper, E.M. (1974) A.B. theses, 178 pp. [12] Delano, J.W. (1979) PLPSC 10th, 275-300. [13] Hughes, S.S. et. al (1988) GCA 52, 2379-2391. [14] Grove, T.L. (1981) PLPSC 12TH, 935-948. [15] Grove, T.L. and Lindsley, D.H. (1978) LPS IX, 430-432. [16] Delano, J.W. (1980) PLPSC 11TH, 251-288. [17] Tatsumoto, M. et. al (1987) PLPSC 17TH, E361-E371.

## LUNAR MARE VOLCANISM: RECENT ADVANCES IN PETROGENESIS

**John W. SHERVAIS**, Depart. of Geological Sciences, University of South Carolina, Columbia SC 29208  
**Scott K. Vetter**, Department of Geology, Centenary College, Shreveport, LA 71134

Mare basalts are subalkaline, low-silica, mafic volcanic rocks which fill broad basins and impact structures in the lunar crust. Nearly all of these basins are concentrated on the lunar nearside due to the offset in the lunar center of mass toward that side. Radiometric ages document the onset of mare volcanism at a minimum of 4.3 AE [1,2]; the youngest basalts dated are about 3.2 AE old [3], but crater density studies suggest that some flows may be younger.

Compositional variations between mare basalt suites reflect variations in the mineralogical and geochemical composition of the lunar mantle which formed during early differentiation to form the lunar crust 4.4-4.5 aeons ago. Three broad suites of mare basalt are recognized: very low-Ti (VLT) basalts with  $\text{TiO}_2 < 1 \text{ wt\%}$ , low-Ti basalts with  $\text{TiO}_2 = 2-4 \text{ wt\%}$ , and high-Ti basalts with  $\text{TiO}_2 = 10-14 \text{ wt\%}$  [4-6]. Important subgroups include the Apollo 12 ilmenite basalts ( $\text{TiO}_2 = 5-6 \text{ wt\%}$ ) [7], aluminous low-Ti mare basalts ( $\text{TiO}_2 = 2-4 \text{ wt\%}$ ,  $\text{Al}_2\text{O}_3 = 10-14 \text{ wt\%}$ ) [8-10], and the recently discovered Apollo 14 Very High potassium (VHK) aluminous low-Ti basalts, with  $\text{K}_2\text{O} = 0.4-1.5 \text{ wt\%}$  [11-13]. All mare basalts are characterized by low alkalis, Si, Al, and Ca, and by high FeO and FeO/MgO, relative to terrestrial basalts. As a result, mare basalts are low in feldspar (<30% modally) and contain abundant pigeonite, olivine, opaque oxides, and metallic iron. The occurrence of free metallic iron reflects the low intrinsic oxygen fugacity of all lunar rocks.

The mare basalt source regions have geochemical characteristics complementary to the highlands crust, and are generally thought to consist of mafic cumulates from the magma ocean which formed the felsic crust by feldspar flotation. The progressive enrichment of mare basalts in Fe/Mg, alkalis, and incompatible trace elements in the sequence VLT basalt → low-Ti basalt → high-Ti basalt is explained by the remelting of mafic cumulates formed at progressively shallower depths in the evolving magma ocean. This model is also consistent with the observed decrease in compatible element concentrations and the progressive increase in negative Eu anomalies [14].

There is increasing evidence, however, that more complex scenarios are required. Mare basalts are too magnesian to be derived from a magma ocean cumulate formed after >95% fractional crystallization, but such high degrees of fractional crystallization are needed to create the necessary trace element rich source [15,16]. The hybridization of Fe- and incompatible element-rich late magma ocean cumulates with more magnesian early magma ocean cumulates may explain this dichotomy. This hybridization is gravitationally driven, with dense, Fe-rich late magma ocean cumulates sinking into the underlying magnesian cumulates. Recent hybridization models generally assume three end members: early magnesian cumulates with low Ti (dominantly olivine + Opx), late Fe, Ti-rich cumulates (Cpx + ilmenite), and a late magma ocean trapped-liquid component similar to KREEP in composition [16, 17]. These end members are mixed in various proportions to create the range in observed mare basalt compositions.

Recent studies of the Apollo 14 aluminous mare basalt suite have revealed a wide variety of previously unknown mare basalt types, many of which seem to require assimilation as an important process in their petrogenesis [8-13]. Two main components have been identified: KREEP, the incompatible element-rich mafic component concentrated in soils and impact breccias [8-10], and lunar granites [11-13]. The Apollo 14 aluminous basalt suite is important because it has many compositional characteristics intermediate between normal, low-alumina mare basalts and high-Ti mare basalts. Apollo 14 high-alumina basalts have high MG#s (similar to low-Al, low-Ti basalts), high alkali and incompatible trace element contents (similar to high-Ti basalts or higher), and compatible trace elements intermediate between high and low Ti basalts [18]. In a cumulate remelting model, these characteristics suggest a mantle source region which lies above the normal low-Ti basalt source and below the high-Ti basalt source. In addition, Apollo 14 high-Al basalts are also high in CaO, suggesting either plagioclase assimilation [15] or plagioclase in the source region.

When data for all mare basalt types (including Apollo 14 aluminous mare basalts and VHK basalts) are plotted on ratio-ratio or ratio-element plots, two distinct trends are observed. One trend is defined by low-Ti basalts *sensu lato* (including VLT, VHK, and high-Al, low-Ti basalts); the other trend is defined by the high-Ti basalt suite. Both trends resemble mixing curves whose incompatible element-rich end points towards KREEP. There is little or no overlap between the two trends, however, and their incompatible element-poor asymptotes point to distinct end-member compositions. If these curves are considered simple mixing trends, up to 65% assimilation of KREEP is indicated. Alternatively, these curves may be due to fractional crystallization, as suggested by fractionation trends on MG# plots. The trends toward a KREEP-like composition suggest that this composition may represent an incompatible element-rich end member mixed into the mare basalt source prior to melting. Fractionation of phase assemblages with bulk distribution coefficients similar to the refractory mineral assemblage will drive the melt composition towards the original KREEP-like mixing component.

These observations suggest that the compositional variations observed in mare basalts result from a complex source hybridization process similar to that suggested by Hughes et al. [16]. In this scenario a late stage magma ocean component similar in composition to KREEP sinks into earlier magma ocean cumulates and the resulting mixture undergoes partial melting to form the mare basalt parent magmas. These magmas subsequently undergo fractional crystallization to create the observed fractionation trends. The major difference between our model and previous models such as Hughes et al [16] is that the KREEPy component mixes with distinct low-Ti and high-Ti mantle source regions, and that there is no significant mixing between these two source regions. Each source region is internally heterogeneous and may mix with different amounts of the KREEP ferrobasalt component. The distinct break between the two cumulate source regions is probably caused by a change in cumulate phase assemblage (ilmenite + clinopyroxene in).

The physical process by which the KREEP component mixes with the cumulate mantle rocks is uncertain; the KREEPy component may sink as solid blocks of crystalline material or as a liquid. For "urKREEP" to sink, it must be extremely Fe-rich, unlike pristine KREEP basalts like 15386, which is probably a mixture of urKREEP and crustal melts [e.g., 19]. We use polytopic vector analysis to estimate the composition of urKREEP from mare basalt compositional trends. Polytopic vector analysis (PVA) differs from factor analysis in that it applies Q-mode analysis to non-orthogonal multivariate sample vectors to extract sample endmember compositions. The data are fit to a polytope of N-1 dimensions (where N = number of variables) and endmembers are defined as vertices of the polytope after it has been modified to eliminate negative values. Advantages of this method are that it works best with constant sum data (e.g., chemical analyses) and that it can define endmembers which lie outside the data cloud. Our preliminary results using this technique suggest that the KREEP component in mare basalts is an Fe-rich ferrobasalt (FeO = 35 wt%) which is fractionated with respect to pristine KREEP 15386. Our calculated urKREEP has incompatible trace element concentrations similar to high-K KREEP or "Super KREEP" 15405.

**REFERENCES:** [1] Taylor et al (1983) *Earth Planet. Sci. Lett.*, 66, 33-47; [2] Dasch et al (1987) *Geochim. Cosmo. Acta*, 51, 3241-3254; [3] Papanastassiou and Wasserburg (1970) *EPSL* 8, 269-278; [4] Papike et al (1976) *Rev. Geophys. Space Phys.* 14, 475-540; [5] BVSP (1981) Pergamon Press, 951 pp; [6] Head (1976) *Rev. Geophys. Space Phys.* 14, 265-300; [7] James and Wright (1972) *Geol. Soc. America Bull.*, 83, 2357-2382; [8] Shervais et al (1985) *Proc. 15th Lunar Planet. Sci. Conf., Jour. Geophys. Res.*, 90, C375-C395; [9] Dickinson et al (1985) *Proc. 15th Lunar Planet. Sci. Conf., J. Geophys. Res.*, 90, C365-C374; [10] Neal et al (1988) *Proc. 18th Lunar & Planet. Sci. Conf.*, 139-1153; [11] Shervais et al (1985) *Proc. 16th Lunar Planet. Sci. Conf., Jour. Geophys. Res.*, 90, D3-D18; [12] Shih et al (1986) *Proc. 16th Lunar and Planet. Sci. Conf., J. Geophys. Res.*, 91, D214-D228; [13] Neal et al (1988) *Proc. 18th Lunar Planet. Sci. Conf.*, 121-137; [14] Taylor & Jakes (1974) *Proc. Lunar Sci. Conf. 5th*, 1287-1305; [15] Kesson & Ringwood (1976) *Earth Planet. Sci. Lett.*, 30, 155-163; [16] Hughes et al (1989) *Proc. 19th Lunar Planet. Sci. Conf.*, 175-188; [17] Binder (1985) *Proc. 16th Lunar Planet. Sci. Conf., J. Geophys. Res.*, 90, D19-D30; [18] Shervais & Taylor (1984) *Origin of the Moon*, 173-201; [19] Warren (1988) *Proc. LPSC 18*, 233-242.

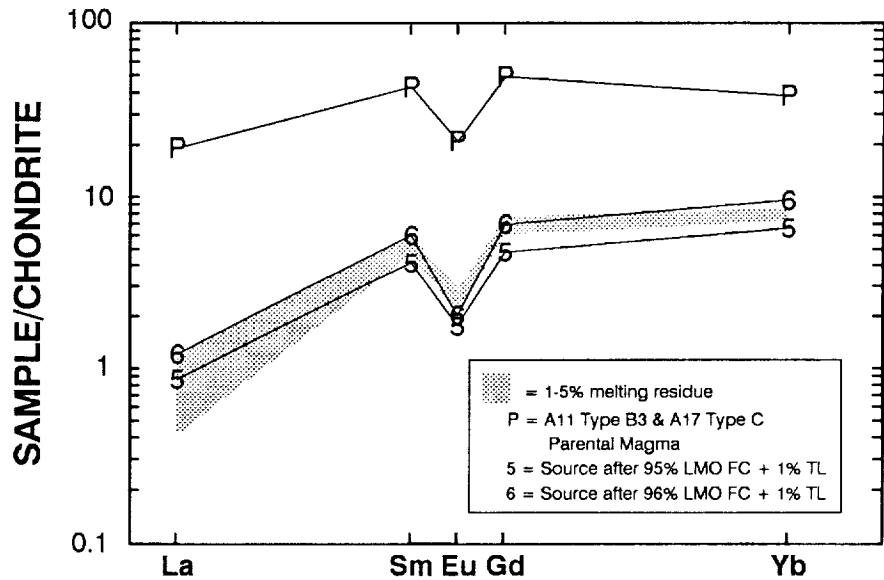
**GEOCHEMICAL CONSTRAINTS (AND PITFALLS) ON REMELTING OF LUNAR MAGMA OCEAN CUMULATES FOR THE GENERATION OF HIGH-TI MARE BASALTS** Gregory A. SNYDER, Lawrence A. TAYLOR, & Clive R. NEAL, Dept. of Geological Sciences, University of Tennessee, Knoxville, TN 37996-1410.

The major and trace element abundances of the most primitive (lowest incompatible element (IE) abundances) basalts from the Apollo 11, low-K (B3) suite and Apollo 17 (Type C) high-Ti suites are nearly indistinguishable (Table 1). It is proposed that both suites were derived from similar source regions and similar processes to arrive at a common parent magma. This parental magma had trace element abundances approximately 10-15 x the bulk moon [1], was LREE depleted and had a pronounced negative Eu anomaly. Further evidence for the similarity of the Apollo 11, B3 and Apollo 17, Type C sources is shown by the modeling of Hughes et al. [2]. Though they did not delineate primitive parental liquids, the chemical composition of their calculated sources for high-Ti Apollo 11, B3 and Apollo 17, Type C basalts are almost identical.

In our modeling, we have adopted a fractionation sequence similar to that of Hughes et al. [3], as this sequence can be justified by both known high pressure phase equilibria and the accumulated knowledge of observed mare basalt mineralogies [3-4]. However, we have determined the most primitive (i.e., lowest IE abundances, highest compatible element abundances) compositions in each suite, either by calculation or simple inspection. We consider these compositions to represent a best estimate of the parental magma for each suite. This convention eliminates confusion in the calculated mineralogy and chemical composition of the source that may be inherent in simply averaging a group of samples; especially those which may have experienced post-magma generation evolutionary processes (e.g. fractional crystallization and AFC). As a refinement to previous work, we have adopted an approach for evolution of the Lunar Magma Ocean (LMO) that includes not only plagioclase flotation and mafic crystal accumulation, but the incorporation of a **trapped instantaneous residual liquid** in the cumulate pile. This model is discussed in further detail in a companion paper in this proceedings volume [5].

Approximately 92-96% fractional crystallization of the LMO (trace elements = 3 x chondrites as per [2-4]) with 1% trapped instantaneous residual liquid is required in order to generate cumulates which have the requisite REE abundances and appropriate relative proportions to generate magmas parental to the Apollo 11, B3 and Apollo 17, Type C basalts (Figure 1). As a lower limit, 1-5% batch melting of the LMO mafic cumulates is assumed. Higher degrees of batch melting may indeed occur, but would require even higher percentages of fractional

crystallization of the LMO in order to generate the appropriate source. The degree of fractional crystallization required may vary somewhat, dependent upon the amount of trapped instantaneous residual liquid in the cumulate. Due to the relative proportions of the REE as calculated in the high-Ti mare basalt source (i.e., LREE depleted with nearly flat HREE), one constraint does seem to be inescapable -- the LMO liquid must have reached a point in its fractional crystallization where **cpx is on the liquidus** (as also pointed out by Nyquist et al. [6] and Paces et al. [7]). Major element considerations also point to the need for ilmenite (and chromite?) in the source [8-9].



Our modeling is consistent with that performed by Hughes et al. [3] on Apollo 15 yellow-brown glass and Apollo 12 mare basalts. Their work also suggested extensive fractional crystallization of the LMO with subsequent low degrees of remelting of the cumulates to generate these basalts. They also pointed to the need for a trapped late-stage ("KREEPy") LMO liquid in the cumulates. Although our work confirms the need for a trapped liquid component in the source, a simple *in situ* trapped instantaneous residual liquid will suffice for the high-Ti basalts (Figure 1). A more complicated model involving convective overturn of the LMO cumulate pile and mixing with a late "KREEPy" liquid [3] is not required.

These conclusions, based on our modeling, are not in agreement with those of Neal et al. [9] in this volume. On the basis of Rb-Sr isotopic systematics for the Apollo 17 Type C basalts, Neal et al. [9] have stated that cpx must have "melted out" of the source. Our present conclusions are consistent, however, with previous Hf and Nd isotopic systematics presented by Unruh et al. [8]. Further work is in progress to resolve this issue.

Table 1

	LMO	AP-11,B3 parent	AP-17,C parent	source* required
SiO <sub>2</sub>	46.0	39.60	38.5	
TiO <sub>2</sub>	0.30	11.10	12.3	
Al <sub>2</sub> O <sub>3</sub>	7.0	9.51	8.7	
FeO	12.4	19.12	18.5	
MnO		0.28	0.26	
MgO	27.6	8.10	9.7	
CaO	5.5	11.07	10.1	
Na <sub>2</sub> O	0.6	0.36		
K <sub>2</sub> O	0.06	0.05	0.07	.0006
Cr <sub>2</sub> O <sub>3</sub>	0.5	0.47	0.61	
Rb	10.35	0.80	1.2	.0105
Sr	34.2	144	160	1.71
Ba	10.8	95	67	.847
La	0.73	6.7	6.3	.068
Ce	1.91	22.5	21.8	.249
Nd	1.42	21.1	23.8	.298
Sm	.462	8.4	9.5	.147
Eu	.174	1.54	1.79	.0253
Gd	.613	13.2	14.8	.265
Tb	.112	2.13		
Dy	.762	14.5	16.9	.415
Er	.498	9.7	9.67	.352
Yb	.495	8.5	8.8	.409
Lu	.076	1.17	1.25	.067

\* (minimum abundances) for 1% batch melting with only opx and olivine in the residue.

Sources: LMO = [10] for major elements; AP-11, B3 basalt = sample 10045 [11] and [12]; AP-17, C = average of 74245, 74275, 74247 for trace elements [13]; [14] and [15] and personal communication for major elements.

**References:** [1] Taylor, S.R. (1982), *Planetary Science: A Lunar Perspective*, LPI, 481 pp.; [2] Hughes, S.S. et al. (1989), *PLPSC* 19, 175-188; [3] Hughes, S.S. et al. (1988), *GCA* 52, 2379-2391; [4] Nakamura, N. (1974), *GCA* 38, 757-775; [5] Snyder, G.A. et al. (1990), **this volume**; [6] Nyquist, L.E. et al. (1976), *PLSC* 7, 1507-1528; [7] Paces, J.B. (1990), *LPSC* 21, 926-927; [8] Unruh, D.M. et al. (1984), *PLPSC* 14, B459-B477; [9] Neal et al. (1990), **this volume**; [10] Warren, P.H. (1986), *PLPSC* 16, D331-D343; [11] Agrell, S.O. et al. (1970), *PLSC* 7, 93-128; [12] Haskin, L.A. et al. (1970), *PLSC* 1, 1213-1231; [13] Rhodes, J.M. (1976), *PLSC* 7, 1467-1489; [14] Warner, R.D. (1979), *PLPSC* 10, 225-247; [15] Neal, C.R. et al. (1990), *GCA* 54, 1817-1833.

**THE SOURCES OF MARE BASALTS: A MODEL INVOLVING LUNAR MAGMA OCEAN CRYSTALLIZATION, PLAGIOCLASE FLOTATION, AND TRAPPED INSTANTANEOUS RESIDUAL LIQUID** Gregory A. SNYDER, Lawrence A. TAYLOR, & Clive R. NEAL, Dept. of Geological Sciences, University of Tennessee, Knoxville, TN 37996-1410.

The magma ocean concept has been an integral part of the lunar literature practically since the return of the first lunar samples [1]. Many variations of the concept have been proposed (e.g. [2-3]), and we offer here a further refinement to this fundamental concept. Several parameters must be considered when developing a model for the mare basalt source regions: (1) the bulk composition of the initial Lunar Magma Ocean (LMO); (2) the relevant phase equilibria with depth for crystallization paths of the LMO; (3) the degree of perfect fractional crystallization of the LMO; (4) the amount and composition of a trapped liquid component; and (5) the depth in the cumulate pile at which melting must occur to generate a mare basalt parent magma. We have dealt with (5) elsewhere in this volume [5] and will concentrate on points (3) and (4) here.

Recently, certain workers [4] have suggested that the source for at least some mare basalts may not have had a significant Eu anomaly, despite the observed negative Eu anomaly found in actual mare basalts. They go on to state that plagioclase separation during generation of the mare basalt source may not be required to give the requisite negative Eu anomaly found in many mare basalts. However, trace element modeling of the high-Ti mare basalts [5] has indicated the need for a source with a significant negative Eu anomaly. To this end, we have developed a model for crystallization of the LMO that is analogous to what is believed to have occurred in certain portions of terrestrial layered mafic intrusions. In this model, the LMO is allowed to fractionally crystallize. Crystallization occurs in the upper portion of the moon-wide melt layer, and mafic crystals settle to the bottom. At successively greater stratigraphic heights, a variable proportion of instantaneous residual liquid is trapped in the cumulate pile. In our model, 1, 5, and 10% trapped instantaneous residual liquids (TIRL) are used, and we assume that perfect adcumulates do not exist.

The trapped liquid is required to elevate the extremely low REE abundances found in the mafic cumulates alone (e.g. see figure 1). Only prohibitively low degrees of melting ( $\ll 1\%$ ) could generate a liquid with the appropriate abundances of the REE seen in mare basalts. However, at these extremely low degrees of partial melting, derived liquids would be extremely LREE enriched and would not match the analyzed REE patterns of mare basalts.

The fractionation sequence used in this model is slightly modified from that used by Hughes et al. [3], as deduced from Walker et al. [7]. This sequence is preferred on the basis of known

mineralogy and phase equilibria. The sequence used is: 0-40% = olivine; 40-55% = opx; 55-90% = 53% plag + 47% opx; 90-100% = 50% cpx + 36% plag + 8% pig + 6% ilm. After approximately half of the LMO has crystallized, plagioclase becomes a liquidus phase [3]. This plagioclase is subsequently floated, and does not become part of the *mafic cumulate* + TIRL pile. Generation of mare basalts from a cumulate containing only mafic minerals, left behind after flotation of plagioclase, is not a unique idea (see [6]). However, previous geochemical models for the genesis of mare basalt sources do not, to our knowledge, include this TIRL component.

The differences are dramatic in the evolution of the REE patterns of the cumulate (+ TIRL) with plagioclase included versus that with the plagioclase removed by flotation. For the case where plagioclase is included in the cumulate pile (the terrestrial case), the required negative Eu anomaly for mare basalt sources does not even begin to emerge until  $> 95\%$  fractional crystallization of the LMO. This is due to the overwhelmingly large positive Eu anomaly imparted to the cumulate pile once the mineral plagioclase appears on the liquidus. Sources which contain a negative Eu anomaly of the appropriate magnitude do not occur until approximately 98% fractional crystallization of the LMO. At this point, the abundances of the REE have become prohibitively high in order to generate a source capable of being remelted to form the parent magmas of mare basalts.

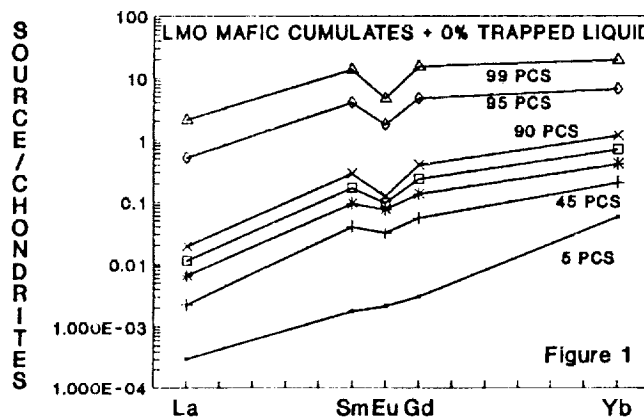
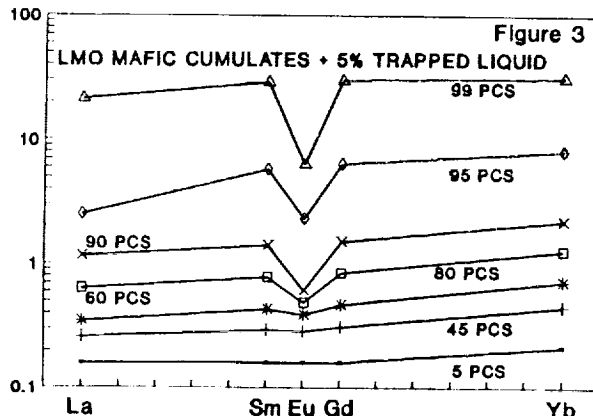
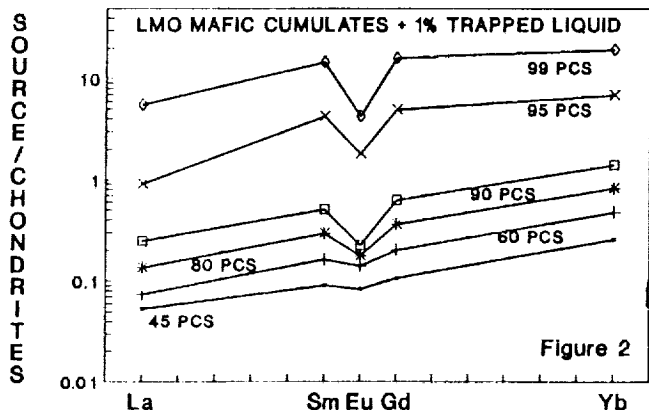
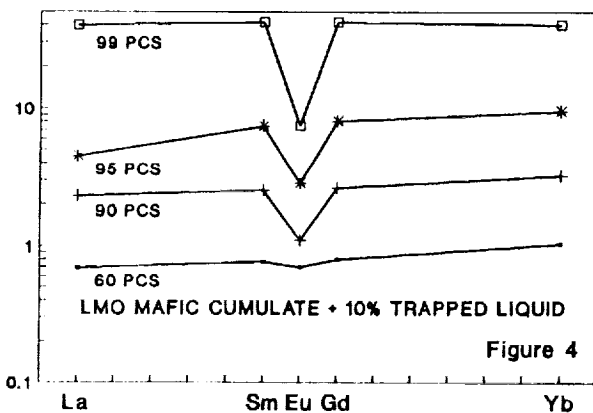


Figure 1

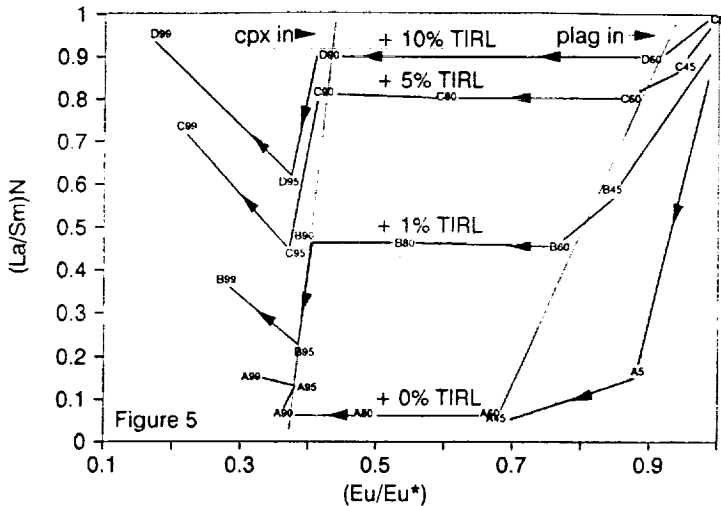


The mafic cumulate + TIRL source (*sans* plagioclase) begins to take on a pronounced negative Eu anomaly once plagioclase becomes a liquidus phase (>45% LMO fractional crystallization). As can be seen in Figures 2-4 (and compared to the crystallization of the mafic cumulate alone in Figure 1; PCS on figures = percent crystallized solids), as the percentage of TIRL decreases, the more LREE depleted the source becomes. This is further illustrated on Figure 5 where  $(La/Sm)_N$  is plotted versus  $Eu/Eu^*$ . As crystallization proceeds ( $Eu/Eu^*$  decreases), LREE depletion decreases initially, levels off, and then takes a drastic drop where cpx becomes a

SOURCE/CHONDRITES



liquidus phase. Simply by varying the percentages of TIRL and the degree of fractional crystallization of the



LMO, a wide range of sources which are LREE depleted, and exhibit a negative Eu anomaly, may be generated (Figure 5).

The source region for a group of high-Ti mare basalts has been successfully modeled using our proposed approach (elsewhere, this volume [5]). Complicated models involving convective overturn of the LMO cumulate pile and selective addition of a late-stage "KREEPy" liquid [3] are not required. In general, mare basalt source regions can be generated by simple fractional crystallization of the LMO, settling of the mafic phases with the entrainment of a small amount of TIRL, and accompanied by the flotation of plagioclase in the latter stages.

References: [1] Warren, P.H. (1985), *Ann. Rev. Earth Planet. Sci.* 13, 201-240; [2] Shih, C.-Y. & Schonfeld, E. (1976), *PLSC* 7, 1757-1792; [3] Hughes, S.S. et al. (1988), *GCA* 52, 2379-2391; [4] Shearer, C.K. & Papike, J.J. (1989), *GCA* 53, 3331-3336; [5] Snyder, G.A. et al. (1990), *this volume*; [6] Taylor, S.R. (1982), *Planetary Science: A Lunar Perspective*, LPI, 481 pp.; [7] Walker, D. et al. (1973), *EPSL* 20, 325-336.

**LUNAR MAGMA TRANSPORT PHENOMENA; F.J. Spera,  
Institute for Crustal Studies & Department of Geological Sciences,  
University of California, Santa Barbara, Santa Barbara, CA  
93106**

An understanding of the first Ga of lunar history requires an appreciation of magma transport phenomena beyond our current reservoir of knowledge. At the risk of oversimplification, a rough sketch of some outstanding problems is outlined here. Lunar magma ocean evolution as well as the segregation, ascent and eruption of magma present formidable but fascinating problems to magma dynamicists.

In order to address the structure and mixedness of the reservoir from which mare basalts were extracted the characteristics and temporal evolution of the Lunar Magma Ocean (LMO) must be considered. Estimates of initial LMO depths vary from  $\approx 200$  km to whole planet melting; most probable values are in the range 300 to 700 km, approximately. Numerous geochemical and petrological LMO models have been put forward mainly from the petrological point of view. These are summarized in (1,2). Recently the high Rayleigh number mixing-length theory of turbulent thermal convection (3) has been used to investigate the question of crystal-melt fractionation in the LMO (4). Quench crust, which forms at the ocean surface at early times is repeatedly disrupted early on by convective stress, meteoritic impact and foundering. A key parameter is the thermal renewal time (5) of the LMO crust; as long as this time remains short, heat transfer will remain near its maximum value based on the Nu-Ra scaling of turbulent convection and cooling will be significant and rapid due to the combined effects of radiative and conductive transport. In the inertial convective regime, velocities are high enough to preclude significant crystal-melt fractionation. Near the ocean bottom however due to the presence of a rigid boundary and because of much higher effective viscosities (and perhaps a finite yield strength) convective velocities are smaller and dense crystals will sink (6). Greater crystallinities near the bottom are primarily due to the relative steepness of the solidus and liquidus (0.5 k/km) compared to the LMO adiabat (0.05 k/km). Because of the intrinsically low permeability of ocean bottom mush, where the solid fraction ( $\phi$ )  $> 0.5$ , Darcy velocities of interstitial pore melts are small despite positive buoyancy. Compaction may be a more significant process in the mobilization by expulsion of trapped pore melts. Turbulent eddies possess sufficient kinetic energy during the early "inertial" era of LMO convection to partially erode the mush layer from time to time. Convective behavior of the LMO changes significantly once a contiguous crust, both in time and space forms because of the insulating effects of a continuous conductive lid

(7,8). Once a coherent conductive lid forms at the top of the LMO, heat transfer rates drop and rms convective velocities also decrease. By the time sufficient olivine and pyroxene crystallize increasing the concentration of  $Al_2O_3$  enough to stabilize plagioclase, convective velocities will have fallen to values low enough to permit crystal flotation of large crystals at least in the upper regions of the LMO adjacent to the nascent lunar crust. Because late stage cumulates are dense, subsolidus convection driven by compositional as well as thermal effects will tend to mix the crystallization products of the LMO. This large scale mechanism for the generation of both lateral and radial heterogeneity will be superimposed upon the earlier effects of doubly-diffusive compositionally-driven convection in the porous mush of a possible LMO sandwich horizon possibly the source of KREEP. The scale of segregation may be studied by forward modelling of the complete set of conservation equations governing porous media and subsolidus viscous convection using the two-point compositional correlation function of (9) as implemented, for example, in (10).

A review of the literature on mare basalt petrogenesis suggests, not surprisingly, that no simple model put forward to date explains the wealth of geochronological, isotopic, geochemical and petrological data. In order to pose some magma transport questions, a generic model which involves a heterogeneous source of age  $\approx 4.4$  Ga that melts to various extents due to radiogenic heating and/or isentropic decompression associated with subsolidus convection in the period 4.2 to 3.0 Ga is adopted. The process by which melt is extracted from the partially molten mare source region is a complex one. It is not certain which of two contrasting models is most correct. In the percolation theory (11,12,13) the matrix is regarded as a deformable porous matrix. Melt segregation is driven by deformation of the matrix (compaction) provided the thickness of the partially molten region  $\delta_{pm} \leq ((1-\phi)W_0\eta_m/g\Delta\rho)^{1/2}$  where  $\phi$ ,  $W_0$  and  $\eta_m$  are the fraction solid, vertical velocity of the matrix (i.e., the rate of convective upwelling), and the effective matrix viscosity. With 5% melting,  $W_0 = .1$  m/a,  $\eta_m = 10^{19}$  Pa s,  $g = 1.6$  ms<sup>-2</sup> and  $\Delta\rho = 500$  kg/m<sup>3</sup>,  $\delta_{pm} \approx 5$  km. For regions of partial melt thicker than this, or if melting takes place over a depth interval, then melt segregation is controlled by the buoyancy and viscosity of the melt and not matrix deformation. In this regime Darcy's law may be used to estimate typical velocities in the range  $10^{-6}$  to  $10^{-9}$  m/s depending on the porosity, melt viscosity, matrix grain size and relationship between porosity and permeability. In a second model for melt extraction, melt accumulates in vein which are oriented parallel to the axis of minimum compressive stress. Once veins grow large enough, an interconnected network can serve to rapidly drain the source region (14, 15). The percolative and vein

models for melt segregation clearly have very different implications for trace element distributions in mare lavas because the time available for equilibration between interstitial or veinlet melt and matrix is quite different. This has not been explored by lunar geochemists. Melt generated by partial fusion of the imperfectly mixed region of frozen LMO cumulates undergoes variable amounts of Polybaric Crystal Fractionation (PCF) or Assimilation while en route to the surface. The relative importance of PCF, perhaps by flow differentiation (16,17,18) and assimilation can be roughly assessed if it is assumed that the dominate mode of magma ascent is by the propagation of buoyancy-driven melt-filled cracks through the lunar lithosphere (19,20,21). Asymptotic crack widths ( $h$ ) and magma ascent rates ( $v$ ) at depths greater than the upper 20 km of pervasively fractured lunar crust for flows in the laminar and turbulent regimes are:  $h = (3\eta Q/2\Delta\rho g)^{1/3}$  and  $h = [\rho^{3/7} Q (\eta/2)^{1/7} / (2(30\Delta\rho g))]^{7/12}$  with  $v = Q/2h$  in which  $\rho$ ,  $\Delta\rho$ ,  $\eta$  and  $Q$  represent the magma density, mean density difference between magma and country rock along the ascent path, magma viscosity and volumetric flux per unit length of fracture. When combined with a simple heat transfer model for cooling from a magma-filled crack (18,22) one may predict the extent of crystal fractionation or likelihood of assimilation as a function of the fracture dimensions, the discharge rate, magma viscosity and density, density differential, the selenotherm and a few other transport properties. In the laminar regime, magma ascent times ( $t_a$ ) from the segregated source region (200 to 500 km) to the surface are proportional to  $\eta/\Delta\rho g$ ; lower lunar gravity that decreases the importance of buoyancy relative to earth is partially offset by the generally lower viscosity of lunar melts relative to terrestrial MORB. In the turbulent regime, ascent rates are proportional to  $\eta^{1/7}/(\Delta\rho g)^{4/7}$  and so other factors remaining constant, magma ascent times are greater compared to terrestrial ones by a factor of about 3. Although volatiles seem to play a limited role in lunar petrogenesis, fire-fountaining is apparently an important process in the production of some pristine glasses. Because of the absence of a lunar atmosphere and the dependence of vapor compressibility on pressure ( $\beta = 1/P$ ) vapor expansion can propel melts to velocities of order 10 to 100 m/s despite intrinsically low volatile concentrations.

## REFERENCES

- (1) Warren, P.H. (1985), *Annu. Rev. Earth Planet Sci.*, p. 201-240.
- (2) Warren, P.H. (1989), *Tectonophysics*, p. 165-199.
- (3) Kraichnan, R.H. (1962), *Phys. Fluids*, p. 1374-1389.
- (4) Tonks, W.B., Melosh, H.J. (1990), In *Origin of the Earth*, in press.
- (5) Crisp, J.A., Baloga, S. (1990), *Jour. Geophy. Res.*, p. 8245-8294.
- (6) Martin, D., Nokes, R. (1989), *Jour. Petrol.*, p. 1471-1500.
- (7) Carrigan, C. (1987), *Geophy. Res. Letters*, p. 915-918.
- (8) Brandeis, G., Marsh, B.D. (1989), *Nature*, p. 613-616.
- (9) Danckwerts, P.V. (1952), *App. Sci. Res.*, p. 279-296.
- (10) Oldenburg, C.O., Spera, F.J., Yuen, D.A., Sewell, G. (1989), *Jour. Geophys. Res.*, p. 9215-9236.
- (11) McKenzie, D. (1984), *Jour. Petrol.*, p. 713-765.
- (12) Ribe, N.M. (1987), *Jour. Volcanol. Geotherm. Res.*, p. 241-253.
- (13) Richter, F.M. (1986), *Earth Planet. Sci. Letters*, p. 333-344.
- (14) Sleep, N.H. (1988), *J. Geophys. Res.*, p. 10255-10272.
- (15) Stevenson, D. (1989), *Geophys. Res. Letters*, p. 1067-1070.
- (16) Irving, A., (1984), *Am. Jour. Sci.*, p. 682-703.
- (17) Spera, F.J., (1981), *Contrib. Mineral. Petrol.*, p. 56-65.
- (18) Spera, F.J., (1984), *Contrib. Mineral. Petrol.*, p. 217-232.
- (19) Spera, F.J., (1986), *Mantle Metasomatism.*, p. 1-21.
- (20) Spence, D.A., Turcotte, D.L., (1990), *Jour. Geophy. Res.*, p. 9463-9472.
- (21) Lister, J.R., (1990), *J. Fluid Mech.*, p. 263-280.
- (22) Bruce, P.M., Huppert, H. (1989), *Nature*, p. 685.

**Titanium-Rich Basalts within the Flamsteed-P Region of Oceanus Procellarum: New Results from High Spatial Resolution CCD Data.** Jessica M. Sunshine and Carle M. Pieters, Department of Geological Sciences, Brown University, Providence, RI 02912.

A variety of basalt types have been identified from samples of the lunar landing sites. In addition, detailed analyses of small foreign fragments in the lunar sample collections continue to lead to the discovery of new basalt groups. Although these efforts have contributed a great deal to our understanding of lunar geologic history, the sample collection is unfortunately not fully representative the compositional diversity of the Moon. Over the last two decades, a variety of distinct basalt types have been identified using remote measurements, approximately 2/3 of which have not been sampled directly [1]. Telescopic and spacecraft data provide the only near-term opportunities to explore the unsampled regions of the lunar surface in further detail.

New high spatial resolution CCD images spanning the Flamsteed-P ring in southern Oceanus Procellarum (see **Figure 1**) have been recently obtained in cooperation with Dr. Patrick Pinet at the Pic-du-Midi Observatory, Toulouse, France. The data consist of two sets of overlapping images each taken at ten narrow spectral channels ranging from 0.40 to 1.05  $\mu\text{m}$  [2]. **Figure 2** shows the spatial extent and resolution of this new CCD data. Previous studies of the Flamsteed region suggest that this area contains young unsampled basalts which are rich in titanium and contain relatively large amounts of olivine and/or iron-rich glass [3]. Such basalts are relatively common in the unsampled western hemisphere, but are absent in the eastern hemisphere [1].

The increased spatial resolution of these images, combined with their spectral range, will allow further evaluation of the mare units within the Flamsteed-P ring. Among the goals of this study are to search for and characterize discrete basalt units, to identify any compositional variation that might indicate in situ differentiation within these basalts, and to determine the sequence of the mare fill within the region.

Preliminary analysis of the new Pic-du-Midi data reveals several spectrally distinct mare units within the Flamsteed-P ring. Examination of the ratio image of the 0.40  $\mu\text{m}$  to 0.73  $\mu\text{m}$  images, which is sensitive to titanium content in mare units, indicates that there are a variety of basalt units within the Flamsteed-P ring. At lower resolution the basalt within the Flamsteed-P ring appeared to be one unit of relatively high titanium content [3]. However, this new high resolution CCD data indicates that the mare in this region is actually composed of at least three distinct units which differ in titanium content.

Continued analysis of these data will concentrate on determining whether these units represent distinct homogeneous flows or compositional variations within one flow, which would be indicative of near-surface differentiation. More quantitative assessment of all the spectral data, including the character of the near-infrared absorptions, will be required. In addition, the morphologic setting of these mare units will be examined to search for the source of the flows and to determine their stratigraphic relationships.

Characterizing these late titanium rich basalts provides an important constraint on our understanding of the source regions for lunar magmas, lunar petrologic evolution, and the thermal history of the Moon. Further examination of the diversity of western lunar basalts, which is critical to our understanding of these processes, will be possible from continued Earth-based studies only for the near side. The upcoming Galileo encounter with the Moon this December, will however provide the first spectral data for basalts within the Orientale Basin, extending our knowledge to also include parts of the farside.

## References

- [1] Pieters, C., *Proc. Lunar and Planet. Sci. Conf. 9th.*, pp. 2825-2849, 1978.
- [2] Chevrel, S. and Pinet, P., (abst.), *LPSC 20th*, pp. 153-154, 1989.
- [3] Pieters, C. M., Head, J. W., Adams, J. B., McCord, T. B., Zisk, S., and Whitford-Stark, J., *J. G. R.*, 85, pp. 3913-3938, 1980.



**Figure 1.** High resolution Lunar Orbiter IV frame 143-H3 showing the Flamsteed-P ring (112 km), including the crater Flamsteed (21 km), in southern Oceanus Procellarum. The white triangle is the approximate location of the Surveyor I landing site.



**Figure 2.** One of the ten different wavelength CCD images ( $0.40 \mu\text{m}$ ) spanning the Flamsteed-P ring. This is a mosaic of two separate images showing the spatial extent and resolution of the newly acquired data.

**APOLLO 15 OLIVINE-NORMATIVE AND QUARTZ-NORMATIVE MARE BASALTS:  
A COMMON ORIGIN BY DYNAMIC MELTING.**

**Scott K. VETTER**, Department of Geology, Centenary College, Shreveport, LA, 71134

**John W. SHERVAIS**, Depart. of Geological Sciences, University of South Carolina, Columbia, SC, 29208.

Two distinct mare basalt groups are represented at Apollo 15: the olivine-normative basalts (ONB) and the quartz-normative basalts (QNB) [1-3]. The ONB and QNB suites are distinguished petrographically by their phenocryst assemblages (the ONBs are olivine-phyric, the QNBs are generally pyroxene-phyric) and chemically by their major element compositions: the QNBs are higher in SiO<sub>2</sub> and MgO/FeO, and lower in FeO\* and TiO<sub>2</sub> than ONBs with similar MgO contents. Experimental data [2,4-7] show that the QNB suite is derived from a more magnesian, olivine-normative parent magma, a conclusion which is supported by the recent discovery of high-SiO<sub>2</sub> olivine-normative basalt clasts in breccia 15498 [8]. Least-squares mixing calculations are consistent with the high-SiO<sub>2</sub> ONBs being parental to the more primitive QNBs by simple removal of low pressure olivine [8]. Based on this relationship we include these high-SiO<sub>2</sub> ONBs as part of the "QNB suite". Relationship between the primitive QNBs and the more evolved QNBs is the result of low pressure pigeonite fractionation. The combination of high Mg#, high SiO<sub>2</sub>, and low TiO<sub>2</sub> in the QNB suite precludes a relationship to the ONB suite by simple removal of low pressure liquidus minerals (olivine and pigeonite) and is consistent with our modeling [8] and earlier studies [2,3].

Despite these significant differences in petrography and major element composition, both groups have similar trace element concentrations and chondrite-normalized abundance patterns. Both groups have LREE/MREE < 1 and MREE/HREE > 1 producing the characteristic Apollo 15 hump shaped REE patterns. Average total abundance of REE of the ONBs is slightly less than the QNBs which is consistent with the more evolved nature of the QNBs. The high SiO<sub>2</sub> QNBs have the lowest REE abundances. Any petrogenetic model for Apollo 15 mare basalts must address the distinctly different major element characteristics but nearly identical trace element compositions. The similarity in trace element concentrations imply compositionally similar source regions and similar percent melting, but these conclusions are not easily reconciled with the observed differences in major element compositions, which require sources with distinct mineralogies or large differences in percent melt.

**PREVIOUS MODELS:** The mare basalt source region has geochemical characteristics that are complementary to the highlands crust, and it is generally thought to comprise mafic cumulates from the magma ocean [9]. Early models of mare basalt petrogenesis, suggested that remelting of these cumulates at different depths resulted in the observed mare chemistries [9]. Despite the appeal of this simple model, there is increasing evidence that more complex scenarios are required. More recent models of mare basalt petrogenesis have stressed two dominant themes: (1) the assimilation of crustal components, e.g., KREEP [10-15], and (2) melting of complex hybrid source regions [16,17,18]. A major problem with the KREEP assimilation model is that the assimilation of KREEP tends to enrich the LREE relative to the MREE and HREE. Any significant amount of KREEP assimilation will not work at Apollo 15 because both the ONBs and QNBs have LREE/MREE slopes < 1. The Apollo 15 basalts also have low overall concentrations of incompatible elements which differ little between the two main suites present. These suites differ mainly in their major element chemistry (unlike the Apollo 14 basalts, which have nearly identical major element compositions). We have tried a variety of KREEP assimilation models on the Apollo 15 mare basalts and none have proved satisfactory.

Hughes et al. [17] have recently presented detailed, quantitative models that account for Apollo 15 ONBs by melting of hybrid source regions. These regions are complex mixtures of early magma ocean cumulates, late magma ocean cumulates, and trapped liquid. The trapped liquid component is late magma ocean with a KREEP-like composition, so these models are similar to the assimilation models in effect, but differ in concept. Hughes et al. [17] apply their model to Apollo 15 green glass, yellow-brown glass, and ONBs, but do not address the more subtle differences observed between the ONB and QNB suites.

**DYNAMIC MELTING MODEL:** We propose that the salient chemical characteristics of the Apollo 15 olivine normative and quartz normative mare basalt suites can be derived from a dynamic melting model without KREEP assimilation. In this model, melt extraction from the mantle source region is incomplete and 5-10% of the melt produced during each melting event is retained in the source region as dikes and veins [18]. During subsequent melting events, trace element concentrations are controlled by remelting of the dikes, whereas major elements are controlled by phase proportions and compositions in the refractory

residuum. This model allows repeated melting of the same source region without total depletion of the incompatible trace elements. Because the refractory residuum is enriched in MgO and depleted in SiO<sub>2</sub> during melting, subsequent melts derived from this region tend to be more mafic and silica-undersaturated.

Three general situations were tested using this approach: (1) Cpx-rich cumulate source in equilibrium with late lunar magma ocean (LMO) ( $La = 30 \times$  chondrite), (2) Olivine + Opx-rich cumulate with 20% Cpx in equilibrium with late LMO ( $La = 30 \times$  chondrite), and (3) Olivine/Opx/Cpx cumulate in equilibrium with an early LMO ( $La = 10 \times$  chondrite). All of our models share the following characteristics: (1) Nine trace elements were included in the calculations (five REE, Ba, Th, Sc, Ti); (2) Following Nyquist et al. [20], a fractionated LMO was used ( $La/Lu = 2 \times$  chondrite); (3) Non-modal melting dominated by pyroxene; (4) We assume that 2-10% of the first stage melt was retained in the source as dikes/veins; (5) The high-SiO<sub>2</sub> ONBs are taken to be parental to the more evolved QNB suite; (6) In each case, the QNB parent magma (= high-SiO<sub>2</sub> ONB) is assumed to be the first melt extracted from the source, and the normal low-SiO<sub>2</sub> ONBs are generated by re-melting of the refractory source region.

Model 1 (Cpx-rich source with late LMO) produces observed trace element concentrations in the QNB parent magma after 25% melting. Remelting of the refractory residue (plus 10% dikes) produces the relative trace element concentrations of the ONB suite after 20% melting; matching the absolute concentrations requires about 25% fractional crystallization. Model 2 (olivine-rich source with late LMO) matches the QNB parent magma after 5% to 7% melting. Primitive ONBs are produced by an additional 5-7% melting of the residue (plus 5-9% dikes). Model 3 (olivine-rich source with early LMO) produces the overall shape of the trace element patterns after 4% melting, but the absolute abundances are too low; approximately 50% fractional crystallization is required to produce the correct absolute abundances. Remelting of this mantle residuum (plus 5% dikes) can produce the ONB suite pattern, but up to 50% fractional crystallization is required to match the observed concentrations.

Dynamic melting can be applied over a wide range of mantle compositions to successfully model mare basalt suites which have similar trace element abundances. It seems clear that model 1 is the most robust because the amount of melting significantly exceeds the amount of trapped/retained magma in the source, so we are not merely remelting the retained magma. However, Nyquist et al [19] have suggested that the Rb/Sr systematics of Apollo 15 ONBs require a source with only 20% Cpx. This constraint favors models 2 and 3 -- which differ mainly in their LMO component. Model 3 may be applicable to a non-hybrid, magma ocean cumulate source region, whereas models 1 and 2 will probably require some hybridization to match the major element characteristics of these basalts.

**REFERENCES** [1] Rhodes J.M. and Hubbard N.J. (1973) Proc. Lunar Planet. Sci. Conf., 4th, 1127-1148; [2] Chappell B.W. and Green D.H. (1973) EPSL, 18, 237-246; [3] Dowty E., et al. (1973) Proc. Lunar Planet. Sci. Conf., 4th, 423-444; [4] Humphries et al., (1972) The Apollo 15 Lunar Samples, 103-107; [5] Lofgren (1975) Lunar Science VI, 515-517; [6] Longhi et al (1972) The Apollo 15 Lunar Samples, 131-134; [7] Grove T. and Walker D. (1977) Proc. Lunar Sci. Conf. 8th 1501-1520; [8] Vetter et al. (1988) Proc. Lunar Planet. Sci. Conf. 18th, 255-271; [9] Taylor, S.R. and Jakes, P. (1974) Proc. Lunar Sci. Conf. 5th, 1287-1305; [10] Binder, A.B. (1985) Proc. Lunar Planet. Sci. Conf. 16th, D19-D30; [11] Shervais J. et al., (1985) Jour. Geophys. Res., 90, C375-C395; [12] Shervais J. et al., (1985) Jour. Geophys. Res., 90, D3-D18; [13] Shih, C-Y. et al., (1986) Proc. Lunar Planet. Sci. Conf. 16th, J. Geophys. Res., 91, D214-D228; [14] Dickinson, T. et al., (1985) Proc. Lunar Planet. Sci. Conf. 15th, 90, C365-C374; [15] Neal C.R., et al (1988) Proc. Lunar Planet. Sci. Conf. 18th, 121-137; [16] Ringwood A. and Kesson S. (1976) Proc. Lunar Sci. Conf. 7th, 1697-1772; [17] Hughes et al. (1989) Geochim. Chem. Acta 52, 2379-2391; [18] Langmuir C. et al. (1977) EPSL 36, 133-156; [19] Nyquist L. et al. (1977) Proc. Lunar Sci. Conf. 8th 1383-1415.

## LUNAR MARE METEORITES

Paul H. Warren and Gregory W. Kallemeyn

Institute of Geophysics and Planetary Physics, University of California, Los Angeles, CA 90024-1567

A total of 11 pieces of the Moon have now been found as meteorites collected by Japanese and U.S. expeditions to Antarctica. With adjustment for obvious "pairing" of samples, the number of apparently distinct Antarctic Moon rocks stands at 8. Lunar meteorites are delivered to the Earth by kinetic energy from random collisions between other objects and the Moon.

The value of this collection as an augmentation to previous sampling of the Moon can be appreciated by noting that the Moon has been directly sampled at only a total of nine sites (six US Apollo sites plus three USSR Luna sites). The Apollo sites were sampled most comprehensively, yielding 22-110 kg of material per site, mostly in the form of rocks (on average, about 135 rocks bigger than 5 g per site), from traverses that extended to points as far as 11 km apart. Sampling by the Luna probes was limited to 52-170 g of soil per site, obtained in the form of short cores. The representativeness of the Apollo and Luna samples is greatly enhanced by the "gardened" nature of the Moon's upper crust, thanks to its history of prolonged impact-bombardment. Thus, a significant fraction of the rocks at a typical point on the surface (especially if the point is in the highlands) originally formed at points many tens, or even hundreds, of km away. However, six km-scale traverse zones, plus three 1-2 cm wide cores, hardly constitute an adequate sample of a heterogeneous, differentiated body with a circumference of 10,900 km. To make matters worse, for technological reasons the Apollo and Luna landings were clustered into a small region of the central nearside. A polyhedron drawn around all six Apollo sites covers only 2.7% of the Moon's surface, and adding the three Luna sites only stretches this coverage to 4.4% (Fig. 1). In contrast, cratering of the lunar surface is probably almost random. There is probably a 1.2 x higher cratering rate on the eastern hemisphere vs. the western hemisphere, but the farside/nearside ratio is probably within 1% (on the high side) of 1.00 [1].

*Short Petrological Descriptions of the Individual Meteorites:* **Y791197** (mass: 52 g), **ALHA81005** (31.4 g), **Y82192/86032** (712 g), and **MAC88104/5** (724 g) are regolith breccias<sup>1</sup> composed of almost pure highlands material [e.g., 2]. **Y793169** (6.1 g, not yet allocated for consortium investigation) is a medium-grained VLT mare basalt (K. Yanai, pers. comm., 1990). **Y793274** (8.7 g) is a regolith breccia composed of VLT-mare and nonmare material in roughly 2:1 proportions [3]. We find a bulk composition with  $\text{Al}_2\text{O}_3 = 17.4$  wt% and  $\text{TiO}_2 = 0.67$  wt%. By mass balance, the mare component of this breccia (assuming an  $\text{Al}_2\text{O}_3$  content of at least 8 wt%) must have  $\text{TiO}_2 < 1.5$  wt%. This meteorite probably originated as a submature soil near a highlands/VLT-mare boundary. **EET87521** (30.7 g) is a fragmental breccia (polymict, but with no indications of a surface regolith history), composed of nearly pure mare material. The mare component consists of relatively coarse-grained (cumulate?) diabases or gabbros, of VLT bulk composition [4,5]. **Asuka-31** (tentative name, 442 g, not yet allocated for consortium investigation) is an uncommonly coarse-grained (cumulate) VLT mare diabase or gabbro, with pyroxenes up to 4 mm across [6]. Note that the four dominantly-mare meteorites are all VLT types, but in detailed petrography and bulk chemistry (based largely on wet-chemical data from [6] and K. Yanai, pers. comm., 1990), they appear at least superficially distinct from one another.

The 8 apparently distinct lunar meteorites do not necessarily represent 8 separate lunar impact sites. Hard evidence from isotopic cosmic-ray exposure (CRE) records (thus far measured only for the 4 highlands samples<sup>2</sup>) guarantees a minimum of 2 separate lunar source craters, and the CRE data are only barely consistent with <3 sources [O. Eugster and K. Nishiizumi, presentations at 21st Lunar & Planetary

1 Y82192/86032 is arguably better classified as a simple fragmental breccia with a minor regolith component.

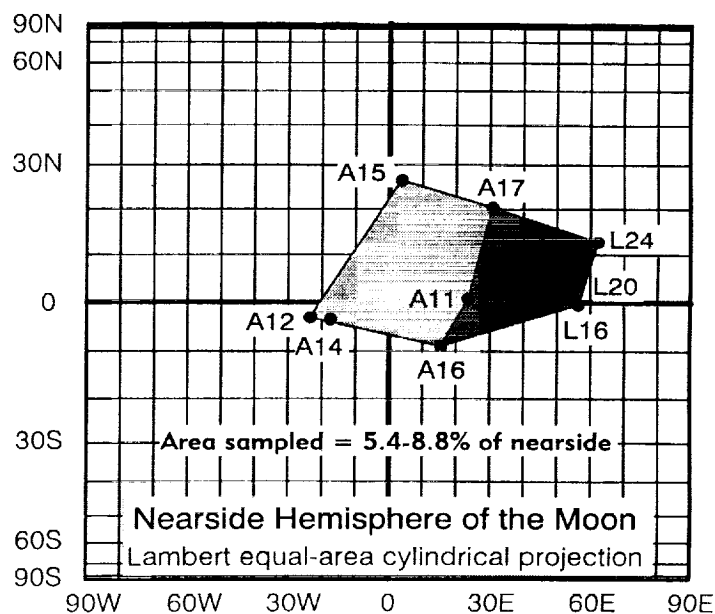
2 The relevant CRE age is the sum of the terrestrial age plus the "4 $\pi$ " exposure (Moon-Earth transit) age. Data for a fifth lunar meteorite, Y793274 [7,8], thus far do not constrain its "4 $\pi$ " exposure history.

## LUNAR MARE METEORITES: Warren P. H. and Kallemeyn G. W.

Sci. Conf., 1990] (see also [9]). Although the 4 samples that have not yet been measured for CRE are all dominantly VLT-mare, and thus totally unlike the 4 measured samples, the petrologic differences among the 4 mare meteorites are relatively minor. It is curious that 3 out of 8 samples are mare, and one of the others (Y793274) is a mixture of mare and nonmare material, dominantly mare. Only 1/6 of the Moon's surface appears (albedos, crater-densities, etc.) to be of mare affinity. The remaining 5/6 of the surface appears to be highlands (nonmare) crust, and the maria are believed to be thin veneers (generally only a few hundred meters thick) covering nonmare materials. Simple probability theory indicates that the probability of finding 4 out of 8 instances of predominantly mare material, through random sampling of a population that is 1/6 mare, is only 0.031. Even ignoring the hybrid Y793274, the probability for 3 out of 7 random samples to be mare is only 0.095. Unfortunately, we cannot expect CRE ages to remove all ambiguity regarding possible source-crater pairing among lunar meteorites, because Monte Carlo models [10] indicate that even considering only objects that are initially ejected clear from the Earth-Moon system and into heliocentric orbits (some lunar meteorites are presumably derived in a more direct fashion), in most cases the Moon-Earth transit times are <1 Ma.

Unless the four dominantly-mare meteorites indeed represent different pieces of ejecta from a single lunar source crater, it is remarkable that they are so completely dominated by VLT materials. The abundance of VLT types in the crust as a whole is difficult to gauge. Remote sensing techniques are far better at distinguishing between low-Ti and high-Ti mare basalts. Pieters [11] has recently used remote sensing to infer high proportions of augite within many large areas traditionally mapped as "pure" highlands. In addition, the minor mare components in ALHA81005, Y791197, Y82192/86032 and MAC88104/5 are also dominantly VLT (see references in [5]). Apparently, VLT types are far more common than previously suspected, and the dichotomy of lunar magmatism into distinct nonmare and mare styles may have been less abrupt than traditionally envisaged.

**References:** [1] Bandermann L. W. and Singer S. F. (1973) *Icarus* 19, 108-113. [2] Ostertag R. et al. (1986) *Proc. 10th Sym. A. M.*, 17-44. [3] Abstracts by Fukuoka, Kurat, Lindstrom, Takeda, and Warren, in *Abstracts, 15th Sym. A. M.* [4] Delaney J. S. (1989) *Nature* 342, 889-890. [5] Warren P. H. and Kallemeyn G. W. (1989) *GCA* 53, 3323-3330. [6] Yanai K. (1990) *Lunar Planet. Sci. XXI*, 1365-1366. [7] Eugster O. (1990) *Abstracts, 15th Sym. A. M.*, 188-190. [8] Takaoka N. and Yoshida Y. (1990) *Abstracts, 15th Sym. A. M.*, 126-128. [9] Eugster, O. (1989) *Science* 245, 1197-1202. [10] Wetherill G. W. (1968) in *Origin and Distribution of the Elements* (L. H. Ahrens, ed.), p. 425-443. [11] Pieters C. M. (1989) *Lunar Planet. Sci. XX*, 848-849.



## A SPINIFEX-TEXTURED MARE BASALT: COMPARISON WITH KOMATIITES

Paul H. Warren, Eric A. Jerde and Gregory W. Kallemeyn

Institute of Geophysics and Planetary Physics, University of California, Los Angeles, CA 90024-1567

Lunar sample 12024,15 is a 14.1-g rocklet from the coarse fraction of a soil sample obtained at the extreme SW end of the Apollo 12 traverse. Marvin [1] noted that 12024,15 has a surface appearance that suggests quenching. As first received in Houston, the sample was covered by a thick (several mm) layer of adhering dust. Following removal of nearly all of the dust, Marvin [1] noted "a microtopography of tongues and ponds of smooth bronzy glass . . . resembling that of quenched slags." Our own binocular examination (3/89) showed that the rock consists largely of microlitic sheets, arranged in groups of typically 20 parallel sheets, 0.6-0.8 mm long and spaced roughly 30-40  $\mu\text{m}$  apart, to form blocks spanning roughly 0.7 x 0.7 mm in two-dimensional view. These blocks appear to resemble tiny unbound books, composed of thick microlitic "pages" of uneven height and width. We have studied petrographically two thin sections and geochemically a 360 mg chip. The bulk composition corresponds to a typical Ap12 ilmenite basalt (e.g., [2,3]). The rock consists of ~10% olivine phenocrysts, traces of chromite and FeNi, and 90% groundmass. The olivine phenocrysts are for the most part remarkably euhedral. In some cases they are slightly skeletal, with roundish enclaves of glassy, groundmass-like material. These phenocrysts are typically ~0.3 mm across, and occur in glomeroporphyritic clusters. The largest individual crystal is 1.0 mm across. The groundmass consists mainly of glass and submicroscopic devitrification products, but also contains abundant platy-textured olivine microlites, especially in thin section 12024,55. These microlites are generally <3  $\mu\text{m}$  in width, but up to 0.7 mm long. The largest "book" of them is 1.2 mm thick. BSE images of 12024,55 (Fig. 1) show that nearly all of its groundmass is book-textured, and the overall groundmass texture is remarkably similar to relatively fine-grained varieties of spinifex typical of the upper portions of komatiite flows. The microlitic sheets of olivine appear at high magnification (Fig. 1, bottom) to be partially-discontinuous chains. The microlites are generally too slender to probe, but one of the fattest ones gave a composition of  $\text{Fo}_{61.0}$ . The phenocrysts are  $\text{Fo}_{68.2-70.7}$  in their interiors, but are zoned in their outermost ~3  $\mu\text{m}$ . If the olivine and chromite phenocrysts are subtracted from the bulk-rock composition to yield the composition of the groundmass that was potentially in equilibrium with the phenocrysts, the predicted equilibrium phenocryst composition is  $\text{Fo}_{70.1}$ .

Marvin's [1] suggestion that 12024,15 represents the very top of a lava flow appears to be essentially confirmed. Besides 12024,15, at least three other Apollo 12 basalts are also olivine-porphyritic vitrophyres (12008, 12009 and 12015), but none of these had final-stage cooling comparable in rapidity to that of 12024,15. In experiments using a synthetic analog of A12 basalt as the starting liquid, Donaldson [4] documented systematic changes in olivine morphology related to cooling rate during growth. On this scale, the 12024,15 phenocrysts grew with  $-dT/dt \sim 1-2 \text{ }^\circ\text{C/hr}$ , probably en route from a mantle source region, or else a deep-crustal staging chamber, to the surface. In contrast, the microlites grew with  $-dT/dt \sim 10^3 \text{ }^\circ\text{C/hr}$ . Some models for the origin of spinifex texture assume that isolation from crystal nuclei is a key preliminary condition, but 12024,15 suggests that rapid cooling rate and ultramafic melt composition are the keys. This new evidence for presence of olivine phenocrysts prior to eruption of a seemingly typical mare magma weakens arguments [e.g., 5] that lunar magmas seldom fractionated between their mantle source regions and the surface. However, the clear absence of plagioclase among the phenocrysts hardly supports the hypothesis [6] that during Ap-12 mare basalt genesis, fractionation in deep-crustal staging chambers was extensive enough to involve important proportions of plagioclase.

**References:** [1] Marvin U. B. (1978) *Apollo 12 Coarse Fines (2-10): Sample Locations, Description, and Inventory*, NASA JSC 14434. [2] Rhodes J. M. et al. (1977) *Proc. Lunar Sci. Conf.* **8**, 1305-1338. [3] Dungan M. A. and Brown R. W. (1977) *Proc. Lunar Sci. Conf.* **8**, 1339-1381. [4] Donaldson C. H. (1976) *Contrib. Min. Pet.* **57**, 187-213. [5] Taylor G. J. (1989) in *(Abstracts for) Workshop on Lunar Volcanic Glasses: Scientific and Resource Potential* (LPI), p. 27-28. [6] Walker D. A. (1983) *Proc. Lunar Planet. Sci. Conf.* **14**, B17-B25.

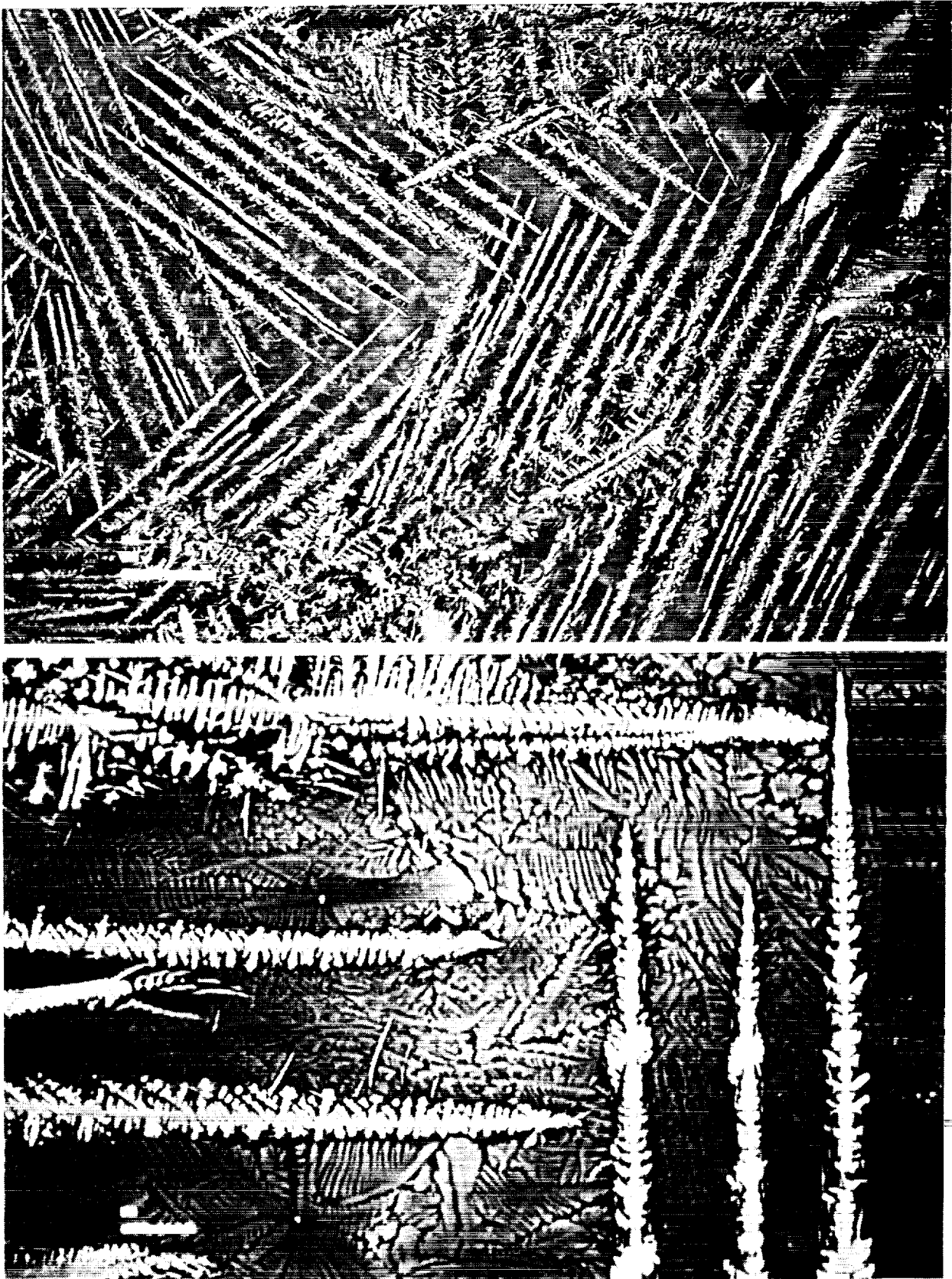


Fig. 1: BSE images of the groundmass of 12024,55: top view is  $1000 \times 690 \mu\text{m}$ , bottom view is  $127 \times 86 \mu\text{m}$ .

# List of Workshop Participants

---

- Jayne C. Aubele  
*Department of Geological Sciences*  
*Brown University*  
 Box 1846  
 Providence RI 02912
- A. Basu  
*Department of Geology*  
*Indiana University*  
 Bloomington IN 47405
- David Batchelor  
*Cosmochemistry Group*  
*Department of Chemistry and Biochemistry*  
*University of Arkansas*  
 Fayetteville AR 72701
- Mark J. Cintala  
 Mail Code SN21  
*NASA Johnson Space Center*  
 Houston TX 77058
- Russell Colson  
*Washington University*  
 Box 1169  
 St. Louis MO 63130
- Cassandra Coombs  
*POD Associates*  
 2309 Renard Place, SE  
 Suite 201  
 Albuquerque NM 87106
- Bonnie Cooper  
 8601 Palmer Highway, #3  
 Texas City TX 77591
- Larry Crumpler  
*Department of Geological Sciences*  
*Brown University*  
 Box 1846  
 Providence RI 02912
- Julius Dasch  
 Mail Code XEU  
*NASA Headquarters*  
 Washington DC 20546
- John Delano  
*Department of Geological Sciences*  
*State University of New York*  
 Albany NY 12222
- Tammy Dickinson  
 Mail Code SL  
*NASA Headquarters*  
 Washington, DC 20546
- Michael J. Drake  
*Lunar and Planetary Laboratory*  
*University of Arizona*  
 Space Science Building  
 Tucson AZ 85721
- Jim Eckert  
*Department of Geological Sciences*  
*University of Tennessee*  
 Knoxville TN 37996-1410
- Don Francis  
*McGill University*  
 3450 University Street  
 Montreal Quebec H3A 2A7  
 Canada
- B. Ray Hawke  
*Planetary Geosciences Division*  
*University of Hawaii*  
 2525 Correa Road  
 Honolulu HI 96822
- James Head III  
*Department of Geological Sciences*  
*Brown University*  
 Box 1846  
 Providence RI 02912
- Paul C. Hess  
*Department of Geological Sciences*  
*Brown University*  
 Box 1846  
 Providence RI 02912
- Petr Jakeš  
*Lunar and Planetary Institute*  
 3303 NASA Road 1  
 Houston TX 77058
- Ralf Jaumann  
 D. L. R.  
 8031 Oberpfaffenhofen  
 NE-OE-PE  
 D-8031 Wessling, WEST GERMANY
- John Jones  
 Mail Code SN2  
*NASA Johnson Space Center*  
 Houston TX 77058
- Susan Keddie  
*Department of Geological Sciences*  
*Brown University*  
 Box 1846  
 Providence RI 02912

- Laszlo Keszthelyi  
Mail Stop 170-25  
California Institute of Technology  
Pasadena CA 91125
- V. R. Keyuchkov  
Vernadsky Institute  
USSR Academy of Sciences  
Kosygin Street 19  
117975 Moscow, USSR V-334
- Gary Lofgren  
Mail Code SN2  
NASA Johnson Space Center  
Houston TX 77058
- John Longhi  
Lamont-Doherty Geological Observatory  
Palisades NY 10964
- Michael Manga  
Department of Earth and Planetary Sciences  
Harvard University  
20 Oxford Street  
Cambridge MA 02139
- Ted A. Maxwell  
Mail Code SL  
NASA Headquarters  
Washington DC 20546
- Gordon A. McKay  
Mail Code SN2  
NASA Johnson Space Center  
Houston TX 77058
- Paul D. Miller  
1117 South Davis  
Arlington TX 76013
- Donald Morrison  
Mail Code SN2  
NASA Johnson Space Center  
Houston TX 77058
- Clive Neal  
Department of Earth Sciences  
University of Notre Dame  
Notre Dame IN 46556
- Laurence E. Nyquist  
Mail Code SN2  
NASA Johnson Space Center  
Houston TX 77058
- James J. Papike  
Department of Geology  
Northrop Hall 313  
Institute of Meteoritics  
University of New Mexico  
Albuquerque NM 87131
- Carle Pieters  
Department of Geological Sciences  
Brown University  
Box 1846  
Providence RI 02912
- Graham Ryder  
Lunar and Planetary Institute  
3303 NASA Road 1  
Houston TX 77058
- Peter Schultz  
Department of Geological Sciences  
Brown University  
Box 1846  
Providence RI 02912
- Ben Schuraytz  
Lunar and Planetary Institute  
3303 NASA Road 1  
Houston TX 77058
- Derek W. G. Sears  
Cosmochemistry Group  
Department of Chemistry and Biochemistry  
University of Arkansas  
Fayetteville AR 72701
- C. K. Shearer  
Department of Geology  
Institute of Meteoritics  
Northrop Hall 313  
University of New Mexico  
Albuquerque NM 87131
- John Shervais  
Department of Geological Sciences  
University of South Carolina  
Columbia SC 29208
- Eugene N. Skyutov  
Vernadsky Institute  
USSR Academy of Sciences  
Kosygin Street 19  
117975 Moscow, USSR V-334
- Gregory Snyder  
Department of Geological Sciences  
University of Tennessee  
Knoxville TN 37996-1410
- Frank J. Spera  
Department of Geological Sciences  
University of California  
Santa Barbara CA 93106
- Jessica Sunshine  
Department of Geological Sciences  
Brown University  
Box 1846  
Providence RI 02912

Larry Taylor  
*Department of Geological Sciences*  
*University of Tennessee*  
*Knoxville TN 37996*

Scott Vetter  
*Department of Geology*  
*Centenary College*  
*Shreveport LA 71134*

Paul H. Warren  
*Institute of Geophysics*  
*University of California*  
*Los Angeles CA 90024-1567*

J. L. Whitford-Stark  
*Geology Department*  
*Sul Ross State University*  
*Alpine TX 79832*

